Addis Ababa University
Addis Ababa Institute of Technology
School of Electrical and Computer Engineering

Direct Torque Control of Five Phase Induction Motor Using Space Vector Modulation

By

Gebrihans Yehdego

Advisor

Dr. Mengesha Mamo

A Thesis Submitted to the Addis Ababa Institute of Technology, School of Graduate Studies, Addis Ababa University, in Partial Fulfillment of the Requirements for the Degree of Masters of Science in Electrical Engineering (Electrical Control Engineering)

June, 2016

Addis Ababa, Ethiopia

Addis Ababa University
Addis Ababa Institute of Technology
School of Electrical and Computer Engineering

Direct Torque Control of Five Phase Induction Motor Using Space Vector Modulation

By

Gebrihans Yehdego

Approval by Board of Examiners

_____	_____	_____
Chair man, Department Graduate Committee	Signature	Date
Dr. Mengesha Mamo	_____	_____
Advisor's Name	Signature	Date
_____	_____	_____
Internal Examiner	Signature	Date
_____	_____	_____
External Examiner	Signature	Date

Acknowledgment

Next to the Almighty God, I would like to express my sincere gratitude to my advisor Dr. Mengesha Mamo for his continuous support and motivation. His guidance during all phases of this study was invaluable. Besides, I would like to thank all my friends for their encouragement throughout my work. Last but not least, I would like to thank my precious parents for their great support and love during my study.

Abstract

In this thesis effective direct torque control for a five phase induction motor with concentrated windings is designed. For demonstrating the superior performance of the five-phase IM, the motors are analyzed on the d_1-q_1 and d_3-q_3 synchronously rotating reference frame. The five-phase VSI output are decoupled into the torque producing (fundamental) and non-torque producing (third) harmonics sets. The third harmonic components can be used to enhance the total torque production and the motor needs to be supplied with the fundamental and the third harmonic of the stator voltages. The fault tolerance simulation results are analyzed. Also the difference between three-phase induction motor and five-phase induction motor is highlighted.

Thus due to the additional degrees of freedom, the five-phase motor drives possess many other advantages when compared to traditional three-phase motor drives. Some of these advantages include, lower torque pulsation, reduction in harmonic currents, reduced stator current per phase without the need to increase the phase voltage, greater reliability, fault tolerant feature and increased power. The performance of direct torque control induction motor has been demonstrated by simulation using a matlab/simulik. By the proper dynamical adjustment and steady state compensation, the direct torque control of the five-phase induction motor achieves a high drive performance. Simulation output results show that the transient response oscillates for 0.03 second with rise time 0.004 second and the steady state value of torque is tracking the load torque with less than 2% error.

Keywords: Induction Motor, Direct Torque Control, d-q Transformation, Space Vector Modulation.

Table of contents

List of Acronyms

DC	Direct Current
AC	Alternating Current
DSP	Digital Signal Processor
IM	Induction Motor
FOC	Field Oriented Control
DTC	Direct Torque Control
VSI	Voltage Source Inverter
SVPWM	Space Vector Pulse Width Modulation
PI	Proportional Integral
SVM	Space Vector Modulation
MMF	Magneto motive force
RFOC	Rotor Field Oriented Control
PWM	Pulse Width Modulation
PID	Proportional Integral Derivative
CSI	Current Source Inverter
IGBT	Insulated Gate Bipolar Transistor

List of Symbols

ω_r	Rotor speed
ω_e	synchronous speed
ω_a	Arbitrary speed
P	Differential operator
V	Voltage
I	Current
R	Resistance
L	Inductance
Lm	Mutual inductance
λ	Flux
θ	Rotor flux angle
Te	Electromagnetic torque
J	Moment of inertia
B	Frictional coefficient
T_L	Load torque
P	Pole pairs
Kp	Proportional gain
Ki	Integral gain
e(t)	Error signal
u(t)	Actuating signal
V_A,V_B,V_C, V_D, V_E	Inverter leg voltages
v_a, v_b, v_c, v_d, v_e	Phase to neutral voltages
V_{Nn}	Voltage between star point of load and negative rail of dc bus
Vdc	DC link voltage
v_1, v_2, v_3,…	Space voltage vectors
S_1, S_2, S_3,…	Switching function
T_1, T_2	Time of application of neighboring space vectors
T_0	Time of application of zero space vectors

T_s	Sampling time
a	$2\pi/5$

Subscripts

S	Associated with stator winding
R	Associated with rotor winding
L	Associated with leakage
α-β	Relates to alpha and beta axis
d-q	Relates to direct and quadrature axis
1-3	Relates to first harmonics and third harmonics component
a-b-c-d-e	Associated with phase domain
Ref	Associated with reference input

List of Figures

List of Tables

Chapter One

Introduction

1.1 Back Ground

The history of electrical motors goes back as far as 1820, when Hans Christian Oersted discovered the magnetic effect of an electric current. One year later, Michael Faraday discovered the electromagnetic rotation and built the first primitive DC motor. Faraday went on to discover electromagnetic induction in 1831, but it was not until 1883 that Tesla invented the AC asynchronous motor. Currently, the main types of electric motors are still the same such as: DC, AC asynchronous and Synchronous, all based on Oersted. Faraday and Tesla's theories developed and discovered more than a hundred years ago [1].

For many years, before the introduction of micro-controllers, digital signal processers (DSP) and high switching frequency semiconductor devices, variable speed actuators were dominated by DC motors. They were used extensively in areas where variable speed operation was required. Since their flux and torque could be controlled independently and easily by the field and armature current. Particularly, the separately excited DC motor has been used mainly for applications where there was a requirement of fast response and four-quadrant operation with high performance near zero speed. However, due to the existence of the commutator and the brushes, DC motors have certain disadvantage. That is, they required periodic maintenance; they cannot be used in explosive or corrosive environments. Nowadays these problems can be overcome by the application of AC induction motors, because of its simplicity, ruggedness, efficiency, low cost, compactness, and economical and volume manufacturing advantages.

The advantages of AC induction motor drives compared with DC motor drives are:

- Induction motors do not require an electrical connection between stationary and rotating parts of the motor.
- Due to the absence of Commutator and Brushes, they have high speed operations.
- Induction motors have comparable and frequently better efficiency than the equivalent DC motor.

- It’s low sensitive to disturbances during operation.
- A DC motor must be regularly required service to check or replace the brushes and the commutator. But induction motor is essentially maintenance free, except for the bearings.
- Protection of an induction motor is simpler than for DC motor. For large DC machines protection of a DC circuit breaker is required which are expensive.
- Generally induction motors have low weight and inertia, high efficiency and a high overload capability, cheaper and more robust, and less proves to any failure at high speeds.
- Furthermore, the motor can work in explosive environments because no sparks are produced.

Taking into account all the advantages outlined above, induction Motors are widely used in industrial, commercial and domestic applications than all the rest of the electric motors. For high performance applications there are two types of control method of induction motor used such as: Scalar control and vector control methods [2]. In scalar control, only the magnitude and frequency, which is based on the steady state model of IM of a space vector variable such as current, voltage and flux linkage, are controlled. Thus during the transient position of space vector the scalar control does not act. While in vector controller it is based on relation which is valid for dynamic states, i.e. not only magnitude and frequency (angular speed) but also instantaneous positions of voltage, current, and flux space vectors are controlled. Thus, the vector control acts on the positions of the space vectors and provides correct orientation for both steady state and transient state. Various methods have been discovered to implement vector control for IM. The most popular vector control methods are the FOC and DTC [3]. Conventional DTC strategy is quite different from that of the FOC. Because it does not need complicated coordinate transformations and decoupling calculations. DTC technique is introduced by Takahashi and Noguchi for low and medium power application and by Depenbrock for high power application [11].

In the recent time, Multi-Phase induction motors such as: five-phase, six phase, seven phase motor and so on, are fast increasing due to their several inherent benefits such as lower torque pulsation, reduction in harmonic currents, reduced stator current per phase without the need to increase the phase voltage, greater reliability, fault tolerant feature and increased power in the same frame as compared to three phase induction motor [20]. Presently the grid power available

is only limited to three-phase so the supply to multi-phase motors is invariably given from power electronic converters. Many applications, such as electric ship propulsion, electric aircraft drives, electric/hybrid electric vehicles, locomotive traction and high power industrial plants, require high power ratings for both the motor and its converter. However, converter ratings cannot be accordingly increased due to power rating limitations of semiconductor devices [4, 5].

Higher torque density in a multi-phase machine is possible, since apart from the fundamental spatial field harmonic, the space harmonic fields can be used to contribute to the total torque production. In a multi-phase machine, with five or more phases, there are additional degrees of freedom, which can be used to enhance the torque production through the injection of higher-order current harmonics. The five-phase voltage source inverter (VSI) inputs are decoupled into the torque producing (fundamental component) and non-torque producing (third) harmonics sets. This third harmonic current injection can be used to enhance the overall torque production [6].

Five-phase voltage source inverter produces 32 output space vector voltages. The higher number of output voltage vectors can be achieved more precise control in electromagnetic torque and stator flux. This thesis will address both the fundamental component and the third harmonic component to improve the ability of a five-phase induction motor performance.

1.2 Statement of the Problem

From many years three-phase induction motor is one of the most common form of electromechanical drive which is used for industrial, commercial and domestic application due to low weight and inertia, high efficiency, high overload capability, lower cost, more robustness, simple mechanical construction, less proves to any failure at high speeds and able to work in explosive environments. But, this three phase induction motor has its own limitation compare to multi-phase induction motor such as: it has only fundamental torque component, the fault tolerance is low and run with high de-rating during phase failure, the over load capability is low and it has only eight space vector voltages that produce high torque ripple.

To overcome these limitations of three phase induction motor drive, DTC of five phase induction motor drive has better performance characteristics. Because, five-phase inverter has thirty two possible space vector voltages. So there is a greater flexibility in controlling five-phase drive

systems. Due to the additional degrees of freedom, it presents unique characteristics for enhancing the torque producing capability of the motor. And also they possess several advantages over conventional three-phase drives such as lower torque pulsation, high fault tolerance feature, reliability, high efficiency, lower torque ripple and reduced current per phase without increasing voltage per phase. Specially, in fault tolerance the motor keeps working at good performance even though one or two phases fail which is not possible in three phase motors.

1.3 Objective of the Thesis

1.3.1 General Objective

The general objective of the thesis is to design and simulate Direct Torque Controller of five-phase induction motor.

1.3.2 Specific Objective

The study in this thesis will address the following specific objectives:

- To study dynamic model of DTC five-phase induction motor using space vector modulation.
- To enhance a third harmonic voltage component that determine the ability of a five-phase induction motor to contribute a third harmonic torque component to the fundamental torque component.
- To design PI torque and flux controller for the induction motor.
- To determine the switching sequence and duty cycle of the inverter circuit using SVPWM technique.
- To simulate the whole integrated DTC based space vector modulation using MATLAB/SIMULINK.

1.4 Methodology

In this study a direct torque control of induction motor is designed using space vector modulation. The SVM is used to generate the triggering pulses which are fed to five-phase VSI in order to produce five-phase voltages. Torque and flux will be controlled independently using space vector modulation algorithm. In brief the following methodologies will be followed.

- Different literatures which are related to this thesis work are studied and concepts adopted.
- Direct torque control of induction motor is studied starting from the concept of different reference frames, transformations and dynamic modeling's.
- The dynamic space vector model of the induction motor are developed which are important for torque and flux estimation and control purposes.
- The fundamental and third harmonic torque components are estimated based on the dynamic model of the plant.
- The PI torque and flux controllers are designed.
- The switching sequence and duty cycle of the five-phase power inverter is designed using space vector pulse width modulation technique.
- Then finally the whole control system is integrated and simulated to check its functionality and accuracy with MATLAB/SIMULINK.

1.5 Literature Review

To start this thesis, many prior research papers have been read about direct torque control of induction motors. Direct torque control method is one of the effective control strategies which allow a torque control in steady state and transient operation of induction motor [2]. The main aim of direct torque control strategies is to effectively control the torque and flux of induction motor. Direct torque control method made the motor more accurate and fast torque response.

A simplified variation of field orientation known as direct torque control was developed by Takahashi and Depenbrock [1, 2]. In direct torque controlled induction motor drives, it is possible to control directly the stator flux linkage and the electromagnetic torque by the selection of an optimum inverter switching state. The selection of the switching state is made to restrict the flux and the torque errors within their respective hysteresis bands and to obtain the fastest torque response and highest efficiency at every instant. Direct flux and torque control with space vector modulation of three phase induction motor schemes are proposed in [8, 12]. The proposed controllers are shown a significant improvement over the classical DTC strategies'. The DTC-SVM strategies operate at a constant switching frequency.

The importance of the multi-phase machine over their three phase counterparts has been explained in [4, 15]. Specifically, many researchers have studied detail on DTC of five-phase induction motor. Five-phase VSI input are decoupled into the torque producing (fundamental component) and non-torque producing (third) harmonics sets. In these research papers [6, 11], DTC of Five-Phase Induction Motor with third Harmonics Elimination principles are introduced. In the proposed control systems they introduced two SVM schemes to cancel out all possible low frequency voltage harmonics.

Paper [9] has recently extended the DTC concept to a five-phase induction motor control and they presented a comparison between the three-phase and five-phase DTC drives. The implementation of the control system was done using 32 bit floating point TMS320C32 DSP. The three-phase inverter has only eight voltage space vectors that can be applied to a motor, while a five-phase inverter has 32 possible voltage space vectors. There is therefore a greater flexibility in controlling a five-phase drive system. The authors achieved high performance in terms of precise and fast flux and torque control and a smaller torque and flux ripple for five-phase induction machine as compared to three phase induction machine.

An application of rotor field oriented control (RFOC) to a five-phase induction motor with the combined fundamental and third harmonic currents was proposed in [10]. In the proposed technique the complete theory and modeling of RFOC of the five-phase induction motor are established. Specifically, investigation is made to improve power density and output torque of the five-phase induction motor by injecting third harmonic of currents. By the proper dynamical adjustment and steady state compensation, the rotor field oriented control of the five-phase induction motor not only achieves a high drive performance, but also controls the fundamental and third harmonic flux and torque to generate the desired nearly rectangular air-gap flux.

Five-Phase Induction Motor Drives With DSP-Based Control System was proposed in [14]. This introduces two kinds of control schemes: vector control and direct torque control. The implementation of these control systems was done using 32 bit floating point TMS320C32 DSP. Vector control of the five-phase induction motor not only achieves high drive performance, but also generates the desired nearly rectangular current waveforms and flux profile in the air-gap resulting in an improvement in air gap flux density and an increase of 10% in output torque. The

DTC method has additional advantages when applied to five-phase IM. The five-phase inverter provides 32 space voltage vectors in comparison to 8 space voltage vectors provided by the three-phase inverter. Direct torque control of the five-phase induction motor reduces the amplitude of the ripples of both the stator flux and the torque, resulting in a more precise flux and torque control.

Bifurcation Analysis of Five-Phase Induction Motor Drives with Third Harmonic Injection was developed in [30]. This paper addresses, for the first time, the bifurcation analysis of a five-phase induction motor drive when a third harmonic is injected for torque enhancement purposes. The main focus of the paper is to present a mathematically based study of the nonlinear dynamics of the proposed drive with torque enhancement. The overall bifurcation analysis for both concentrated and distributed winding machines, that the harmonic injection provides not only torque enhancement but also more robust controllers.

1.6 Thesis Organization

This thesis work is arranged in five chapters. The first chapter introduces back ground of induction motors, statement of the problem, objectives, methodology and literature review. The second chapter is explains the Mathematical modeling of induction motor and Direct Torque Control techniques. In addition, the different types of d-q reference frames and space vector concepts are elaborated. Design of PI controllers for the torque and flux control system is also explained in this chapter. In the third chapter, concepts and mathematical explanations of space vector modulation design are discussed. The calculating method for the reference voltages, time duration of the space vectors and switching time of each transistor are also discussed. On the fourth chapter, system simulation setup and simulation results are presented and analyzed. Concluding ideas and respective recommendations are given in chapter five.

Chapter Two

Dynamic Modeling of DTC Five-Phase Induction Motor

2.1 Introduction

Direct torque control is a controller method that used to control the stator flux and the torque directly and independently by selecting the appropriate inverter switching state. It has been gaining more popularity since its introduction due to its exceptional dynamic response and less dependence on machine parameters. DTC with a lookup table is more used in controlling the induction motor because it is considered a simple and robust method. The common disadvantages of conventional DTC are high torque ripple and slow transient response to the step changes in torque during start-up. Recently, to overcome this problem many researchers are doing to replace the lookup table DTC with the DTC space vector modulation in the five-phase IM drive. This type of control further reduces the torque ripple because it can produce the voltage reference which accurately compensates the differences between the commanded torque and flux values and their actual values from measurement and estimation.

In five-phase motors with sinusoidal distributed stator windings, the absence of back EMF for non-torque-producing harmonics (mostly the 3^{rd} harmonic) will result in considerable harmonic current. This causes deformation of the phase current and extra copper losses (while not causing torque pulsation). For sinusoidal results, the lookup table DTC and even the DTC using SVM (with one pair of closest vectors plus the zero-vector) cannot be used in a sinusoidal wound five-phase motor. At least two pairs of voltage vectors with the zero-vector are required for the harmonic free operation [7].

The main features of direct torque control are given as follows:

- ✓ Direct control of flux and torque.
- ✓ Indirect control of stator currents and voltages.
- ✓ Completely a motion-sensor less control method.
- ✓ Not sensitive for rotor parameters because its need only stator flux and torque estimator.
- ✓ High dynamic performance even at locked rotor.

Comparison of Conventional DTC and SVM DTC Method

The principle behind direct torque control of induction motor drive is to control the flux linkage and electromagnetic torque directly by the selecting proper inverter switching state with the help of lookup table or SVM. The conventional DTC includes two level and three level hysteresis controllers, three level for torque and two level for flux linkage. Even though it has many advantages like no feedback control, no traditional PWM algorithm, no vector transformation, it has some drawbacks like variable switching frequency, difficult to control flux and torque at low speed, current and torque distortion during the change of the sector, a high sampling frequency needed for digital implementation of hysteresis controllers, inherent steady state torque and flux ripple. Due to hysteresis band controller, steady state torque and flux ripple is more in direct torque control of induction motor which is undesirable from smooth response point of view. In the journal paper [12], Direct Flux and Torque Control with Space Vector Modulation (DTC-SVM) schemes are proposed in order to overcome the drawbacks of the classical DTC of Induction motor. The DTC-SVM strategy operates at a constant switching frequency is shown in figure 2.1-1.

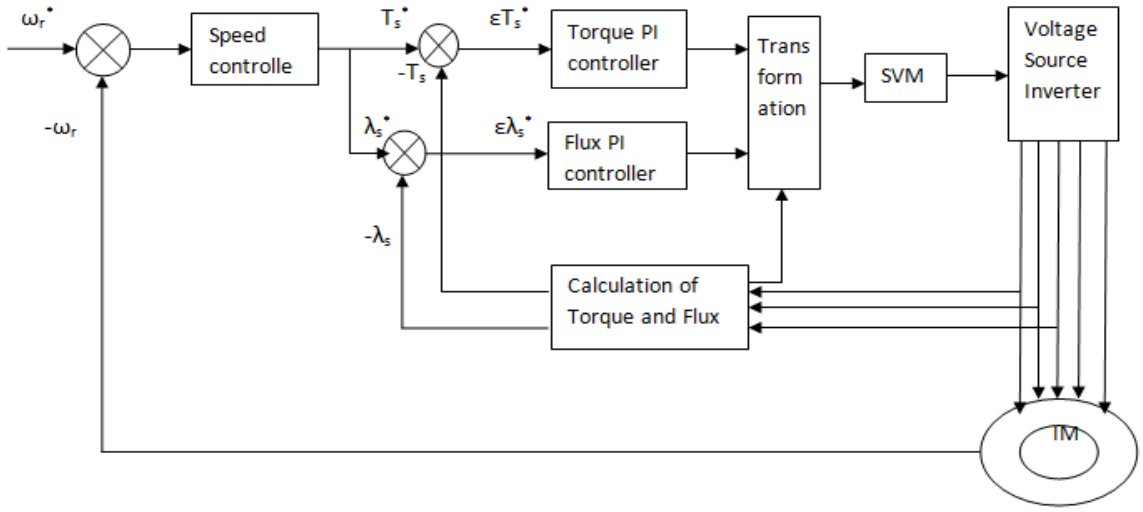

Figure 2.1-1 Direct Torque Control with SVM

Compared with the steady-state performance of lookup table DTC, DTC-SVM results in much lower torque ripple. Because; it uses the zero-vector instead of backward active vectors to reduce torque ripple. The control algorithm in DTC-SVM methods are based on averaged values

whereas the switching signals for the inverter are calculated by space vector modulator. The objective of this DTC-SVM scheme is to estimate a reference stator voltage vector V_{ref} and modulate it by SVM technique in order to drive the power gates of the inverter with a constant switching frequency [8, 13].

2.2 Winding Design of Induction Motor

An n-phase symmetrical induction machine, such that the spatial displacement between any two consecutive stator phases equals $\alpha = 2\pi/n$, is considered. This will always be the case if the number of phase is an odd prime number. There are two common types of stator winding systems such as: sinusoidally distributed winding and concentrated winding. In the case of single-induction motor five-phase, if the machine is designed with a concentrated stator winding, the spatial harmonics interact with the current harmonics producing an air gap field. This additional field rotates at fundamental speed if the order of the current and spatial harmonics is the same. This fact leads to increase the torque density by injecting the third stator current harmonics using the d_3-q_3 components. The fundamental component is generated using the d_1-q_1 subspace, while the harmonics are injected using the d_3-q_3 components. Therefore, the third stator current harmonic injection can be used to enhance the torque production and the motor needs to be supplied with the fundamental and the third harmonic of the voltage [14]. If the induction motor is wound with the concentrated windings figure 2.2-1, the air-gap flux can be made to take on a quasi-rectangular rather than sinusoidal shape by using the harmonics [15].

On the other hand, if the five-phase induction motor is with a sinusoidally distributed winding, the sinusoidal output voltages should contain only the fundamental component and they can lead to torque ripple or to be free of low-order harmonics [16]. Hence, the reference voltage space vector is nonzero only in the plane and the SVPWM scheme has to ensure that zero average voltage space vectors is applied in all the other planes, so that undesirable low order harmonics do not appear in the output. This is most easily done utilizing the analytical expressions for computation of the application times of the active vectors, such as those developed in [17] for a five-phase VSI.

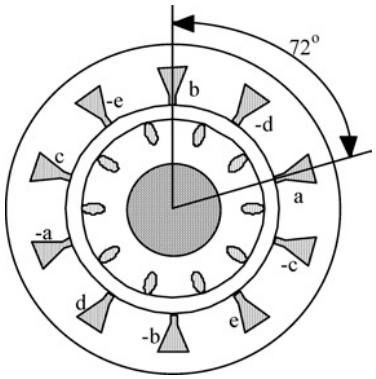

Figure 2.2-1 Five-phase concentrated-winding induction machines

2.3 Reference Frame

Based on speed of reference frame there are four main reference frames of motion, which could be used to model the five-phase induction machine. These are arbitrary reference frame, stationary reference frame, rotor reference frame and synchronous reference frame. The two commonly employed coordinate transformations with induction machine are the stationary and the synchronous reference frame [22].

1. **Arbitrary reference frame:** In this Reference frame speed is unspecified (ω) and the d-q axis can rotate at an arbitrary speed, there is no relative speed between the four coils d_s, q_s, d_r and q_r.
2. **Stationary reference frame**: In this case the d-q axis is not rotate so, the reference frame speed is zero ($\omega = 0$). It is best suited for studying stator variables only, for example variable speed stator fed IM drives, because stator d-axis variables are exactly identical to stator phase A-variable.
3. **Rotor reference frame**: The reference frame speed is equal to the rotor speed ($\omega = \omega_r$). Since in this reference frame the d-axis of the reference frame is moving at the same relative speed as the rotor phase A winding and coincident with its axis, it is best suited when analysis is confined to rotor variables as rotor d-axis variable is identical to phase-rotor variables.
4. **Synchronous reference frame:** When the reference frame is rotating at synchronous speed, both the stator and rotor are rotating at different speeds relative to it. The reference frame

speed is equal to synchronous speed ($\omega = \omega_e$). Synchronously rotating reference frame is suitable when analog computer is employed because both stator and rotor d-q quantities becomes steady DC quantities. It is also best suited for studying multi-machine system.

The IM may be modeled with respect to its stator, its rotor or its synchronous speed. These are known as referencing frames. In this research, a synchronous frame is taken as a reference frame for modeling. It makes easier to apply a direct control as all variables are seen constant with respect to the synchronous frame. The synchronous frame is also called excitation frame subscribed by **e** notation.

2.4 Dynamic Model of Five-Phase Induction Motor

The traditional per-phase equivalent circuit shown in figure 2.4-1 has been widely used in steady-state analysis and design of induction motors, but it is not appropriate to predict dynamic performance of the motor. The concept of direct torque control has opened up a new possibility that induction motors can be controlled to achieve dynamic performance as good as that of DC or brushless DC motors. In order to understand and analyze direct torque control, the dynamic model of the induction motor is necessary. It has been found that the dynamic model equations developed on a rotating reference frame is easier to describe the characteristics of induction motors. It is the objective of the article to derive and explain induction motor model in relatively simple terms by using the concept of space vectors and d-q variables. [19]

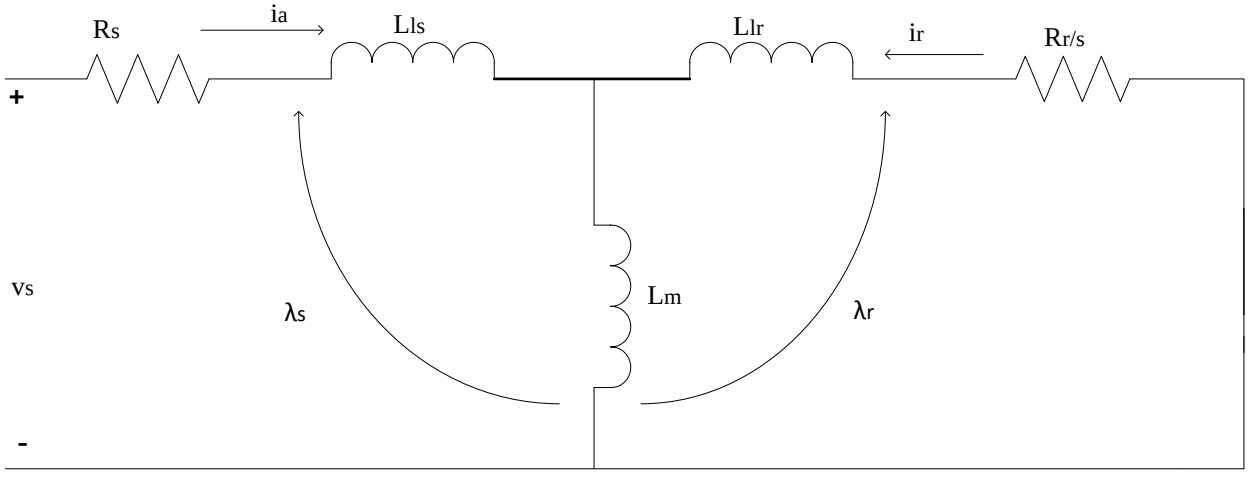

Figure 2.4-1 Conventional Per-phase Equivalent Circuit

When describing a five-phase IM by a system of equations, the following simplifying assumptions are made:

- the five-phase motor is symmetrical, only the fundamental and the third harmonic is considered, while the higher harmonics of the spatial field distribution and of the magneto motive force (MMF) in the air gap are disregarded,
- the effects of anisotropy, magnetic saturation, iron losses and eddy currents are neglected,
- the coil resistances and reactance are taken to be constant,

Taking into consideration the above stated assumptions; the dynamic behavior of five-phase induction motor is described by the following equations written in terms of space vectors in the stationary reference frame [6].

$$v_s = R_s i_s + \frac{d}{dt}(\lambda_s) \tag{2.1}$$

$$v_r = 0 = R_r i_r + \frac{d}{dt}(\lambda_r) - \omega_r \lambda_r \tag{2.2}$$

Where, $\omega_r = \frac{d}{dt}\theta_r$ is the speed of the rotor motor in electrical frequency unit and

$$\lambda_s = L_s i_s + L_m i_r \tag{2.3}$$

$$\lambda_r = L_r i_r + L_m i_s \tag{2.4}$$

The above 4 equations (2.1-2.4) constitute a dynamic model of the induction motor on a stationary stator reference frame in space vector form. These model equations may be simplified by eliminating flux linkages as:

$$v_s = R_s i_s + \frac{d}{dt}(L_s i_s + L_m i_r) \tag{2.5}$$

$$= (R_s + L_s p) i_s + L_m p i_r$$

$$0 = R_r i_r + \frac{d}{dt}(L_r i_r + L_m i_s) - \omega_r (L_r i_r + L_m i_s) \tag{2.6}$$

$$= (R_r + L_r(p - \omega_r)) i_r + L_m (p - \omega_r) i_s$$

From equation (2.5) and (2.6), the dynamic equivalent circuit model on a stationary reference frame can be drawn as in figure 2.4-2.

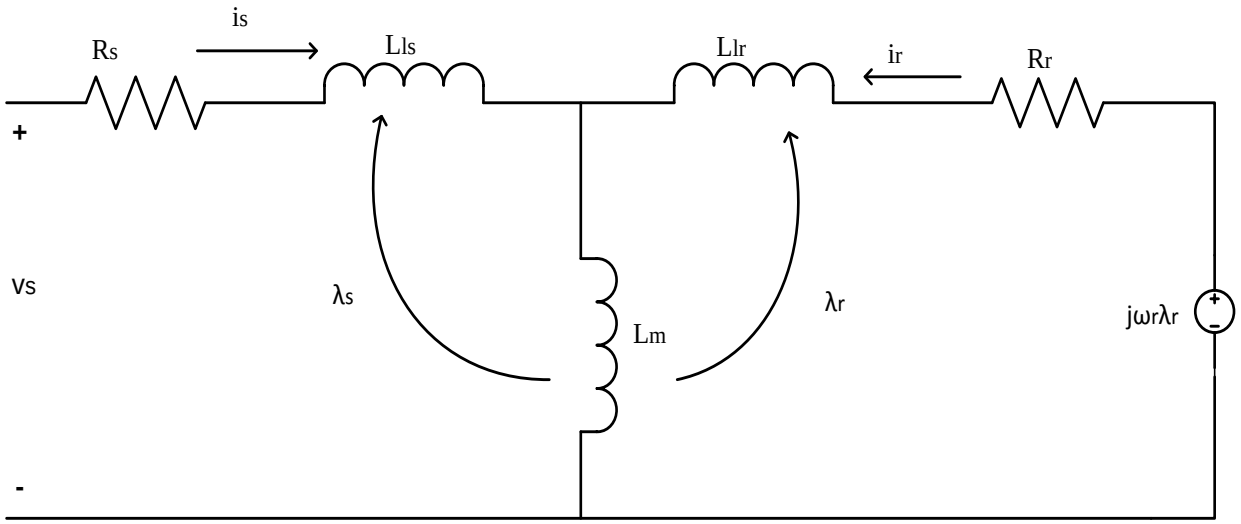

Figure 2.4-2 Dynamic Equivalent Circuit on a Stationary Reference Frame

For steady-state operation with excitation frequency ω_e, p in equation (2.5-2.6) may be replaced by $j\omega_e$ and after some algebraic manipulation, we get

$$v_s = (R_s + j\omega_e L_s)i_s + j\omega_e L_m i_r \quad (2.7)$$

$$v_r = 0 = (R_{r/s} + j\omega_e L_r)i_r + j\omega_e L_m i_s \quad (2.8)$$

This exactly describes the conventional steady-state equivalent circuit of figure 2.4-1. Now, the previous procedure can be generalized so that the dynamic model is described on an arbitrary reference frame rotating at a speed ω_a, where equation (2.1-2.8) is a special case with $\omega_a = 0$.

Depending on a specific choice of ω_a, many forms of dynamic equivalent circuit can be established. Among them, the synchronous frame form can be obtained by choosing $\omega_a = \omega_e$. This form is very useful in describing the concept of direct torque control of induction motors and PM synchronous motors because at this rotating frame, space vector is not rotating. Another possible reference frame used in direct torque control is the rotor reference frame by choosing $\omega_a = \omega_r$.

2.5 D-Q Reference Frame Transformation

The d–q–0 reference frame transformation has long been used successfully in the analysis and control of three-phase electric machines [4].The same approach is used for five-phase drive. The five-phase motor system as shown in figure 2.5-1, five-dimensional machine variables can be transformed into d_1-q_1 and d_3-q_3 reference frames and a zero sequence variables [20]. However; the d_3-q_3 components do not contribute to torque production in a sinusoidal distribution of the flux around the air-gap is assumed. A zero-sequence component does not exist in any star-connected multiphase system without neutral conductor for odd phase numbers, but only can exist if the phase number is even. Since rotor winding is short-circuited, zero-sequence components cannot exist. As stator to rotor coupling takes place only in d_1–q_1 equations, rotational transformation is applied only to these two pairs of equations. Its form is similar to a three-phase machine [4, 21].

The mathematical model of five-phase induction motor are transformed into a stationary (α-ß) and synchronous (d-q) reference frames. These reference frames are decoupled into the torque producing (fundamental component) and non-torque producing (third) harmonics sets. During operation of a five-phase VSI, it produces 32 space vectors in the d_1-q_1 and d_3-q_3 sub-spaces. The 30 space vectors are active space vectors and the two zero space vectors. Each active space vector maps simultaneously into both d_1-q_1 and d_3-q_3 sub-space. Large vectors of the d_1-q_1 plane map into small vectors of the d_3-q_3 plane, medium length vectors map into medium length vectors, while small vectors of the d_1-q_1 plane map into large vectors of the d_3-q_3 plane [16, 17].

The fundamental component and the harmonics of order $10k \pm 1$ (k = 0, 1, 2, 3...) are applied on the d_1-q_1 reference frame circuit in figure 2.5-1(a) to produce a rotating MMF and torque (harmonics produce torque pulsation). The harmonics of order $10k \pm 3$ (k = 0, 1, 2, 3...) which are applied onto the remaining d_3-q_3 frame in figure 2.5-1(b) [20]. These components can be represented by the following complex space vector on a stationary reference frame [15].

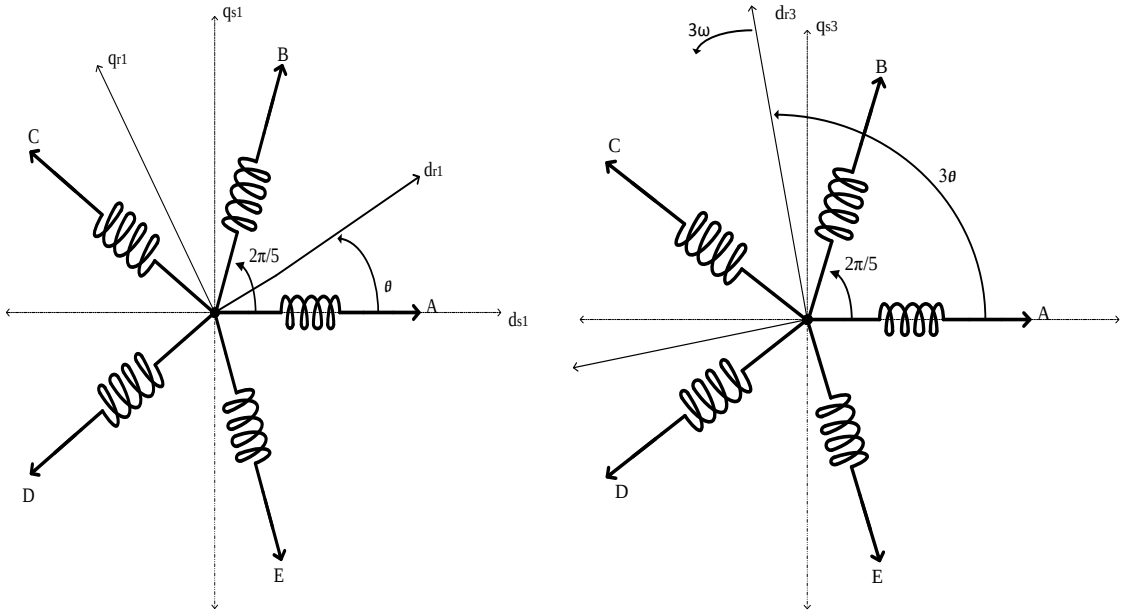

(a) d1-q1 frame (b) d3-q3 frame

Figure 2.5-1 Vector diagram of five-phase induction motor

As shown in figure 2.5-1 the stator of induction motor consists of five-phase balanced concentrated windings with each phase separated from each other by 72 degrees in space. When these current flow through these windings, five-phase rotating magnetic field is produced. This field rotates at synchronous speed in revolution per minute. By faraday's law, this rotating stator magnetic field induces voltages in the rotor windings causing balanced currents to flow in the short circuited rotor. As a result, a rotor MMF is formed. These output voltages can be transformed in to two axis coordinates by Clark and park transformation.

2.5.1 Clark and Park Transformation

The Clarke and Parke transformation is a transformation of coordinates that designed to transform multi-phase stationary coordinate system in to two axes stationary and rotating coordinate system respectively. Clarke transform uses five-phase voltages v_a, v_b, v_c, v_d and v_e to calculate voltages in the two-phase orthogonal stator axis, v_α and v_β. These two voltages in the fixed coordinate stator phase are transformed to the v_d and v_q voltage components in the d-q frame with the Park transform.

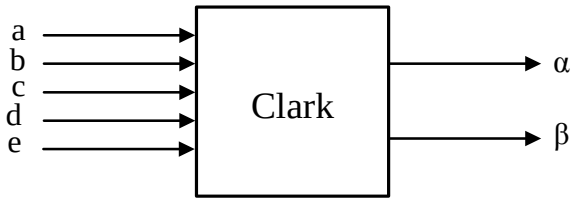

Figure 2.5-2 the (a, b, c, d, e) → (α-β) projection (Clarke transformation)

Park transformation is used to transform from the stationary reference frame (α-β) in to the rotating reference frame (d-q).

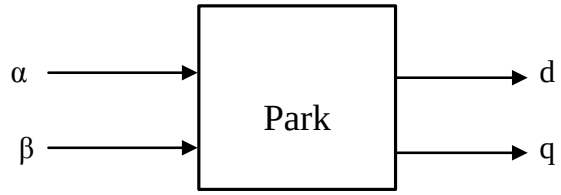

Figure 2.5-3 the (α-β) → (d-q) projection (Park transformation)

Considering squirrel-cage induction motor, the transformations are usually based on the following assumptions:

- Slot harmonics and deep bar effects are not considered.
- Space harmonics of the flux linkage distribution are neglected.
- Iron losses are not taken into account.
- Saturation is neglected.
- Neutral point is isolated.

2.5.2 Space Vector Definition

Assume v_a, v_b, v_c, v_d and v_e are the instantaneous balanced five-phase voltage:

$$v_a + v_b + v_c + v_d + v_e = 0 \quad (2.9)$$

Thus, it is possible to define the stator voltage space vector as follows [6, 20]:

$$v_{\alpha\beta 1} = k(v_a + av_b + a^2 v_c + a^{*2} v_d + a^* v_e) \quad (2.10)$$

$$v_{\alpha\beta 3} = k(v_a + a^{*2}v_b + av_c + a^{*}v_d + a^2 v_e) \quad (2.11)$$

Where $a,\ a^2,\ a^*,\ a^{*2}$ are the spatial operators

$$a = e^{j\frac{2\pi}{5}} \qquad a^2 = e^{j\frac{4\pi}{5}}$$

$$a^* = e^{j\frac{-2\pi}{5}} \qquad a^{*2} = e^{j\frac{-4\pi}{5}}$$

$$v_{\alpha\beta 1} = v_{\alpha_1} + jv_{\beta_1} \qquad v_{\alpha\beta 3} = v_{\alpha_3} + jv_3$$

K is the transformation constant, chosen as k = 2/5

The 32 space vectors are transformed into two orthogonal sub-spaces using equation (2.10) and (2.11) in the form of power variant. In other words, power per-phase in original and transformed domain is now kept constant, rather than the total power. The scaling factor is therefore set to $2/5$ rather than $\sqrt{2/5}$ [32]. This choice is more convenient in discussion of SVPWM, since it makes the magnitude of the reference voltage space vector equal to the peak value of the desired sinusoidal output phase voltage. The zero-sequence component is identically equal to zero because of the assumption of isolated neutral point.

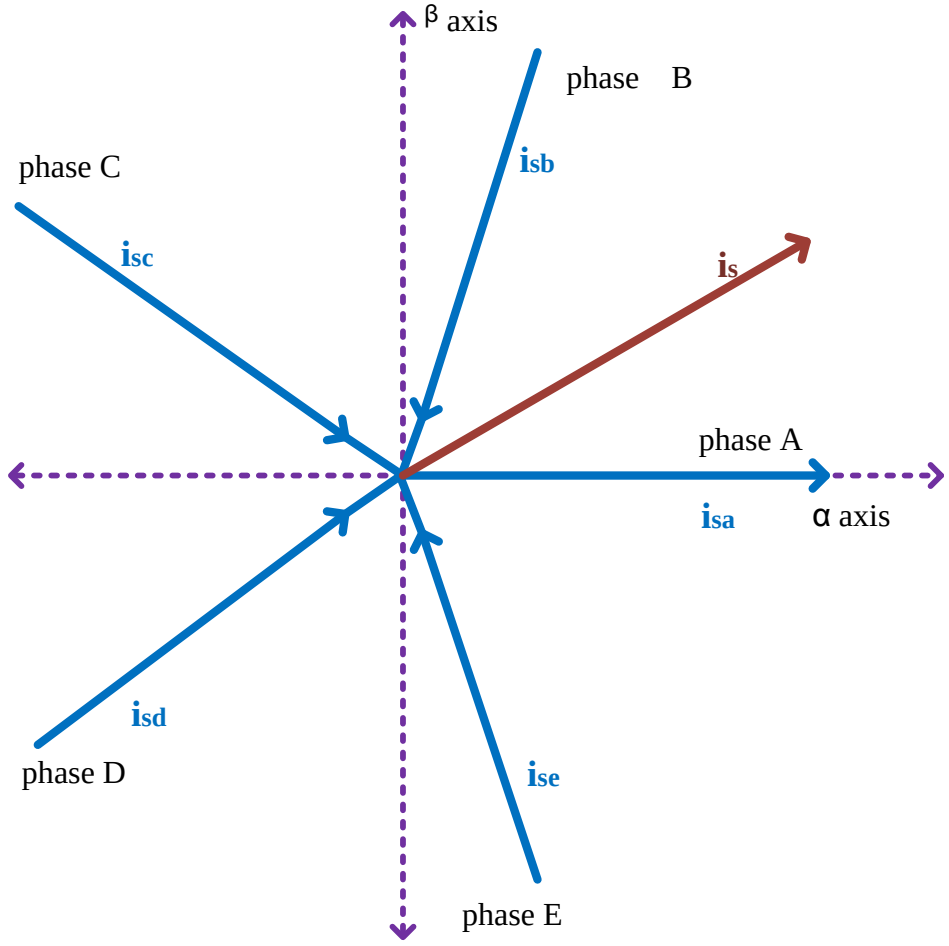

Figure 2.5-4 Stationary transformation of five dimensional axis to α-β axis

The transformation of five-phase induction motor variables can be made in two steps, these are:

i. Five-phase to two phase transformation
ii. Two phase stationary to two phase synchronously rotating frame transformation

I. Five-phase to two phase transformation

A transformation from the five-phase stationary coordinate system to the two-phase (α-β) stationary coordinate system is called Clarke Transformation. The idea of Clarke transformation is that the rotating stator current vector that is the sum of the five-phase currents can also be generated by a bi-phased system placed on the fixed axis α and β.

The space vector defined by equation (2.10) and (2.11) can be expressed utilizing two-axis theory. The real part of the space vector is equal to the instantaneous value of the direct-axis stator voltage component, v_α and whose imaginary part is equal to the quadrature-axis stator voltage component, v_β. Thus, the stator voltage space vector, in the stationary reference frame attached to the stator, can be expressed as [20]:

$$V_{\alpha\beta 1} = v_{\alpha_1} + jv_{\beta_1} \tag{2.12}$$

$$V_{\alpha\beta 3} = v_{\alpha_3} + jv_3 \tag{2.13}$$

In symmetrical five-phase machines with stationary *as-bs-cs-ds-es* axes at 72 degree apart as shown in figure 2.5-5, the alpha and beta axis stator voltages v_α and v_β are fictitious quadrature-phase (two-phase) voltage components, which are related to the actual five-phase stator voltages as follows [20, 25]:

$$\begin{aligned}
v_{\alpha 1} &= k(v_a + v_b * \cos\left(\frac{2\pi}{5}\right) + v_c * \cos\left(\frac{4\pi}{5}\right) + v_d * \cos\left(\frac{4\pi}{5}\right) + v_e * \cos\left(\frac{2\pi}{5}\right)) \\
v_{\beta 1} &= k(0 + v_b * \sin\left(\frac{2\pi}{5}\right) + v_c * \sin\left(\frac{4\pi}{5}\right) - v_d * \sin\left(\frac{4\pi}{5}\right) - v_e * \sin\left(\frac{2\pi}{5}\right) \\
v_{\alpha 3} &= k(v_a + v_b * \cos\left(\frac{6\pi}{5}\right) + v_c * \cos\left(\frac{2\pi}{5}\right) + v_d * \cos\left(\frac{2\pi}{5}\right) + v_e * \cos\left(\frac{6\pi}{5}\right) \\
v_{\beta 3} &= k(0 + v_b * \sin\left(\frac{6\pi}{5}\right) + v_c * \sin\left(\frac{2\pi}{5}\right) - v_d * \sin\left(\frac{2\pi}{5}\right) - v_e * \sin\left(\frac{6\pi}{5}\right)
\end{aligned} \tag{2.14}$$

In matrix form of the five-phase to two phase transformation of the stator voltage ((a, b, c, d, e) to (α-β)) is given as:

$$\begin{bmatrix} v_{\alpha 1} \\ v_{\beta 1} \\ v_{\alpha 3} \\ v_{\beta 3} \end{bmatrix} = \frac{2}{5} \begin{bmatrix} 1 & \cos\left(\frac{2\pi}{5}\right) & \cos\left(\frac{4\pi}{5}\right) & \cos\left(\frac{4\pi}{5}\right) & \cos\left(\frac{2\pi}{5}\right) \\ 0 & \sin\left(\frac{2\pi}{5}\right) & \sin\left(\frac{4\pi}{5}\right) & -\sin\left(\frac{4\pi}{5}\right) & -\sin\left(\frac{2\pi}{5}\right) \\ 1 & \cos\left(\frac{6\pi}{5}\right) & \cos\left(\frac{2\pi}{5}\right) & \cos\left(\frac{2\pi}{5}\right) & \cos\left(\frac{4\pi}{5}\right) \\ 0 & \sin\left(\frac{6\pi}{5}\right) & \sin\left(\frac{2\pi}{5}\right) & -\sin\left(\frac{2\pi}{5}\right) & \sin\left(\frac{4\pi}{5}\right) \end{bmatrix} \begin{bmatrix} v_a \\ v_b \\ v_c \\ v_d \\ v_e \end{bmatrix} \quad (2.15)$$

Similarly, for stator current the matrix forms of a five-phase to two phase transformation ((a, b, c, d, e) to (α-β)) is also given as:

$$\begin{bmatrix} i_{\alpha 1} \\ i_{\beta 1} \\ i_{\alpha 3} \\ i_{\beta 3} \end{bmatrix} = \frac{2}{5} \begin{bmatrix} 1 & \cos\left(\frac{2\pi}{5}\right) & \cos\left(\frac{4\pi}{5}\right) & \cos\left(\frac{4\pi}{5}\right) & \cos\left(\frac{2\pi}{5}\right) \\ 0 & \sin\left(\frac{2\pi}{5}\right) & \sin\left(\frac{4\pi}{5}\right) & -\sin\left(\frac{4\pi}{5}\right) & -\sin\left(\frac{2\pi}{5}\right) \\ 1 & \cos\left(\frac{6\pi}{5}\right) & \cos\left(\frac{2\pi}{5}\right) & \cos\left(\frac{2\pi}{5}\right) & \cos\left(\frac{4\pi}{5}\right) \\ 0 & \sin\left(\frac{6\pi}{5}\right) & \sin\left(\frac{2\pi}{5}\right) & -\sin\left(\frac{2\pi}{5}\right) & \sin\left(\frac{4\pi}{5}\right) \end{bmatrix} \begin{bmatrix} i_a \\ i_b \\ i_c \\ i_d \\ i_e \end{bmatrix} \quad (2.16)$$

Equations (2.15) and (2.16) are valid only for balanced system otherwise zero sequence components are introduced.

The simplified diagram of a five-phase induction motor in figure 2.5-5 shows the stator winding for each phase displaced $2\pi/5$ radians in space and their wave forms. The transformation of stator variables to a two-phase reference frame (indicated by subscripts α-β), where the coils are perpendicular, guarantees that there is no interaction between perpendicular windings as long as there is no saturation.

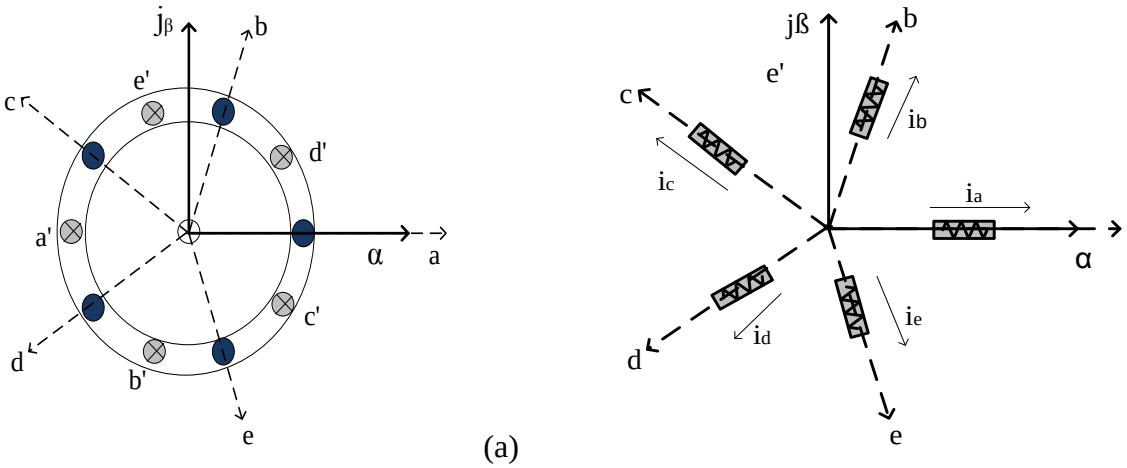

(a)

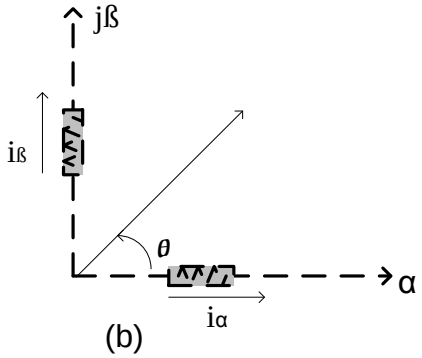

(b)

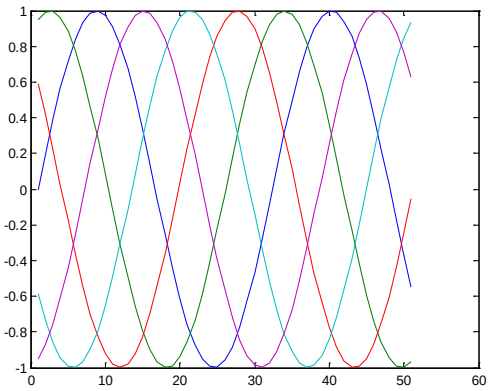

(c)

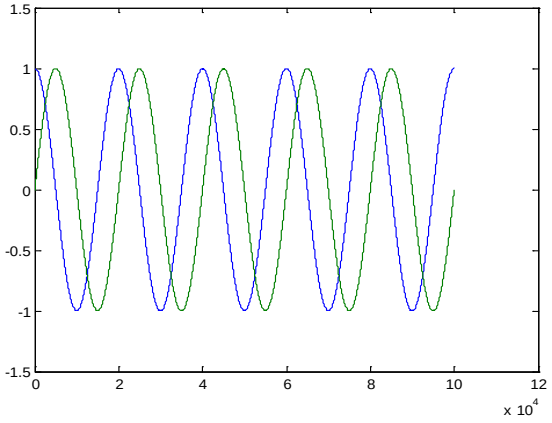

(d)

Figure 2.5-5 (a) five-phase windings, (b) two-phase axes equivalent (c) five-phase reference frame wave form and (d) two phase reference frame wave form

II. Two phase stationary to two phase synchronously rotating frame transformation

A transformation from the α-β stationary coordinate system to the d-q rotating coordinate system is called Park Transformation. The d-q reference frame is rotating at speed ω_e with respect to α-β axes as shown in figure 2.5-6. The angle between α and d axes is $\theta_e = \omega_e t$.

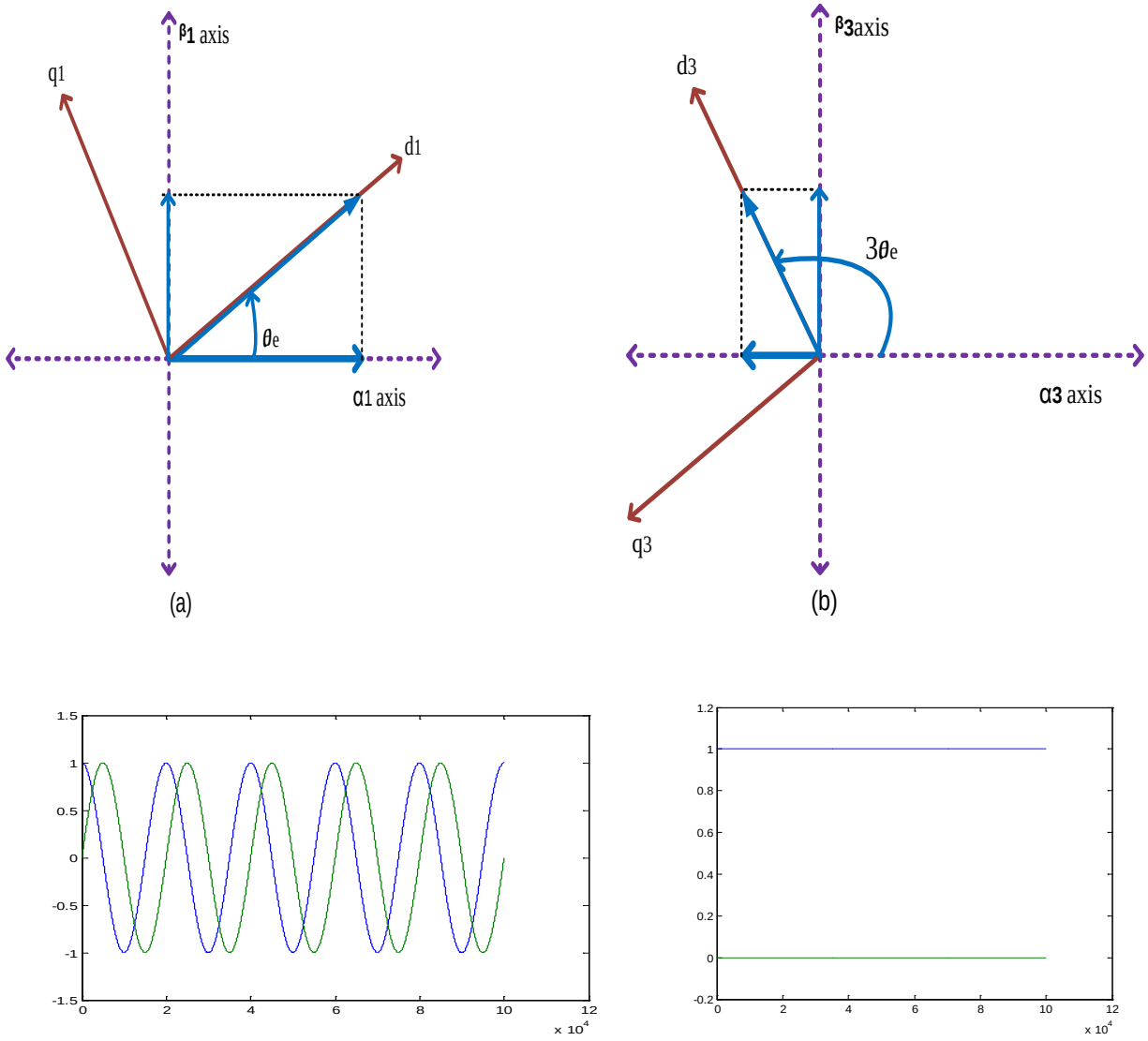

Figure 2.5-6 (a) d_1-q_1 reference frame, (b) d_3-q_3 reference frame, (c) two phase reference frame wave form and (d) rotating reference frame wave form

The voltage v_α, v_β can be converted to voltages on d-q axis according to the following relations:

$$v_{d1} = v_{\alpha1} * \cos(\theta_e) + v_{\beta1} * \sin(\theta_e) \quad (2.17)$$

$$v_{q1} = -v_{\alpha1} * \sin(\theta_e) + v_{\beta1} * \cos(\theta_e) \quad (2.18)$$

$$v_{d3} = v_{\alpha3} * \cos(3\theta_e) + v_{\beta3} * \sin(3\theta_e) \quad (2.19)$$

$$v_{q3} = -v_{\alpha3} * \sin(3\theta_e) + v_{\beta3} * \cos(3\theta_e) \quad (2.20)$$

In matrix form of the two phase stationary to two phase synchronously rotating frame transformation is given as:

$$\begin{bmatrix} v_{d1} \\ v_{q1} \\ v_{d3} \\ v_{q3} \end{bmatrix} = \begin{bmatrix} \cos(\theta_e) & \sin(\theta_e) & 0 & 0 \\ -\sin(\theta_e) & \cos(\theta_e) & 0 & 0 \\ 0 & 0 & \cos(3\theta_e) & \sin(3\theta_e) \\ 0 & 0 & -\sin(3\theta_e) & \cos(3\theta_e) \end{bmatrix} \begin{bmatrix} v_{\alpha1} \\ v_{\beta1} \\ v_{\alpha3} \\ v_{\beta3} \end{bmatrix} \quad (2.21)$$

In the reverse way; the transformation of rotating frame parameters to stationary frame is given according to the following relations:

$$v_{\alpha1} = v_{d1} * cos(\theta_e) - v_{q1} * sin(\theta_e)$$

$$v_{\beta1} = v_{d1} * sin(\theta_e) + v_{q1} * cos(\theta_e)$$

$$v_{\alpha3} = v_{d3} * cos(3\theta_e) - v_{q3} * sin(3\theta_e) \quad (2.22)$$

$$v_{\beta3} = v_{d3} * sin(3\theta_e) + v_{q3} * cos(3\theta_e)$$

In matrix form representation is given as:

$$\begin{bmatrix} v_{\alpha1} \\ v_{\beta1} \\ v_{\alpha3} \\ v_{\beta3} \end{bmatrix} = \frac{2}{5} \begin{bmatrix} \cos(\theta_e) & -\sin(\theta_e) & 0 & 0 \\ \sin(\theta_e) & \cos(\theta_e) & 0 & 0 \\ 0 & 0 & \cos(3\theta_e) & -\sin(3\theta_e) \\ 0 & 0 & \sin(3\theta_e) & \cos(3\theta_e) \end{bmatrix} \begin{bmatrix} v_{d1} \\ v_{q1} \\ v_{d3} \\ v_{q3} \end{bmatrix} \quad (2.23)$$

The general Park transformation v_d and v_q can be also obtained directly from v_a, v_b, v_c, v_d and v_e. The matrix equation corresponding to this transformation is given as [25].

$$\begin{bmatrix} v_{d1} \\ v_{q1} \\ v_{d3} \\ v_{q3} \end{bmatrix} = \frac{2}{5} \begin{bmatrix} \cos(\theta_e) & \cos\left(\theta_e - \frac{2\pi}{5}\right) & \cos\left(\theta_e - \frac{4\pi}{5}\right) & \cos\left(\theta_e - \frac{6\pi}{5}\right) & \cos\left(\theta_e - \frac{8\pi}{5}\right) \\ -\sin(\theta_e) & -\sin\left(\theta_e - \frac{2\pi}{5}\right) & -\sin\left(\theta_e - \frac{4\pi}{5}\right) & -\sin\left(\theta_e - \frac{6\pi}{5}\right) & -\sin\left(\theta_e - \frac{8\pi}{5}\right) \\ \cos(3\theta_e) & \cos\left(3(\theta_e - \frac{2\pi}{5})\right) & \cos\left(3(\theta_e - \frac{4\pi}{5})\right) & \cos\left(3(\theta_e - \frac{6\pi}{5})\right) & \cos\left(3(\theta_e - \frac{8\pi}{5})\right) \\ -\sin(3\theta_e) & -\sin\left(3(\theta_e - \frac{2\pi}{5})\right) & -\sin\left(3(\theta_e - \frac{6\pi}{5})\right) & -\sin\left(3(\theta_e - \frac{6\pi}{5})\right) & -\sin\left(3(\theta_e - \frac{8\pi}{5})\right) \end{bmatrix} \begin{bmatrix} v_a \\ v_b \\ v_c \\ v_d \\ v_e \end{bmatrix} \quad (2.24)$$

Since the actual stator variables either to be generated or to be measured are all in stationary a-b-c-d-e frame, synchronous frame transform should be executed in the control. The most popular transform between stationary a-b-c-d-e frame quantities to synchronously rotating d-q quantities is given in equation (2.24).

2.5.3 D-Q Dynamic Model of Induction Motor in the Synchronous Frame

The mathematical model of IM variables such as: stator voltage, rotor voltage, stator flux linkage and rotor flux linkage are represented in the synchronous reference frame [6, 30].

The stator voltage equations:

$$v_{ds1} = R_s * i_{ds1} + \frac{d}{dt}(\lambda_{ds1}) - \omega_e \lambda_{qs1} \quad (2.25)$$

$$v_{qs1} = R_s * i_{qs1} + \frac{d}{dt}(\lambda_{qs1}) + \omega_e \lambda_{ds1} \quad (2.26)$$

$$v_{ds3} = R_s * i_{ds3} + \frac{d}{dt}(\lambda_{ds3}) - 3\omega_e \lambda_{qs3} \quad (2.27)$$

$$v_{qs3} = R_s * i_{qs3} + \frac{d}{dt}(\lambda_{qs3}) + 3\omega_e \lambda_{ds3} \quad (2.28)$$

The rotor voltage equations:

$$v_{dr1} = 0 = R_r * i_{dr1} + \frac{d}{dt}(\lambda_{dr1}) - (\omega_e - \omega_r)\lambda_{qr1} \quad (2.29)$$

$$v_{qr1} = 0 = R_r * i_{qr1} + \frac{d}{dt}(\lambda_{qr1}) + (\omega_e - \omega_r)\lambda_{dr1} \quad (2.30)$$

$$v_{dr3} = 0 = R_r * i_{dr3} + \frac{d}{dt}(\lambda_{dr3}) - 3(\omega_e - \omega_r)\lambda_{qr3} \quad (2.31)$$

$$v_{qr3} = 0 = R_r * i_{qr3} + \frac{d}{dt}(\lambda_{qr3}) + 3(\omega_e - \omega_r)\,\lambda_{dr3} \quad (2.32)$$

The stator flux linkages equations:

$$\lambda_{ds1} = L_s i_{ds1} + L_m i_{dr1} \quad (2.33)$$

$$\lambda_{qs1} = L_s i_{qs1} + L_m i_{qr1} \quad (2.34)$$

$$\lambda_{ds3} = L_s i_{ds3} + L_m i_{dr3} \quad (2.35)$$

$$\lambda_{qs3} = L_s i_{qs3} + L_m i_{qr3} \quad (2.36)$$

The rotor flux linkages equations:

$$\lambda_{dr1} = L_r i_{dr1} + L_m i_{ds1} \quad (2.37)$$

$$\lambda_{qr1} = L_r i_{qr1} + L_m i_{qs1} \quad (2.38)$$

$$\lambda_{dr3} = L_{lr} i_{dr3} + L_m i_{ds3} \quad (2.39)$$

$$\lambda_{qr3} = L_{lr} i_{qr3} + L_m i_{qs3} \quad (2.40)$$

Where λ_{ds}, λ_{qs}: d-axis and q-axis stator flux linkages

λ_{dr}, λ_{qr}: d-axis and q-axis rotor flux linkages

R_s, R_r: Stator and rotor resistance

v_{ds}, v_{qs}: d-axis and q-axis stator voltage

v_{dr}, v_{qr}: d-axis and q-axis rotor voltage

i_{ds}, i_{qs}: d-axis and q-axis stator current

i_{dr}, i_{qr}: d-axis and q-axis rotor current

ω_e, ω_r: synchronous speed and rotor speed

L_{ls}, L_{lr}, L_m : Stator self inductance, rotor self inductance and mutual inductance respectively.

Figure 2.5-7 shows a dynamic equivalent circuit of an induction machine based on equation (2.25) through (2.40) [11].

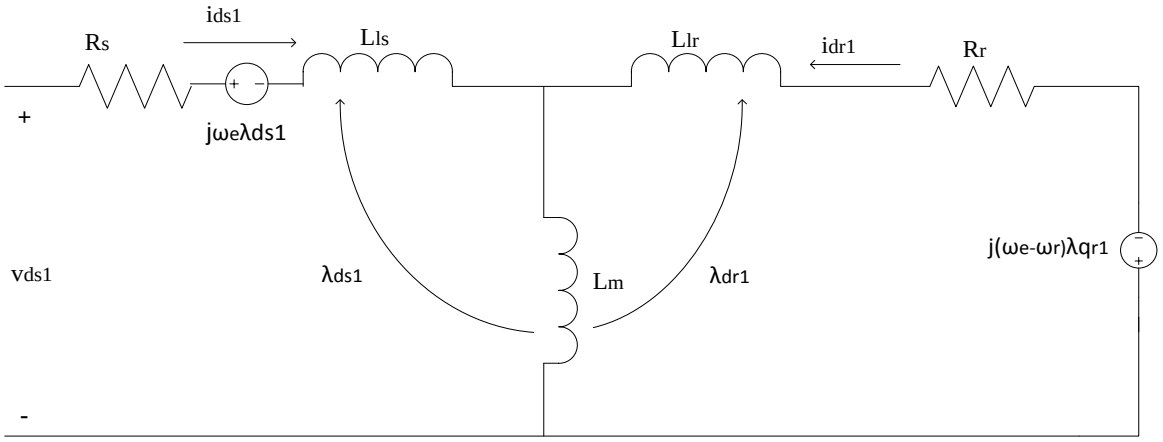

(a)

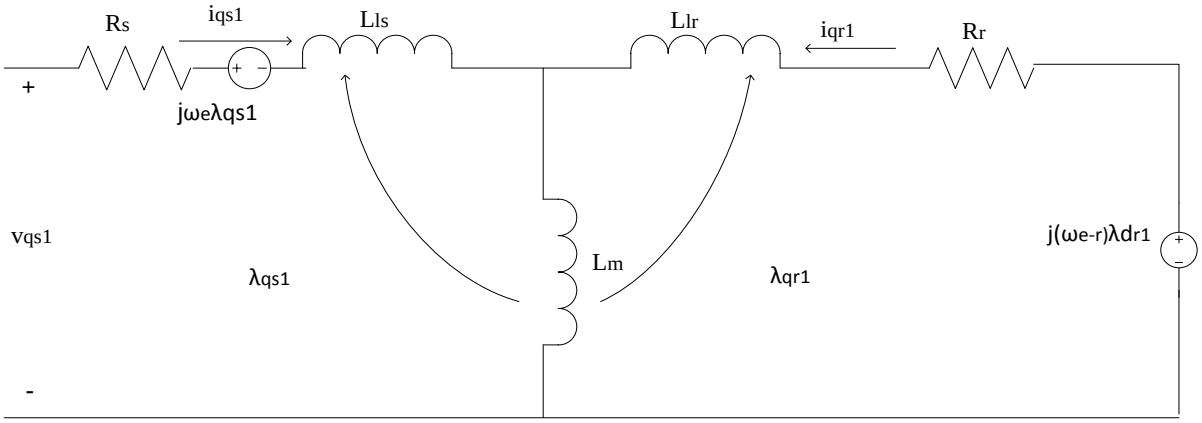

(b)

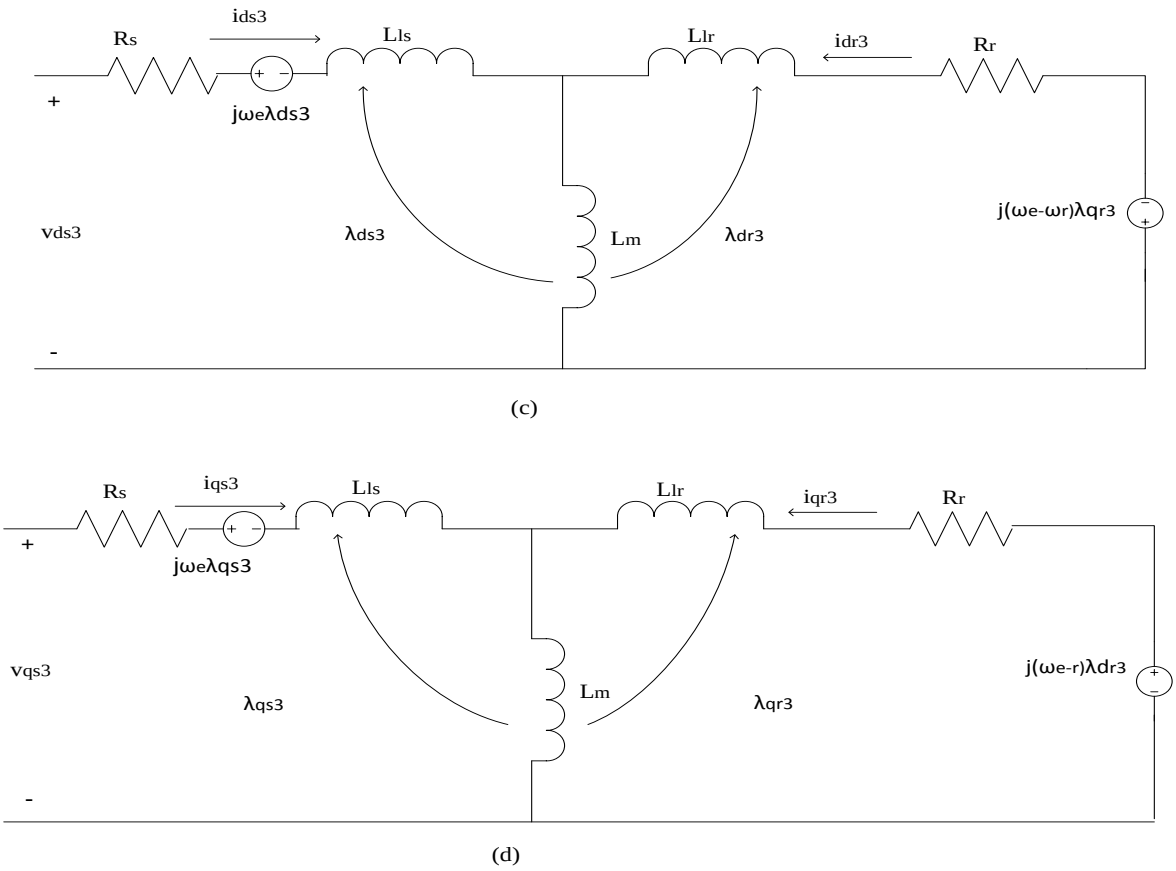

Figure 2.5-7 Dynamic Equivalent Circuits on a Synchronous Reference Frame

The d-q space vector method is generally used to describe the model of the induction motor. The advantage of this method is as follows:

- Reduction of the number of dynamic equations,
- Possibility of analysis at any supply voltage waveform,
- The equations can be represented in various rectangular coordinate systems.

2.6 Direct Torque Control of Induction Motor

It is one of the most excellent and efficient control strategies of induction motor. This technique is based on decoupled control of torque and stator flux and today it is one of the most actively researched control techniques where the aim is to control effectively the torque and flux.

2.6.1 Principle of DTC Scheme

The basic functional blocks used to implement the DTC-SVM scheme is shown in figure 2.6-1. Three phase AC supply is given to the diode bridge rectifier which produces a DC voltage. A high value dc link capacitor is used to reduce the ripple content in the DC voltage. The filtered DC is the power supply to the inverter switches. The IGBT inverter switches are controlled by the space vector modulation algorithm. The output of the inverter is connected to the stator terminals of induction motor [8].

In the proposed system, flux and torque estimators are used to determine the actual value of the flux linkage and torque. Instead of the switching table and hysteresis controllers in conventional DTC, a PI controller and numeric calculation are used to determine the duration time of voltage vectors, such that the error vector in flux and torque can be fully compensated. Four proportional integral (PI) type controllers regulate the flux and torque error. Since the controllers produce the voltage command vector, appropriate space voltage vector can be generated with SVM and fixed switching frequency can be achieved. The output of the PI flux and torque controllers can be interpreted as the reference stator voltage components in d-q co-ordinate system. These DC voltage commands are then transformed into stationary frame α-β, the command values are delivered to SVM block. The SVM block performs the space vector modulation of V_{ref} to obtain the gate drive pulses for the inverter circuit [8].

Thus, the basic principle of DTC is to directly select stator voltage vectors according to the torque and flux errors which are the differences between the references torque and stator flux linkage and their actual values. The governing equation for torque for this scheme is due to the cross-product of stator flux linkage and stator current space vectors. The torque and stator flux linkage equations are computed from measured motor terminal quantities that is, stator voltages and currents. An optimal voltage vector for the switching of VSI is selected among the thirty nonzero voltage vectors and two zero voltage vectors by the space vector modulation algorithm. In order to control the voltage reference vector, controlling of the stator flux and torque is required.

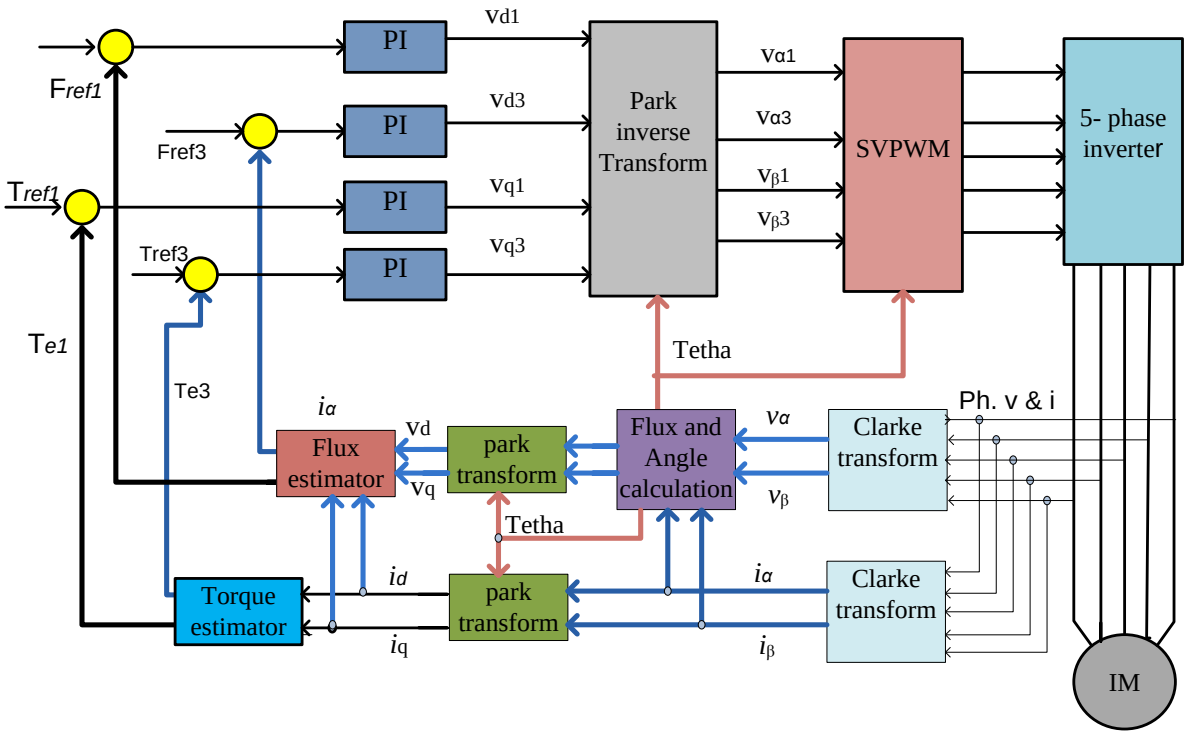

Figure 2.6-1 Schematic of proposed DTC-SVM

2.6.2 Stator Flux Control

The stator flux linkage of the induction motor can be controlled easily by controlling the direct and quadrature stator voltages which are taken from the output of the inverter. From the stator voltage equation (2.25), the stator flux equation can be derived. However; the stator resistance can be assumed constant during a large number of converter switching periods T_s. The voltage vector applied to the induction motor remains also constant during one period T. Thus, the stator flux is estimated by integrating the difference between the input voltage and the voltage drop across the stator resistance as given by equations(2.41)- (2.44) [18].

$$\lambda_{ds1} = \int_0^t (v_{ds1} - R_s i_{ds1})\, dt \qquad (2.41)$$

$$\lambda_{qs1} = \int_0^t (v_{qs1} - R_s i_{qs1})\, dt \qquad (2.42)$$

$$\lambda_{ds3} = \int_0^t (v_{ds3} - R_s i_{ds3})\, dt \tag{2.43}$$

$$\lambda_{qs3} = \int_0^t (v_{qs3} - R_s i_{qs3})\, dt \tag{2.44}$$

Where, $\lambda_{ds} = \lambda_{ds1} + \lambda_{ds3}$

$$\lambda_{qs} = \lambda_{qs1} + \lambda_{qs3}$$

$$i_{ds} = i_{ds1} + i_{ds3}$$

$$i_{qs} = i_{qs1} + i_{qs3}$$

The stator flux linkage phasor and angle is given by

$$\lambda_s = \sqrt{{\lambda_{ds}}^2 + {\lambda_{qs}}^2} \tag{2.45}$$

$$\theta = \tan^{-1}(\frac{\lambda_{qs}}{\lambda_{ds}}) \tag{2.46}$$

Where, $\lambda_{ds}, v_{ds}, i_{ds}$ and $\lambda_{qs}, v_{qs}, i_{qs}$ are the d-axis and q-axes quantities of stator flux linkage space vector, stator voltage space vector and stator current space vector component respectively. By comparing the sign of the components stator flux (λ_{ds} & λ_{qs}) and the amplitude of stator flux, can be localize the sector of the reference stator voltage vector [23, 24].

2.6.3 Direct Torque Control

Torque is estimated as a cross product of estimated stator flux linkage vector and measured motor current vector. The estimated torque is then compared with their reference values. The total electromagnetic torque of five-phase IM is the sum of the first harmonic and third harmonic torqe [10].

The electromagnetic torque is given by

$$T_{e1} = \left(\frac{5}{2}\right)\left(\frac{P}{2}\right)\left(\lambda_{ds1} i_{sq1} - \lambda_{qs1} i_{ds1}\right) \tag{2.47}$$

$$T_{e3} = (3)\left(\frac{5}{2}\right)\left(\frac{P}{2}\right)\left(\lambda_{ds3} i_{qs3} - \lambda_{qs3} i_{ds3}\right) \quad (2.48)$$

$$T_e = T_{e1} + T_{e3} \quad (2.49)$$

The mechanical equation is given by

$$T_e = T_L + J\frac{d\omega}{dt} + B\omega \quad (2.50)$$

2.7 PI Controller

PI or two term controllers are the most widely used controllers in industries today. The name PI

Comprises the first letter P stands for Proportional term in the controller and I stands for the Integral term in the controller. PI controller is applied in speed, torque, current and position control.

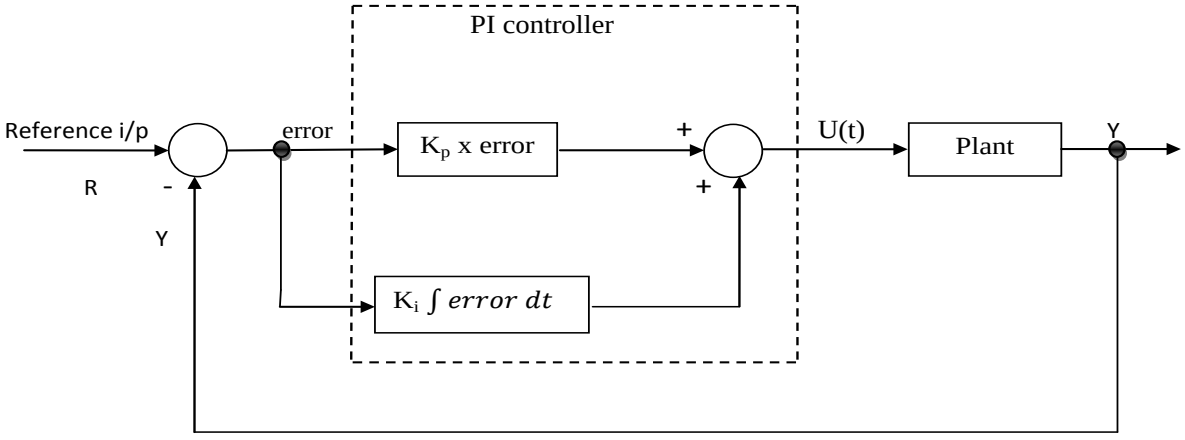

Figure 2.7-1 PI controller

The expression of PI control in time domain is:

$$u(t)=K_p\ [R(t) - Y(t)\ ]+K_i \int_0^t [R(t) - Y(t)\ ]dt$$

$$u(t)=K_p e(t) + K_i \int_0^t e(t)dt \quad (2.51)$$

Where: *u(t)* is the controller's output signal

e(t) is the controller's input error signal

K_p is proportional control gain

K_i is integral control gain

The Laplace transform of equation (2.51) and the structure of PI controller will be given as:

$$U(s) = K_p E(s) + \frac{K_i}{s} E(s) = E(s)\left(K_p + \frac{K_i}{s}\right) \qquad (2.52)$$

$$D(s) = \frac{U(s)}{E(s)} = K_p + \frac{K_i}{s} = \frac{K_p s + K_i}{s}$$

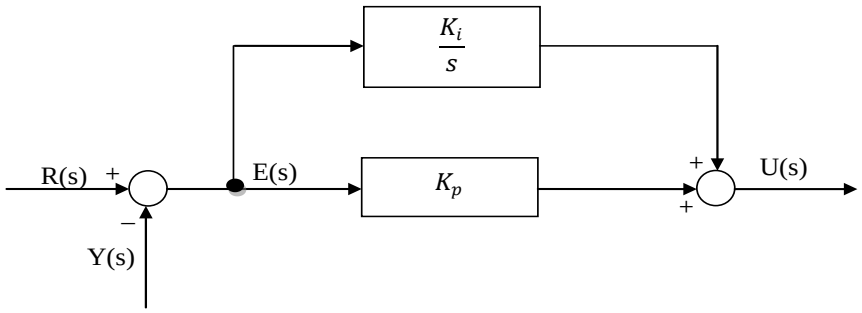

Figure 2.7-2 structure of PI control

A proportional controller (K_p) will have the effect of reducing the rise time and will reduce, but never eliminate the steady state error. If K_p is increasing the stead state error will be decreased but may cause the controller signal to be large which may lead to saturation or limiting problems with the system actuator. An integral control (K_i) will have the effect of eliminating the steady state error, but it may make the transient response worse [25].

2.7.1 Controller Design

Four PI controllers have been used in this thesis. Two torque controller and two flux controller are designed. The PID controller performs especially well when the system has first order

dynamics (a single pole). PI controller is a type of state-feedback controller. And in general, for the system with first-order dynamics the PI control is sufficient, and the D is not needed [26].

The direct synthesis technique is used to calculate the controller parameters based on the knowledge of the process model. It simply attempts to find a controller that gives desired closed-loop transfer function.

If $\tilde{G}$ is the approximated process model and $\left(\frac{Y}{Y_{sp}}\right)_d$ is the desired closed loop transfer function, the expression for the controller will be given by equation 2.53 [27].

$$G_c = \frac{1}{\tilde{G}}\left(\frac{\left(\frac{Y}{Y_{sp}}\right)_d}{1-\left(\frac{Y}{Y_{sp}}\right)_d}\right) \qquad (2.53)$$

The specification of $\left(\frac{Y}{Y_{sp}}\right)_d$ is the key design decision and will be considered during the design. Ideally, we would like the closed loop transfer function to have the value of unity so that the controlled variable tracks set-point changes instantaneously without any error. However, this ideal situation, called perfect control, cannot be achieved by feedback control because the controller does not respond until the error is detected. For processes without time delays; the reasonable first-order model is given by

$$\frac{Y}{Y_{sp}} = \frac{1}{\tau_c S+1} \qquad (2.54)$$

Where: τ_c is the desired closed-loop time constant. Substituting this expression in the above equation and solving the controller transfer function becomes:

$$G_c = \frac{1}{\tilde{G}}\left(\frac{1}{\tau_c s}\right) \qquad (2.55)$$

2.7.2 Torque PI Controller Design

The transfer function of the PI controller is given by:

$$G_c(s) = K_p + K_i$$

$$G_c(s) = K_p\left(1 + \frac{1}{\tau_i s}\right) \qquad (2.56)$$

From the expression we can see that K_p / τ_i is the gain of the integral controller and K_p is the gain of the proportional controller.

The electromagnetic torque which is given in equation (2.47) has direct relationship with the q-axis stator current. In order to relate q-axis stator voltage V_{qs} with the electromagnetic torque, first we have to analyze the relationship between the q-axis stator current and q-axis stator voltage. From the mathematical model in equation (2.26) and (2.28), equation (2.56) and (2.57) are given as follows:

$$I_{qs1} = \frac{K_{q1}V_{qs1}}{1 + \tau_{q1}s} - f\left(I_{qr1}, \omega_{e1}, \lambda_{ds1}\right) \qquad (2.56)$$

$$I_{qs3} = \frac{K_{q1}V_{qs3}}{1 + \tau_{q3}s} - f\left(I_{qr3}, \omega_{e3}, \lambda_{ds3}\right) \qquad (2.57)$$

Thus, the closed loop transfer function of the electromagnetic torque is given by equation (2.58) and equation (2.59)

$$T_{e1} = G_p = \frac{K_{T1}}{1+\tau_{q1}s}V_{qs1} - f(I_{qr1},\ \omega_{e1}, \lambda_{ds1}, I_{dr1}) \qquad (2.58)$$

$$T_{e3} = G_p = \frac{K_{T3}}{1+\tau_{q3}s}V_{qs3} - f(I_{qr3},\ \omega_{e3}, \lambda_{ds3}, I_{dr3}) \qquad (2.59)$$

Where: K_T is the plant gain and τ_q is the plant time constant and are given by the following expressions.

$$K_{T1} = K_{m1}K_{q1}\,, \qquad K_{m1} = \left(\frac{5}{2}\right)\left(\frac{p}{2}\right)L_m i_{dr}$$

$$K_{q1} = \frac{1}{R_s}, \qquad \tau_{q1} = \frac{L_s}{R_s}$$

And the simplified block diagram representation with PI controller will be shown in figure 2.7-3

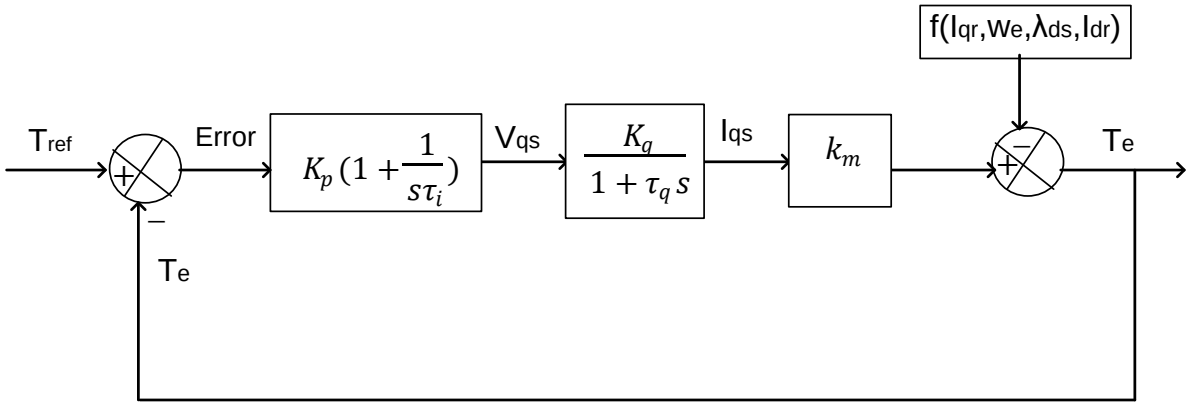

Figure 2.7-3 Electromagnetic torque PI controller block diagram

In the block diagram representation the $f(I_{qr},\ \omega_e, \lambda_{ds}, I_{dr})$ block which is summation of more than two terms makes the closed loop transfer function too complicated. For simplicity of PI controller parameter calculation, this part of the block diagram is ignored. Its effect is compensated by tuning the controller parameter after performing the design calculation. The first order desired closed loop transfers function from the reference input to the plant and the expressions for the PI controller settings using the direct synthesis technique are given by equation (2.58).

$$\frac{G_p(s)G_c(s)}{1+G_p(s)G_c(s)} = \frac{T_e}{V_{qsref}} = \left(\frac{Y}{Y_{sp}}\right)_d = \frac{1}{\tau_c s+1} \tag{2.58}$$

$$G_c(s) = K_p\left(1+\frac{1}{s\tau_i}\right), \text{ and } \quad G_p = \frac{K_T}{1+\tau_q s}$$

$$K_p = \frac{1}{K_T}\frac{\tau_q}{\tau_c} \quad , \quad \tau_i = \tau_q$$

By adjusting the closed loop transfer function to have a time constant $\tau_c = 0.01$ seconds the settings for the proportional controller and integral controller will be

$$K_p = 7.291, K_i = 114.286 \text{ and } \tau_i = 0.0638$$

2.7.3 Flux PI Controller Design

The closed loop transfer function of the stator direct axis flux from the state space model of the induction motor in equation (2.25), (2.33), (2.37) is given by expression in equation (2.59).

$$\lambda_{ds1} = G_p(s) = \frac{K_{\lambda 1}}{\tau_{\lambda 1} S+1} V_{ds1} - f(i_{dr1}, \lambda_{qs1,} \omega_e) \quad (2.59)$$

$$\lambda_{ds3} = G_p(s) = \frac{K_{\lambda 3}}{\tau_{\lambda 3} S+1} V_{ds3} - f(i_{dr3}, \lambda_{qs3,} \omega_e) \quad (2.60)$$

$$K_{\lambda 1} = \tau_{\lambda 1} = \frac{L_s}{R_s} = 0.0638, \quad \text{and} \quad K_{\lambda 3} = \tau_{\lambda 3} = \frac{L_s}{R_s} = 0.0638$$

And by following exactly the same design criteria in PI torque controller the settings for the flux controller is given by

$$K_p = 100, K_i = 1567.4 \text{ and } \tau_i = 0.0638$$

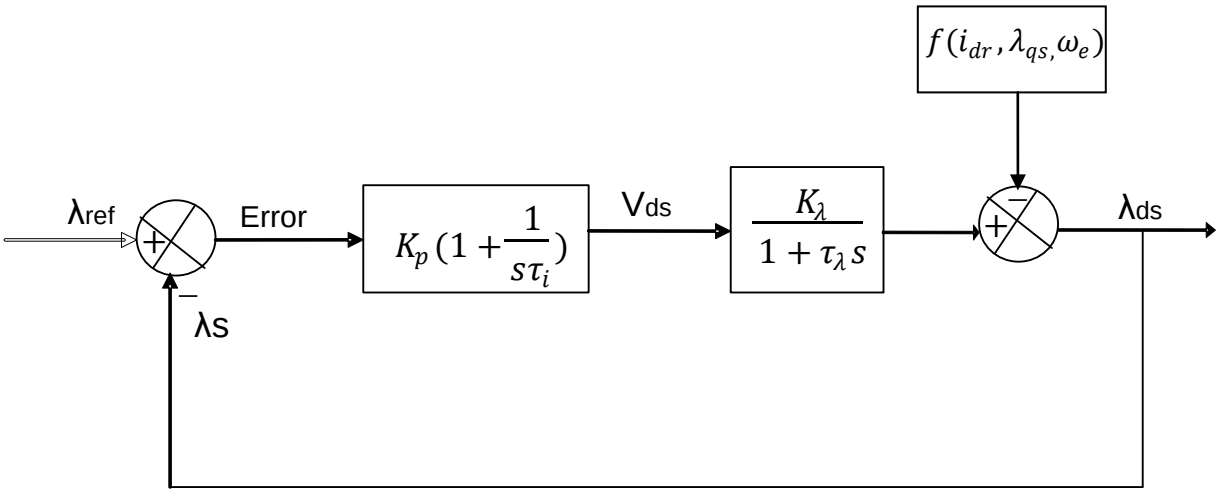

Figure 2.7-4 Flux PI controller block diagram

Chapter Three

Space Vector PWM of Five-phase Voltage Source Inverter

3.1 Introduction

Theory of Space vector pulse width modulation; when three phase supply is given to the stator of the induction machine a three phase rotating magnetic field is produced. Due to this field flux, a three phase rotating voltage vector is generated which lags the flux by 90^0. This field can also be realized by a logical combination of the inverter switching which is the basic concept of SVPWM [13].

Space vector pulse width modulation has become one of the most popular PWM techniques because of its easier digital implementation and better dc bus utilization, when compared to the ramp-comparison sinusoidal PWM method. SVPWM for three-phase voltage source inverter has been extensively discussed in the literature and. However, for multi-phase VSIs, there are only application specific SVPWM techniques available in the literature and more research work is needed in this area. There is a lot of flexibility available in choosing the proper space vector combination for an effective control of multi-phase VSIs because of large numbers of space vectors. With reference to five-phase VSI, there are a very few journal papers found in the literature. In this research the large space vector of SVPWM schemes for five-phase VSI are formulated and elaborated.

3.2 Voltage Source Inverter

The process of converting DC to AC power is called inversion. Inverter is an electronic device which creates the variable frequency from the fixed DC source in order to drive an induction motor at a variable speed. Depending on the type of DC source supplying the inverter; it can be classified as voltage source inverters (VSI) and current source inverters (CSI).

The DC source is usually rectified from the three phase input power. There is a DC link connected between the rectifier and the inverter. A capacitive-output DC link is used for a VSI

and an inductive output link is employed in CSI. The circuit diagram for a two-level voltage source inverter for power applications is shown in figure 3.2-1.

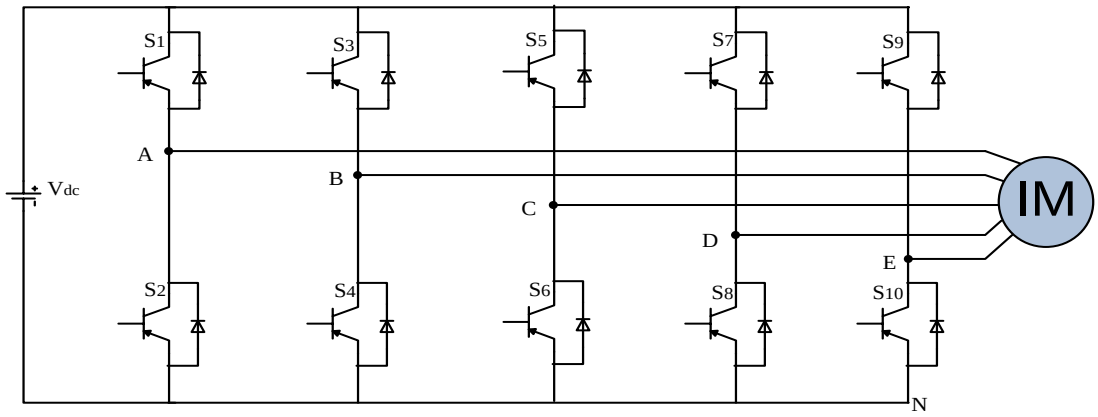

Figure 3.2-1 Five-phase voltage source inverter power circuit

A basic five-phase VSI is a ten step bridge inverter, consisting of minimum ten power electronics switches. Each switch in the circuit consists of two power semiconductor devices, connected in anti-parallel. One of these is a fully controllable semiconductor, such as a IGBT, while the second one is a diode. A step can be defined as the change in firing from one switch to the next switch in proper sequence. For a ten step inverter each step is 36^0 intervals for one cycle of 360^0. That means the switches would be gated at regular intervals of 36^0 in proper sequence to get a five-phase AC output voltage at the output terminal of VSI.

The ten switches are divided into two groups; upper five switches as positive group (i.e. S1, S3, S5, S7, S9) and lower five as negative group of switches (i.e. S2, S4, S6, S8, S10). There are two possible conduction modes to the switches such as [28]:

1) 180^0 conduction mode and
2) 72^0 conduction mode.

In each pattern the gating signals are applied and removed at an interval of 36^0 of the output voltage waveform.

3.2.1 Five-phase 180^0 Degree Conduction Mode VSI

By referring to figure 3.2-1, each switch conducts for 180^0 of a cycle. Switch pair in each arm, i.e. S_1-S_2; S_3-S_4; S_5-S_6; S_7-S_8 and S_9-S_{10} are turned on with a time interval of 180^0. It means that S_1 conducts for 180^0 and S_2 for the next 180^0.

In the ten-step 180^0conduction mode of operation, five switches are on at a time, two from positive group and three from negative group or vice versa, each switch conducts for 180^0 of a cycle. But no two switches of the same leg should be turned on simultaneously in both cases as this condition would short circuit the DC source.

3.2.2 Five-phase 72^0 Degree Conduction Mode VSI

The power circuit diagram of this inverter is the same as shown in figure 3.2-1for the 72 degree mode VSI, each switch conducts for 72^0 of a cycle. Like 180^0 mode, 72^0 mode inverter also require ten steps, each of 36^0duration for completing one cycle of the output AC voltage.

As shown in figure 3.2-2 below; in the conduction mode 72^0 S_1 conducts with S_6 for 36^0 then conducts with S_8 for another 36^0. S_3 will conducts for 72^0 (from 72^0 to144^0) 36^0 (from 72^0 to 108^0) with S_8 and then conducts another 36^0 (from 108^0 to 144^0) with S_{10}. S_5 will conducts 72^0 (from 144^0 to 216^0) with S_{10} for 36^0 (from $144^0$to 180^0) and then conducts for another 36^0 (from 180^0 to 216^0) with S_2. S_7 will conducts 72^0 (from 216^0 to 288^0) with S_2 for 36^0 (from 216^0 to 252^0) and then conducts for another 36^0 (from 252^0 to 288^0) with S_4. S_9 will conducts 72^0 (from 288^0 to 360^0) with S_4 for 36^0 (from 288^0 to 324^0) and then conducts for another 36^0 (from 324^0 to 360^0) with S_6. Simply, the72^0 conduction mode sequence can be written as follows:-

S_6 S_1, S_1 S_8, S_8 S_3, S_3 S_{10}, S_{10} S_5, S_5 S_2, S_2 S_7, S_7 S_4, S_4 S_9, S_9 $S_6$and S_6 S_1

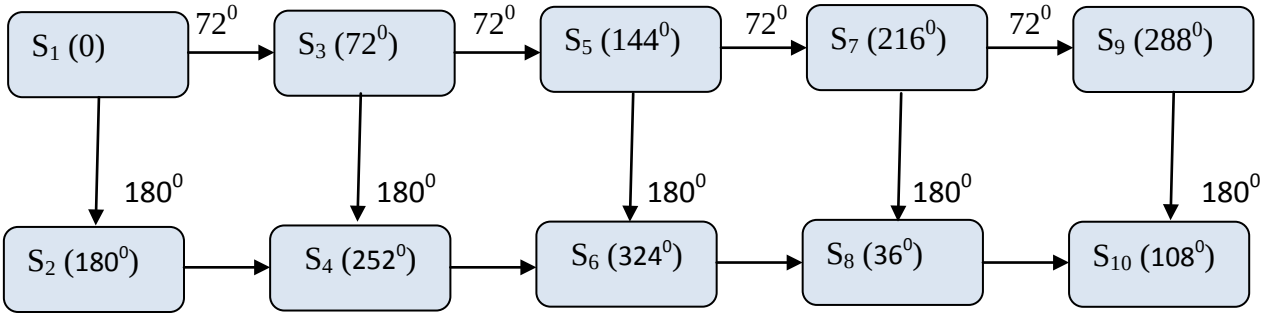

Figure 3.2-2 Five-Phase 72^0 Degree conduction Mode VSI

In this conduction mode the chances of short circuit of the DC link voltage source is avoided as each switch conduct for 72^0 in one cycle, so there is an interval of 36^0 in each cycle when no switch is in conduction mode and the output voltage at this time interval is zero [3].

3.3 Switching States of the VSI

The operating status of the switches in the voltage source inverter in figure 3.2-1 can be represented by switching states. As indicated in Table 3.3-1, switching state '1' denotes that the upper switch in an inverter leg is on and the inverter terminal voltage V is positive ($+V_{dc}$) while '0' indicates that the inverter terminal voltage is zero due to the conduction of the lower switch. There are thirty two possible combinations of switching states in the VSI as listed in Table 3.3-2. For example, the switching state [10000] corresponds to the conduction of S_1, S_4, S_6, S_8 and S_{10} in the inverter legs A, B, C, D and E, respectively. Among the thirty two switching states, [11111] and [00000] are zero states and the others are active states.

Table 3.3-1 Definition of Switching States

Switching state	Leg A			Leg B			Leg C			Leg D			Leg E		
	S_1	S_2	V_A	S_3	S_4	V_B	S_5	S_6	V_C	S_7	S_8	V_D	S_9	S_{10}	V_E
1	On	Off	V_{dc}	On	Off	V_{dc}	on	Off	V_{dc}	On	off	V_{dc}	on	Off	V_{dc}
0	Off	On	0	Off	On	0	off	On	0	Off	on	0	off	On	0

Table 3.3-2 Switching States and Phase voltages for the five-phase inverter

Space vector	On-off	v_a	v_b	v_c	v_d	v_e	Theta in degree
v_1	11001	$0.4V_{dc}$	$0.4V_{dc}$	$-0.6V_{dc}$	$-0.6V_{dc}$	$0.4V_{dc}$	0
v_2	11000	$0.6V_{dc}$	$0.6V_{dc}$	$-0.4V_{dc}$	$-0.4V_{dc}$	$-0.4V_{dc}$	36
v_3	11100	$0.4V_{dc}$	$0.4V_{dc}$	$0.4V_{dc}$	$-0.6V_{dc}$	$-0.6V_{dc}$	72
v_4	01100	$-0.4V_{dc}$	$0.6V_{dc}$	$0.6V_{dc}$	$-0.4V_{dc}$	$-0.4V_{dc}$	108

v_5	01110	$-0.6V_{dc}$	$0.4V_{dc}$	$0.4V_{dc}$	$0.4V_{dc}$	$-0.6V_{dc}$	144
v_6	00110	$-0.4V_{dc}$	$-0.4V_{dc}$	$0.6V_{dc}$	$0.6V_{dc}$	$-0.4V_{dc}$	180
v_7	00111	$-0.6V_{dc}$	$-0.6V_{dc}$	$0.4V_{dc}$	$0.4V_{dc}$	$0.4V_{dc}$	216
v_8	00011	$-0.4V_{dc}$	$-0.4V_{dc}$	$-0.4V_{dc}$	$0.6V_{dc}$	V_{dc}	252
v_9	10011	$0.4V_{dc}$	$-0.6V_{dc}$	$-0.6V_{dc}$	$0.4V_{dc}$	$0.4V_{dc}$	288
v_{10}	10001	$0.6V_{dc}$	$-0.4V_{dc}$	$-0.4V_{dc}$	$-0.4V_{dc}$	$0.6V_{dc}$	324
v_{11}	10000	$0.8V_{dc}$	$-0.2V_{dc}$	$-0.2V_{dc}$	$-0.2V_{dc}$	$-0.2V_{dc}$	0
v_{12}	11101	$0.2V_{dc}$	$0.2V_{dc}$	$0.2V_{dc}$	$-0.8V_{dc}$	$0.2V_{dc}$	36
v_{13}	01000	$-0.2V_{dc}$	$0.8V_{dc}$	$-0.2V_{dc}$	$-0.2V_{dc}$	$-0.2V_{dc}$	72
v_{14}	11110	$0.2V_{dc}$	$0.2V_{dc}$	$0.2V_{dc}$	$0.2V_{dc}$	$-0.8V_{dc}$	108
v_{15}	00100	$-0.2V_{dc}$	$-0.2V_{dc}$	$0.8V_{dc}$	$-0.2V_{dc}$	$-0.2V_{dc}$	144
v_{16}	01111	$-0.8V_{dc}$	$0.2V_{dc}$	$0.2V_{dc}$	$0.2V_{dc}$	$0.2V_{dc}$	180
v_{17}	00010	$-0.2V_{dc}$	$-0.2V_{dc}$	$-0.2V_{dc}$	$0.8V_{dc}$	$-0.2V_{dc}$	216
v_{18}	10111	$0.2V_{dc}$	$-0.8V_{dc}$	$0.2V_{dc}$	$0.2V_{dc}$	$0.2V_{dc}$	252
v_{19}	00001	$-0.2V_{dc}$	$-0.2V_{dc}$	$-0.2V_{dc}$	$-0.2V_{dc}$	$0.8V_{dc}$	288
v_{20}	11011	$0.2V_{dc}$	$0.2V_{dc}$	$-0.8V_{dc}$	$0.2V_{dc}$	$0.2V_{dc}$	324
v_{21}	01001	$-0.4V_{dc}$	$0.6V_{dc}$	$-0.4V_{dc}$	$-0.4V_{dc}$	$0.6V_{dc}$	0
v_{22}	11010	$0.4V_{dc}$	$0.4V_{dc}$	$-0.6V_{dc}$	$0.4V_{dc}$	$-0.6V_{dc}$	36
v_{23}	10100	$0.6V_{dc}$	$-0.4V_{dc}$	$0.6V_{dc}$	$-0.4V_{dc}$	$-0.4V_{dc}$	72
v_{24}	01101	$-0.6V_{dc}$	$0.4V_{dc}$	$0.4V_{dc}$	$-0.6V_{dc}$	$0.4V_{dc}$	108
v_{25}	01010	$-0.4V_{dc}$	$0.6V_{dc}$	$-0.4V_{dc}$	$0.6V_{dc}$	$-0.4V_{dc}$	144
v_{26}	10110	$0.4V_{dc}$	$-0.6V_{dc}$	$0.4V_{dc}$	$0.4V_{dc}$	$-0.6V_{dc}$	180

v_{27}	00101	$-0.4V_{dc}$	$-0.4V_{dc}$	$0.6V_{dc}$	$-0.4V_{dc}$	$0.6V_{dc}$	216
v_{28}	01011	$-0.6V_{dc}$	$0.4V_{dc}$	$-0.6V_{dc}$	$0.4V_{dc}$	$0.4V_{dc}$	252
v_{29}	10010	$0.6V_{dc}$	$-0.4V_{dc}$	$-0.4V_{dc}$	$0.6V_{dc}$	$-0.4V_{dc}$	288
v_{30}	10101	$0.4V_{dc}$	$-0.6V_{dc}$	$0.4V_{dc}$	$-0.6V_{dc}$	$0.4V_{dc}$	324
v_0	00000	0	0	0	0	0	0
v_{31}	11111	0	0	0	0	0	0

3.4 Space Vector Representation of a Five-phase VSI

In order to introduce space vector representation of the five-phase inverter output voltages, an ideal sinusoidal five-phase supply source is considered first in figure 3.2-1. Let the phase voltages of a five-phase pure balanced sinusoidal supply be given with equation (3.1).

$$v_a = \sqrt{2}\mathrm{V}\cos(\omega t)$$

$$v_b = \sqrt{2}\mathrm{V}\cos(\omega t - 2\pi/5)$$

$$v_c = \sqrt{2}\mathrm{V}\cos(\omega t - 4\pi/5) \qquad (3.1)$$

$$v_d = \sqrt{2}\mathrm{V}\cos(\omega t + 4\pi/5)$$

$$v_e = \sqrt{2}\mathrm{V}\cos(\omega t + 2\pi/5)$$

The Space vector of phase voltages is defined using power variant transformation, as follow:

$$\vec{v} = \frac{2}{5}(v_a + a v_b + a^2 v_c + a^{*2} v_d + a^* v_e) \qquad (3.2)$$

Substitution of equation (3.1) into equation (3.2) yields for an ideal sinusoidal source the space vector is given as

$$\vec{v} = \sqrt{5} V exp(j\omega t) \qquad (3.3)$$

However, the voltages are not sinusoidal any more with the inverter supply. They are in general of quasi-square waveform. Leg voltages (i.e. voltages between points A, B, C, D, E and the negative rail of the DC bus N in figure 3.2-1) are considered first. Table 3.4-1 summarizes the values of leg voltages in the ten 36 degrees intervals and includes the numbers of the switches that are conducting [16].

Table 3.4-1 Leg voltages of the five-phase VSI

Switching state (mode)	Switches ON	Space vector	Leg voltage V_A	Leg voltage V_B	Leg voltage V_C	Leg voltage V_D	Leg voltage V_E
1	1,3,6,8,9	v_1	V_{dc}	V_{dc}	0	0	V_{dc}
2	1,3,6,8,10	v_2	V_{dc}	V_{dc}	0	0	0
3	1,3,5,8,10	v_3	V_{dc}	V_{dc}	V_{dc}	0	0
4	2,3,5,8,10	v_4	0	V_{dc}	V_{dc}	0	0
5	2,3,5,7,10	v_5	0	V_{dc}	V_{dc}	V_{dc}	0
6	2,4,5,7,10	v_6	0	0	V_{dc}	V_{dc}	0
7	2,4,5,7,9	v_7	0	0	V_{dc}	V_{dc}	V_{dc}
8	2,4,6,7,9	v_8	0	0	0	V_{dc}	V_{dc}
9	1,4,6,7,9	v_9	V_{dc}	0	0	V_{dc}	V_{dc}
10	1,4,6,8,9	v_{10}	V_{dc}	0	0	0	V_{dc}

For calculation of leg voltage space vectors, individual leg voltage values from Table 3.4-1 are inserted in the equation 3.2-2 which defines the voltage space vector. The leg voltage space vector for the first switching state mode is given as:

$$v_1 = \frac{2}{5}(V_A + aV_B + a^2V_C + a^{*2}V_D + a^*V_E)$$

$$= \frac{2}{5}(V_{dc} + aV_{dc} + 0 + 0 + a^*V_{dc})$$

$$= \frac{2}{5}V_{dc}(1 + \cos(2\pi/5) + \sin(2\pi/5) + 0 + 0 + \cos(2\pi/5) - \sin(2\pi/5))$$

$$= \frac{2}{5} V_{dc} \exp(j0) \, (1 \; + 2\cos(2\pi/5))$$

$$= \frac{2}{5} V_{dc} \, 2\cos(\pi/5) \exp(j0) \tag{3.4}$$

Similarly, the other leg voltages can be calculated in the same manner of equation (3.4) and the results are tabulated in Table 3.4-2

Table 3.4-2 Leg voltage space vectors of the five-phase VSI

Leg voltage space vectors	
v_1	$2/5 \, V_{dc} \, 2\cos(\pi/5) \exp(j0)$
v_2	$2/5 \, V_{dc} \, 2\cos(\pi/5) \exp(j \, \pi/5)$
v_3	$2/5 \, V_{dc} \, 2\cos(\pi/5) \exp(j \, 2\pi/5)$
v_4	$2/5 \, V_{dc} \, 2\cos(\pi/5) \exp(j \, 3\pi/5)$
v_5	$2/5 \, V_{dc} \, 2\cos(\pi/5) \exp(j \, 4\pi/5)$
v_6	$2/5 \, V_{dc} \, 2\cos(\pi/5) \exp(j\pi)$
v_7	$2/5 \, V_{dc} \, 2\cos(\pi/5) \exp(j \, 6\pi/5)$
v_8	$2/5 \, V_{dc} \, 2\cos(\pi/5) \exp(j \, 7\pi/5)$
v_9	$2/5 \, V_{dc} \, 2\cos(\pi/5) \exp(j \, 8\pi/5)$
v_{10}	$2/5 \, V_{dc} \, 2\cos(\pi/5) \exp(j \, 9\pi/5)$

Phase to neutral voltages of the star connected load are most easily found by defining a voltage difference between the star point *n* of the load and the negative rail of the DC bus *N*. The following correlation then holds true:

$$V_A = v_a + v_{nN} \tag{3.5}$$

$$V_B = v_b + v_{nN} \tag{3.6}$$

$$V_C = v_c + v_{nN} \tag{3.7}$$

$$V_D = v_d + v_{nN} \tag{3.8}$$

$$V_E = v_e + v_{nN} \tag{3.9}$$

Since the phase voltages in a star connected load sum to zero, summation of the equations (3.5)-(3.9) yields [29]:

$$v_{nN} = \frac{1}{5}(V_A + V_B + V_C + V_D + V_E) \tag{3.10}$$

Substitution of equation (3.10) into equation (3.5)-(3.9) yields phase voltages of the load in the following form:

$$v_a = \frac{4}{5}V_A - \frac{1}{5}(V_B + V_C + V_D + V_E) \tag{3.11}$$

$$v_b = \frac{4}{5}V_B - \frac{1}{5}(V_A + V_C + V_D + V_E) \tag{3.12}$$

$$v_c = \frac{4}{5}V_C - \frac{1}{5}(V_A + V_B + V_D + V_E) \tag{3.13}$$

$$v_d = \frac{4}{5}V_D - \frac{1}{5}(V_A + V_B + V_C + V_E) \tag{3.14}$$

$$v_e = \frac{4}{5}V_E - \frac{1}{5}(V_A + V_B + V_C + V_D) \tag{3.15}$$

The ten distinct intervals of 36 degrees duration in equation (3.11)-(3.15) can be determined using the values of the leg voltages in table 3.4-1. Table 3.4-3 gives the phase voltages for different switching states, obtained using equation (3.11)-(3.15) and table 3.4-1.

Table 3.4-3 Phase voltages of a star connected load supplied from a five-phase VSI.

Switching state	Switches ON	Space vector	v_a	v_b	v_c	v_d	v_e
1	1,3,6,8,9	v_{1ph}	$2/5\,V_{dc}$	$2/5\,V_{dc}$	$-3/5\,V_{dc}$	$-3/5\,V_{dc}$	$2/5\,V_{dc}$
2	1,3,6,8,10	v_{2ph}	$3/5\,V_{dc}$	$3/5\,V_{dc}$	$-2/5\,V_{dc}$	$-2/5\,V_{dc}$	$-2/5\,V_{dc}$
3	1,3,5,8,10	v_{3ph}	$2/5\,V_{dc}$	$2/5\,V_{dc}$	$2/5\,V_{dc}$	$-3/5\,V_{dc}$	$-3/5\,V_{dc}$
4	2,3,5,8,10	v_{4ph}	$-2/5\,V_{dc}$	$3/5\,V_{dc}$	$3/5\,V_{dc}$	$-2/5\,V_{dc}$	$-2/5\,V_{dc}$
5	2,3,5,7,10	v_{5ph}	$-3/5\,V_{dc}$	$2/5\,V_{dc}$	$2/5\,V_{dc}$	$2/5\,V_{dc}$	$-3/5\,V_{dc}$

6	2,4,5,7,10	v_{6ph}	$-2/5\,V_{dc}$	$-2/5\,V_{dc}$	$3/5\,V_{dc}$	$3/5\,V_{dc}$	$-2/5\,V_{dc}$
7	2,4,5,7,9	v_{7ph}	$-3/5\,V_{dc}$	$-3/5\,V_{dc}$	$2/5\,V_{dc}$	$2/5\,V_{dc}$	$2/5\,V_{dc}$
8	2,4,6,7,9	v_{8ph}	$-2/5\,V_{dc}$	$-2/5\,V_{dc}$	$-2/5\,V_{dc}$	$3/5\,V_{dc}$	$3/5\,V_{dc}$
9	1,4,6,7,9	v_{9ph}	$2/5\,V_{dc}$	$-3/5\,V_{dc}$	$-3/5\,V_{dc}$	$2/5\,V_{dc}$	$2/5\,V_{dc}$
10	1,4,6,8,9	v_{10ph}	$3/5\,V_{dc}$	$-2/5\,V_{dc}$	$-2/5\,V_{dc}$	$-2/5\,V_{dc}$	$3/5\,V_{dc}$

Time domain waveforms of phase to neutral voltages of the star connected load are shown in figure 3.4-1 for the five-phase inverter operation in the ten-step mode. Phase voltages are of non-zero value throughout the period and their value alternates between positive and negative $2/5\,V_{dc}$ and $3/5\,V_{dc}$. The waveforms of the phase-to-neutral voltages show ten distinct steps, each of 36 degrees duration and hence the name of this mode of operation, ten-step mode.

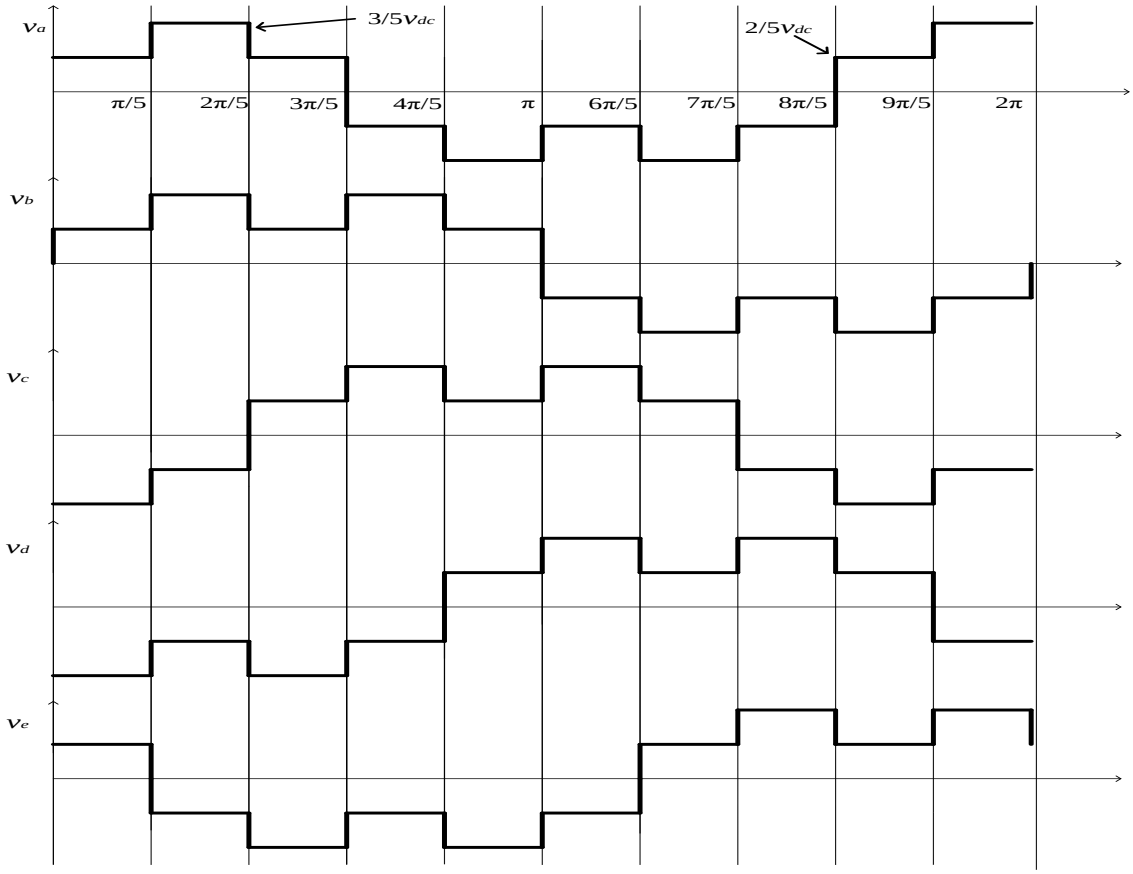

Figure 3.4-1 Five-phase voltage in ten-step mode of operation

To determine the space vectors of phase-to-neutral voltages, the instantaneous values of phase voltages in table 3.4-3 are inserted into equation (3.2). The phase voltage space vectors for the ten-step mode of operation turn out to be same as those of the leg voltages given in table 3.4-2.

A typical space vector diagram for the two-level inverter is shown in figure 3.4-2, where the thirty active vectors V_1 to V_{30} form a regular decagon with ten equal sectors (I to X). The zero vector V_0 and V_{31} lies on the center of the decagon. It obtained directly from equation (3.2) and equation (3.11)-(3.15). The voltage components are normalized with respect to the inverter DC link voltages V_{dc}.

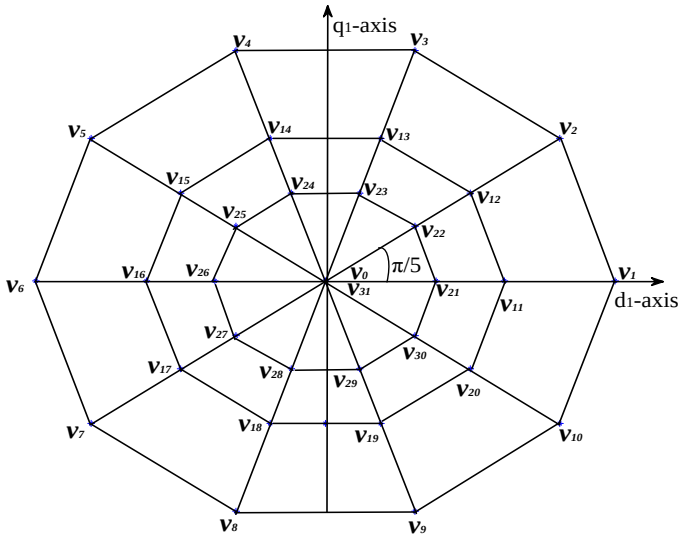

a) d1-q1 space vector voltage

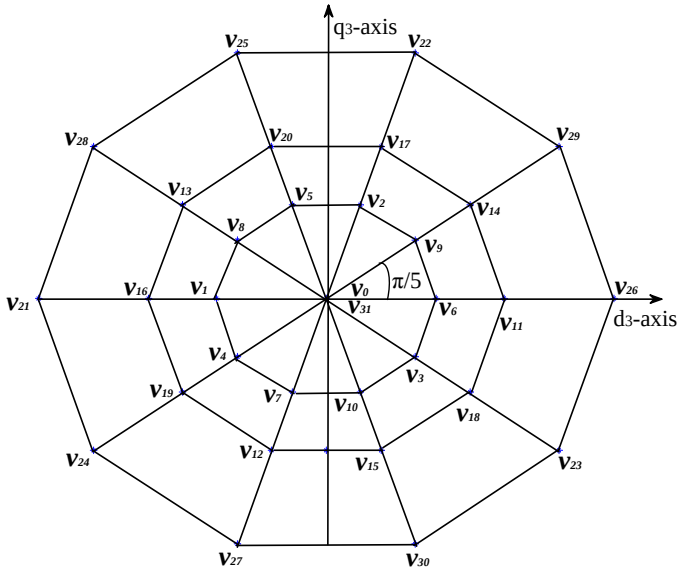

b) d_3-$q_3$space vector voltage

Figure 3.4-2 Five-phase VSI phase voltage space vectors

3.5 Space Vector Modulation

Nowadays, when fast and cheap semiconductor devices are available, it is more desirable to use the PWM technique in the low and middle power range. Since a PWM controlled inverter is able to control both the amplitude and frequency of the output voltage and does not require an additional voltage control on the DC side. This practice is based on multiple pulses in each half AC period, with variable width. Pulse width modulation is the process of modifying the width of the pulses in a pulse train in direct proportion to a small control signal. There are different types of pulse width modulations. Among them, the well known are Sinusoidal pulse width modulation (SPWM) and space vector pulse width modulation (SVPWM) [25].

3.5.1 Comparison of Sine PWM and Space Vector PWM

In summary, the basic difference between sine pulse wide modulation and space vector pulse wide modulation are given below [16, 25].

- SVPWM is more sophisticated method compared with sine PWM.
- Sine PWM is unable to make full use of the inverter's supply voltage and the asymmetrical nature of the PWM switching.

- Space Vector PWM generates less harmonic distortion in the output voltage or currents in comparison with sine PWM.
- Space Vector PWM provides more efficient use of supply voltage in comparison with sine PWM.
- In sine PWM the locus of the reference vector is the inside of the circle with the radius of 1/2Vdc. In Space Vector PWM the locus of the reference vector is the inside of a circle with radius of $2/5\, V_{dc}\, 2\cos(\pi/5)\cos(\pi/10)$.

∴ VoltageUtilization of Space Vector PWM is 1.23108 times of Sine PWM

To implement the space vector PWM, the voltage equations in the *a-b-c-d-e* reference frame can be transformed into the stationary α-β reference frame that consists of the horizontal (α) and vertical (β) axes, as a result, ten non-zero vectors with different amplitudes and two zero vectors are possible. Ten nonzero vectors ($V_1 - V_{10}$) shape the axes of a decagonal as depicted in figure 3.4-2, and feed electric power to the load or DC link voltage is supplied to the load. The angle between any adjacent two non-zero vectors is 36 degrees. Meanwhile, two zero vectors (V_0 and V_{31}) are at the origin and apply zero voltage to the load.

The objective of space vector PWM technique is to approximate the reference voltage vector V_{ref} using the thirty two switching patterns. One simple method of approximation is to generate the average output of the inverter in a small period T to be the same as that of V_{ref} in the same period [25].

3.5.2 Principle of Space Vector PWM

There are some principles of space vector pulse wide modulation:

- Treats the sinusoidal voltage as a constant amplitude vector rotating at constant frequency.
- This PWM technique approximates the reference voltage V_{ref} by a combination of the large active vectors and the two zero vectors V_0 and V_{31}.
- V_{ref} is generated by two adjacent non-zero vectors and two zero vectors.
- Coordinate Transformation; A five-phase voltage vector is transformed into a vector in the synchronous d-q coordinate frame which represents the spatial vector sum of the five-phase voltage.
- The vectors (V_1 to V_{10}) divide the plane into ten sectors (each sector is 36 degrees).

3.6 Realization of Space Vector PWM

The space vector PWM is realized based on the following three steps:

1. Determine V_α, V_β, V_{ref}, and angle (α).
2. Determine time duration T_1, T_2, T_0.
3. Determine the switching time of each transistor (S_1 to S_{10}).

3.6.1 Determine V_α, V_β, V_{ref}, and Angle (α)

The Voltage Space vector and its components in α-β plane are shown in figure 3.6-1. The SVPWM scheme discussed in this section considers the outer-most decagon of space vectors in α-β plane. The input reference voltage vector is synthesized from two active neighboring and zero space vectors [16, 28].

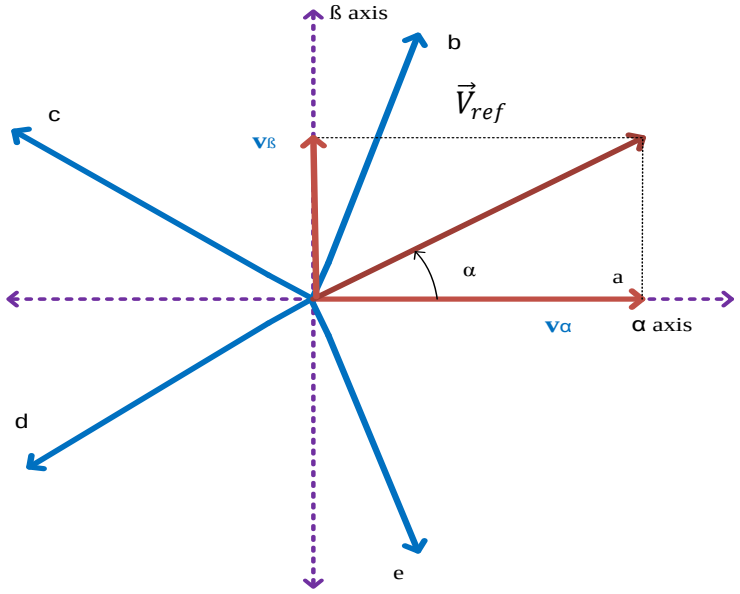

Figure 3.6-1 Space Vector Voltages and its components in α-β

The synchronous voltages V_d and V_q in section 2.7 are generated by the PI controller of figure 2.7-1. From the park inverse transformation of synchronous voltage, the stationary voltage V_α, V_β and V_{ref} can be determined as follows:

$$v_\alpha = v_d * cos(\theta_e) - v_q * sin(\theta_e) \tag{3.16}$$

$$v_\beta = v_d * sin(\theta_e) + v_q * cos(\theta_e) \quad (3.17)$$

$$\begin{bmatrix} v_\alpha \\ v_\beta \end{bmatrix} = \begin{bmatrix} \cos(\theta_e) & -\sin(\theta_e) \\ \sin(\theta_e) & \cos(\theta_e) \end{bmatrix} \begin{bmatrix} V_d \\ V_q \end{bmatrix} \quad (3.18)$$

$$|V_{ref}| = \sqrt{{V_\alpha}^2 + {V_\beta}^2} \quad (3.19)$$

$$\alpha = \tan^{-1}(\frac{v_\beta}{v_\alpha}) \quad (3.20)$$

The voltage $V_\alpha, V_\beta, V_{ref}$ and angle (α), are calculated by using the above equations. The five-phase output voltages in the full bridge inverter at any instant of time in figure 3.2-1 can be represented by a set of thirty two base space vectors according to thirty two switching positions of the inverter. In figure 3.4-2 shows these base vectors V_1 through V_{30} and the two zero vectors which correspond to switching positions resulting in zero output voltage.

3.6.2 Determine Time Duration T_1, T_2, T_0

With considering that T_s is sufficiently small, then the reference voltage V_{ref} could be constant during T_s. When the reference voltage V_{ref} falls into sector I as shown in figure 3.6-2 the reference voltage V_{ref} can be found by two adjacent active vectors V_1 and V_2 and one zero vector V_0. The equation of the reference voltage V_{ref} can be written as follows [16, 25]:-

$$\int_0^{T_s} \vec{V}_{ref}\, dt = \int_{T_0}^{T_1} \vec{V}_1\, dt + \int_{T_1}^{T_1+T_2} \vec{V}_2\, dt + \int_{T_1+T_2}^{T_s} \vec{V}_0 \quad (3.21)$$

$$T_s \vec{V}_{ref} = T_1 \vec{V}_1 + T_2 \vec{V}_2 \quad (3.22)$$

$$T_s = T_1 + T_2 + T_0 \quad (3.23)$$

Whereas:

$$\vec{V}_{ref} = V_{ref}\, e^{j\alpha}$$

$$\vec{V}_1 = \frac{2}{5} V_{dc}\, 2\cos(\frac{\pi}{5}) \exp(j0)$$

$$\vec{V}_2 = \frac{2}{5} V_{dc}\, 2\cos(\frac{\pi}{5}) \exp(j\,\pi/5)$$

$$\vec{V}_0 = 0$$

Then, it can be simplified in to equation (3.24).

$$T_s|V_{ref}|\begin{bmatrix}\cos(\alpha)\\ \sin(\alpha)\end{bmatrix} = T_1\,\frac{2}{5}V_{dc}\,2\cos\left(\frac{\pi}{5}\right)\begin{bmatrix}1\\0\end{bmatrix} + T_2\,\frac{2}{5}V_{dc}\,2\cos\left(\frac{\pi}{5}\right)\begin{bmatrix}\cos\left(\frac{\pi}{5}\right)\\ \sin\left(\frac{\pi}{5}\right)\end{bmatrix} \qquad (3.24)$$

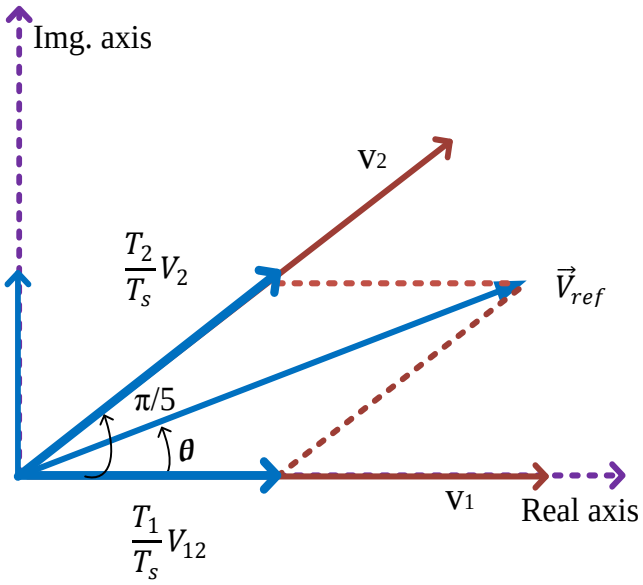

Figure 3.6-2 Principle of space vector time calculation for a five-phase VSI

By collecting the same terms of equation (3.24) will get the following equations:

$$\begin{cases} Realpart & T_sV_{ref}\cos(\alpha) = T_1\,\frac{2}{5}V_{dc}\,2\cos\left(\frac{\pi}{5}\right) + T_2\,\frac{2}{5}V_{dc}\,2\cos\left(\frac{\pi}{5}\right)\cos\left(\frac{\pi}{5}\right) \\ Imaginerypart & T_sV_{ref}\sin(\alpha) = T_2\,\frac{2}{5}V_{dc}\,2\cos\left(\frac{\pi}{5}\right)\sin\left(\frac{\pi}{5}\right) \end{cases} \qquad (3.25)$$

By solving equation (3.25), T_1 and T_2 can be expressed as below;

$$\begin{cases} T_1 = \dfrac{T_s\,V_{ref}\,\sin\left(\frac{\pi}{5}-\alpha\right)}{V_1\sin\left(\frac{\pi}{5}\right)} & (3.26) \\ T_2 = \dfrac{T_s\,V_{ref}\,\sin(\alpha)}{V_2\sin\left(\frac{\pi}{5}\right)} & (3.27) \\ T_0 = T_s - T_1 - T_2 & (3.28) \end{cases}$$

Where: $V_1 = |\vec{V}_1| = V_2 = |\vec{V}_2| = \frac{4}{5}V_{dc}\cos(\frac{\pi}{5})$

$$V_{ref} = |\vec{V}_{ref}|, \qquad 0 \le \alpha \le 36^0$$

Where T_1,T_2,T_0 represents the time widths for vectors V_1,V_2,V_0.T_0 is the period in a sampling period for null vectors should be filled. As each switching period (half of sampling period) T_s starts and ends with zero vectors i.e. there will be four zero vectors per T_s, duration of each null vector is T_s /4. Figure 3.6-3 gives switching pattern for all sectors.

Table 3.6-1 Shows the switching sequence Time T_1, T_2 and T_0 for all sectors

Sector	T_1	T_2	T_0
I	$T_s * a * \sin\left(\frac{\pi}{5} - \alpha\right)$	$T_s * a * \sin(\alpha)$	$T_s - T_1 - T_2$
II	$T_s * a * \sin\left(\frac{2\pi}{5} - \alpha\right)$	$T_s * a * \sin\left(\alpha - \frac{\pi}{5}\right)$	$T_s - T_1 - T_2$
III	$T_s * a * \sin\left(\frac{3\pi}{5} - \alpha\right)$	$T_s * a * \sin\left(\alpha - \frac{2\pi}{5}\right)$	$T_s - T_1 - T_2$
IV	$T_s * a * \sin\left(\frac{4\pi}{5} - \alpha\right)$	$T_s * a * \sin\left(\alpha - \frac{3\pi}{5}\right)$	$T_s - T_1 - T_2$
V	$T_s * a * \sin(\pi - \alpha)$	$T_s * a * \sin\left(\alpha - \frac{4\pi}{5}\right)$	$T_s - T_1 - T_2$
VI	$T_s * a * \sin\left(\frac{6\pi}{5} - \alpha\right)$	$T_s * a * \sin(\alpha - \pi)$	$T_s - T_1 - T_2$
VII	$T_s * a * \sin\left(\frac{7\pi}{5} - \alpha\right)$	$T_s * a * \sin\left(\alpha - \frac{6\pi}{5}\right)$	$T_s - T_1 - T_2$
VIII	$T_s * a * \sin\left(\frac{8\pi}{5} - \alpha\right)$	$T_s * a * \sin\left(\alpha - \frac{7\pi}{5}\right)$	$T_s - T_1 - T_2$
IX	$T_s * a * \sin\left(\frac{9\pi}{5} - \alpha\right)$	$T_s * a * \sin\left(\alpha - \frac{8\pi}{5}\right)$	$T_s - T_1 - T_2$
X	$T_s * a * \sin(2\pi - \alpha)$	$T_s * a * \sin\left(\alpha - \frac{9\pi}{5}\right)$	$T_s - T_1 - T_2$

Switching Time Duration at Any Sector:

The general equation of Switching Time Duration at Any Sector can be calculated as follows:

$$\int_0^{T_s} \vec{V}_{ref}\, dt = \int_0^{T_n} \vec{V}_n\, dt + \int_{T_n}^{T_n+T_{n+1}} \vec{V}_{n+1}\, dt + \int_{T_n+T_{n+1}}^{T_s} \vec{V}_0\, dt \qquad (3.29)$$

$$T_s * \vec{V}_{ref} = T_n\vec{V}_n + T_{n+1}\vec{V}_{n+1} \quad (3.30)$$

Where:

T_n, T_{n+1} *and* T_0 are the switching times of space vector voltages V_n, V_{n+1} *and* V_0 respectively.

$$\vec{V}_{ref} = V_{ref}\, e^{j\left(\alpha-\left(\frac{n-1}{5}\pi\right)\right)}$$

$$\vec{V}_n = \frac{2}{5}V_{dc}\, 2\cos(\tfrac{\pi}{5})\exp\left(j\frac{n-1}{5}\pi\right)$$

$$\vec{V}_{n+1} = \frac{2}{5}V_{dc}\, 2\cos(\tfrac{\pi}{5})\exp\left(j\frac{n}{5}\pi\right)$$

$$T_s|V_{ref}|\begin{bmatrix}\cos\left(\alpha-\left(\frac{n-1}{5}\pi\right)\right)\\ \sin\left(\alpha-\left(\frac{n-1}{5}\pi\right)\right)\end{bmatrix} = \frac{2}{5}V_{dc}\,2\cos\left(\frac{\pi}{5}\right)\left[\begin{bmatrix}\cos\left(\frac{n-1}{5}\pi\right)\\ \sin\left(\frac{n-1}{5}\pi\right)\end{bmatrix}+\begin{bmatrix}\cos\left(\frac{n}{5}\pi\right)\\ \sin\left(\frac{n}{5}\pi\right)\end{bmatrix}\right]\begin{bmatrix}T_n\\ T_{n+1}\end{bmatrix} \quad (3.31)$$

By collecting the same terms i.e. the real part and imaginary part of equation (3.31) will get the following equations:

$$\left[T_sV_{ref}\cos\left(\alpha-\left(\frac{n-1}{5}\pi\right)\right)\right] = \begin{bmatrix}\frac{2}{5}V_{dc}\,2\cos\left(\frac{\pi}{5}\right)\cos\left(\frac{n-1}{5}\pi\right)\\ \frac{2}{5}V_{dc}\,2\cos\left(\frac{\pi}{5}\right)\cos\left(\frac{n}{5}\pi\right)\end{bmatrix}\begin{bmatrix}T_n\\ T_{n+1}\end{bmatrix} \quad (3.32)$$

$$\left[T_sV_{ref}\sin\left(\alpha-\left(\frac{n-1}{5}\pi\right)\right)\right] = \begin{bmatrix}\frac{2}{5}V_{dc}\,2\cos\left(\frac{\pi}{5}\right)\sin\left(\frac{n-1}{5}\pi\right)\\ \frac{2}{5}V_{dc}\,2\cos\left(\frac{\pi}{5}\right)\sin\left(\frac{n}{5}\pi\right)\end{bmatrix}\begin{bmatrix}T_n\\ T_{n+1}\end{bmatrix} \quad (3.33)$$

By solving the above equations, T_1 and T_2 can be expressed as:

$$\begin{cases} T_n = \dfrac{T_s * V_{ref} * \sin\left(\frac{n}{5}\pi-\alpha\right)}{V_n * \sin\left(\frac{\pi}{5}\right)} & (3.34)\\ T_{n+1} = \dfrac{T_s * V_{ref} * \sin\left(\alpha-\frac{n-1}{5}\pi\right)}{V_n * \sin\left(\frac{\pi}{5}\right)} & (3.35)\\ T_0 = T_s - T_n - T_{n+1} & (3.36)\end{cases}$$

Where: n is the sector numbers from n = 1 to 10

$$V_n = |\vec{V}_n| = \frac{4}{5} * V_{dc} * \cos(\tfrac{\pi}{5})$$

3.6.3 Determine the Switching Time of each Transistor

From the switching pattern figure 3.6-3, it is seen that in the first half of the switching cycle zero space vector is applied, followed by two active space vectors and then by the second zero space vector. The sequence followed in the second half cycle is the mirror image of the first one. The total number of state changes in one PWM switching period is thus twenty, since each switch changes state twice in one switching period.

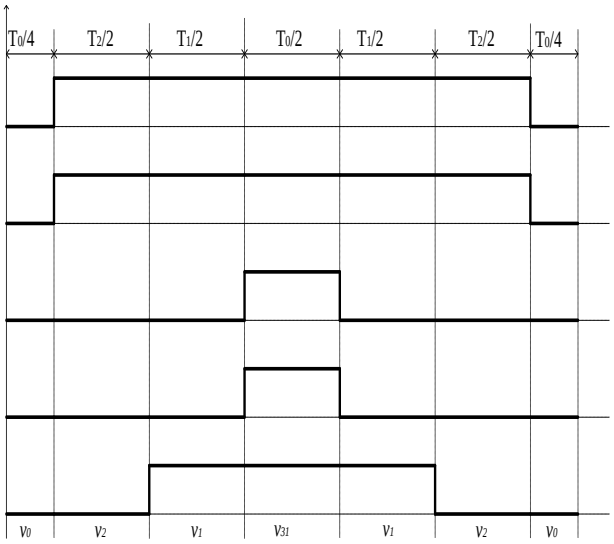

(a) Sector I

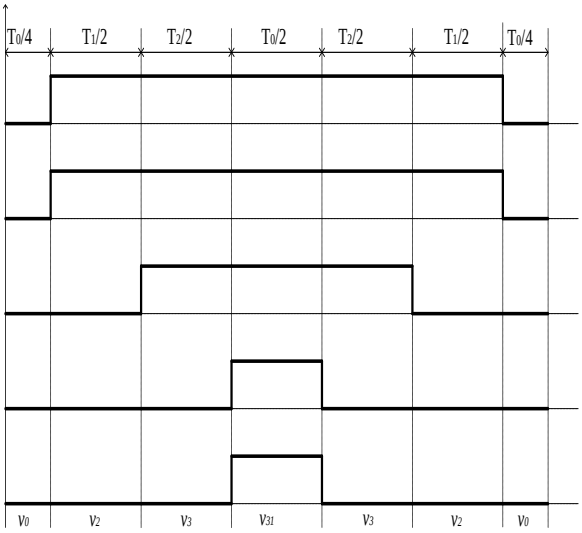

(b) Sector II

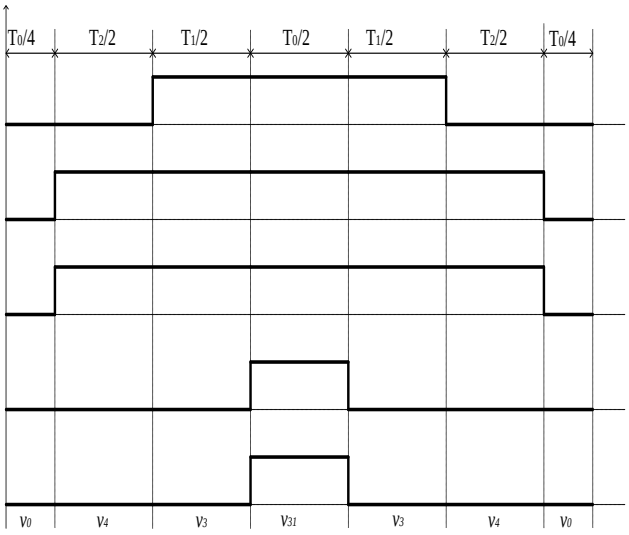

(c) Sector III

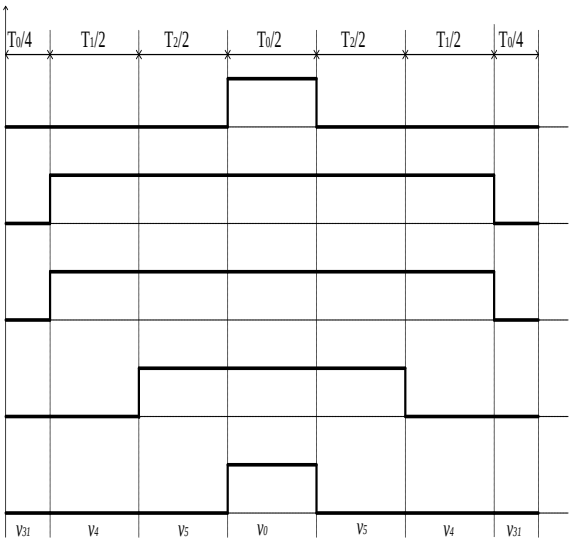

(d) Sector IV

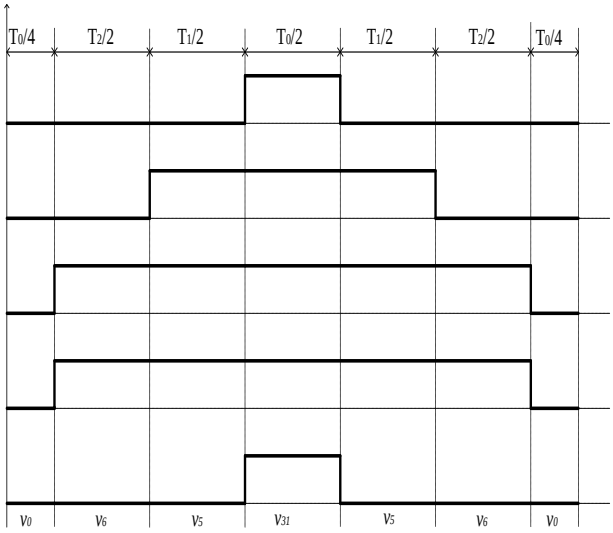

(e) Sector V

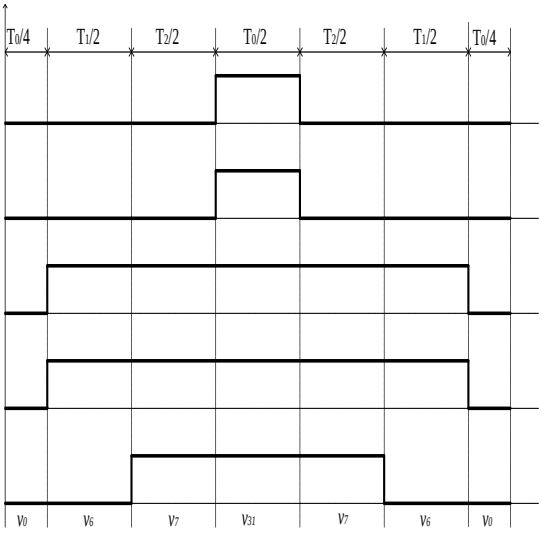

(f) Sector VI

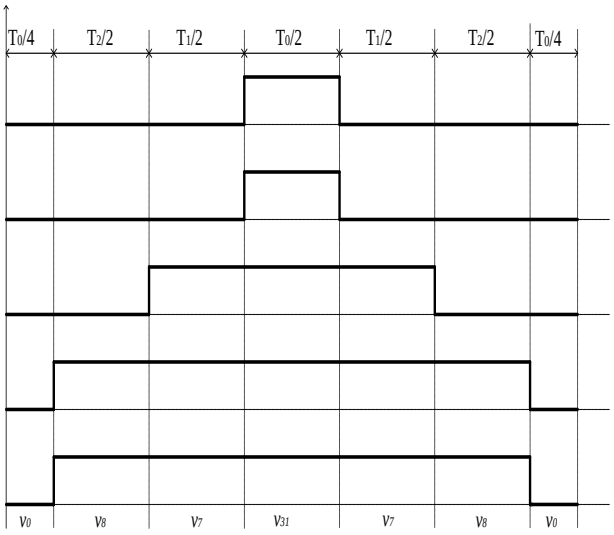

(g) Sector VII

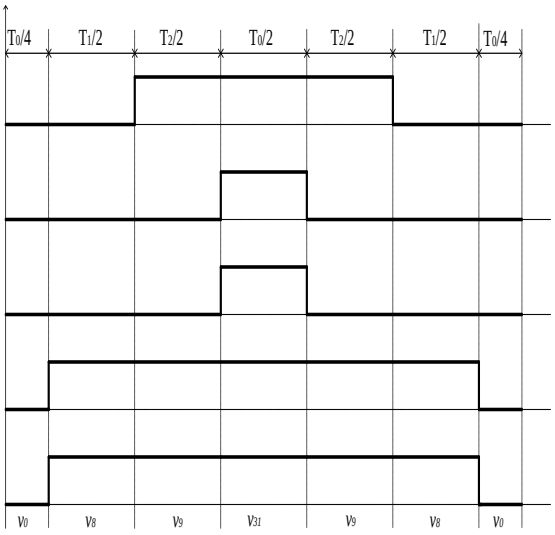

(h) Sector VIII

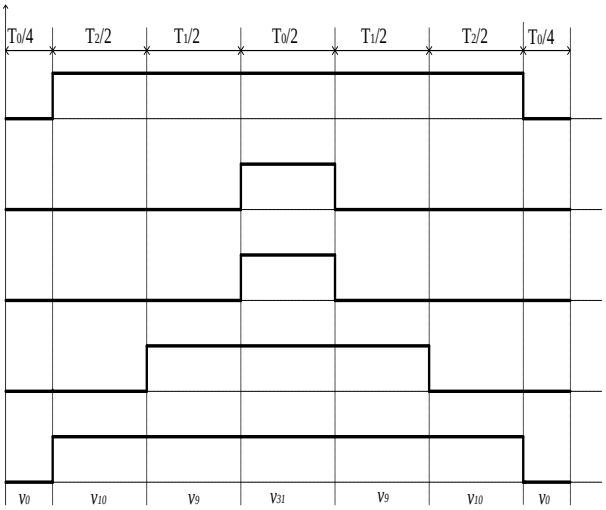

(i) Sector IX

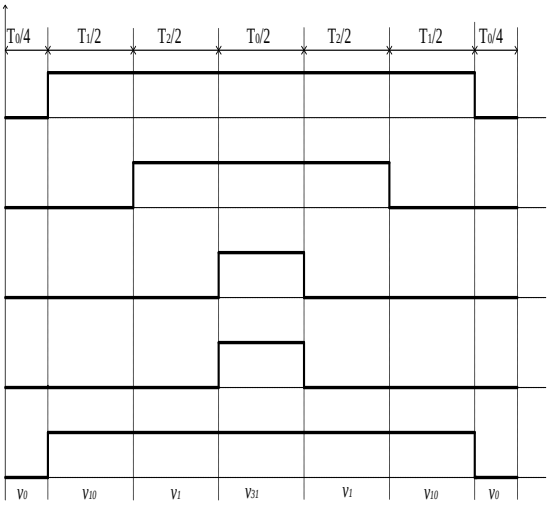

(j) Sector X

Figure 3.6-3 space vector PWM switching patterns with large space vector at each sector

Based on figure 3.6-3 the switching time at each sector is summarized in table 3.6-2.

Table 3.6-2 the switching time at each sector

Sector	Upper switches	Lower switches
I	$S_1 = T_1 + T_2 + T_0/2$ $S_3 = T_1 + T_2 + T_0/2$ $S_5 = T_0/2$ $S_7 = T_0/2$ $S_9 = T_1 + T_0/2$	$S_2 = T_0/2$ $S_4 = T_0/2$ $S_6 = T_1 + T_2 + T_0/2$ $S_8 = T_1 + T_2 + T_0/2$ $S_{10} = T_2 + T_0/2$
II	$S_1 = T_1 + T_2 + T_0/2$ $S_3 = T_1 + T_2 + T_0/2$ $S_5 = T_2 + T_0/2$ $S_7 = T_0/2$ $S_9 = T_0/2$	$S_2 = T_0/2$ $S_4 = T_0/2$ $S_6 = T_1 + T_0/2$ $S_8 = T_1 + T_2 + T_0/2$ $S_{10} = T_1 + T_2 + T_0/2$

III	$S_1 = T_1 + T_0/2$ $S_3 = T_1 + T_2 + T_0/2$ $S_5 = T_1 + T_2 + T_0/2$ $S_7 = T_0/2$ $S_9 = T_0/2$	$S_2 = T_2 + T_0/2$ $S_4 = T_0/2$ $S_6 = T_0/2$ $S_8 = T_1 + T_2 + T_0/2$ $S_{10} = T_1 + T_2 + T_0/2$
IV	$S_1 = T_0/2$ $S_3 = T_1 + T_2 + T_0/2$ $S_5 = T_1 + T_2 + T_0/2$ $S_7 = T_2 + T_0/2$ $S_9 = T_0/2$	$S_2 = T_1 + T_2 + T_0/2$ $S_4 = T_0/2$ $S_6 = T_0/2$ $S_8 = T_1 + T_0/2$ $S_{10} = T_1 + T_2 + T_0/2$
V	$S_1 = T_0/2$ $S_3 = T_1 + T_0/2$ $S_5 = T_1 + T_2 + T_0/2$ $S_7 = T_1 + T_2 + T_0/2$ $S_9 = T_0/2$	$S_2 = T_1 + T_2 + T_0/2$ $S_4 = T_2 + T_0/2$ $S_6 = T_0/2$ $S_8 = T_0/2$ $S_{10} = T_1 + T_2 + T_0/2$
VI	$S_1 = T_0/2$ $S_3 = T_0/2$ $S_5 = T_1 + T_2 + T_0/2$ $S_7 = T_1 + T_2 + T_0/2$ $S_9 = T_2 + T_0/2$	$S_2 = T_1 + T_2 + T_0/2$ $S_4 = T_1 + T_2 + T_0/2$ $S_6 = T_0/2$ $S_8 = T_0/2$ $S_{10} = T_1 + T_0/2$
VII	$S_1 = T_0/2$ $S_3 = T_0/2$ $S_5 = T_1 + T_0/2$ $S_7 = T_1 + T_2 + T_0/2$ $S_9 = T_1 + T_2 + T_0/2$	$S_2 = T_1 + T_2 + T_0/2$ $S_4 = T_1 + T_2 + T_0/2$ $S_6 = T_2 + T_0/2$ $S_8 = T_0/2$ $S_{10} = T_0/2$

VIII	$S_1 = T_2 + T_0/2$ $S_3 = T_0/2$ $S_5 = T_0/2$ $S_7 = T_1 + T_2 + T_0/2$ $S_9 = T_1 + T_2 + T_0/2$	$S_2 = T_1 + T_0/2$ $S_4 = T_1 + T_2 + T_0/2$ $S_6 = T_1 + T_2 + T_0/2$ $S_8 = T_0/2$ $S_{10} = T_0/2$
XV	$S_1 = T_1 + T_2 + T_0/2$ $S_3 = T_1 + T_2 + T_0/2$ $S_5 = T_0/2$ $S_7 = T_0/2$ $S_9 = T_1 + T_0/2$	$S_2 = T_0/2$ $S_4 = T_0/2$ $S_6 = T_1 + T_2 + T_0/2$ $S_8 = T_1 + T_2 + T_0/2$ $S_{10} = T_2 + T_0/2$
X	$S_1 = T_1 + T_2 + T_0/2$ $S_3 = T_2 + T_0/2$ $S_5 = T_0/2$ $S_7 = T_0/2$ $S_9 = T_1 + T_2 + T_0/2$	$S_2 = T_0/2$ $S_4 = T_1 + T_0/2$ $S_6 = T_1 + T_2 + T_0/2$ $S_8 = T_1 + T_2 + T_0/2$ $S_{10} = T_0/2$

The analytical expression for leg voltages averaged over one switching cycle and expressed in terms of the DC bus of the five-phase VSI can be deduced from the switching pattern shown in figure 3.6-3 For sector I can be calculate as follow:

$$V_A = \frac{V_{dc}}{2T_s}\left(-\frac{T_0}{2} + T_2 + T_1 + T_0 + T_1 + T_2 - \frac{T_0}{2}\right)$$

$$V_B = \frac{V_{dc}}{2T_s}\left(-\frac{T_0}{2} + T_2 + T_1 + T_0 + T_1 + T_2 - \frac{T_0}{2}\right)$$

$$V_C = \frac{V_{dc}}{2T_s}\left(-\frac{T_0}{2} - T_2 - T_1 + T_0 - T_1 - T_2 - \frac{T_0}{2}\right)$$

$$V_D = \frac{V_{dc}}{2T_s}\left(-\frac{T_0}{2} - T_2 - T_1 + T_0 - T_1 - T_2 - \frac{T_0}{2}\right)$$

$$V_E = \frac{V_{dc}}{2T_s}\left(-\frac{T_0}{2} - T_2 + T_1 + T_0 + T_1 - T_2 - \frac{T_0}{2}\right)$$

Chapter Four

System Model Simulation and Results

4.1 System Model Simulation

MATLAB/Simulink is a software package which is used to model, simulate, and analyze of dynamic systems. The mathematical equations presented in chapter two and chapter three is used to model the five phase induction motor in Matlab/Simulink R2013a environment. Figure 4.1-1 depicts the complete Simulink model of DTC of five phase induction motor.

The overall system simulation block includes different sub-functional blocks such as: PI controller blocks, Coordinate Transformation blocks, SVPWM block, VSI block and IM modeling block are sub functional blocks.

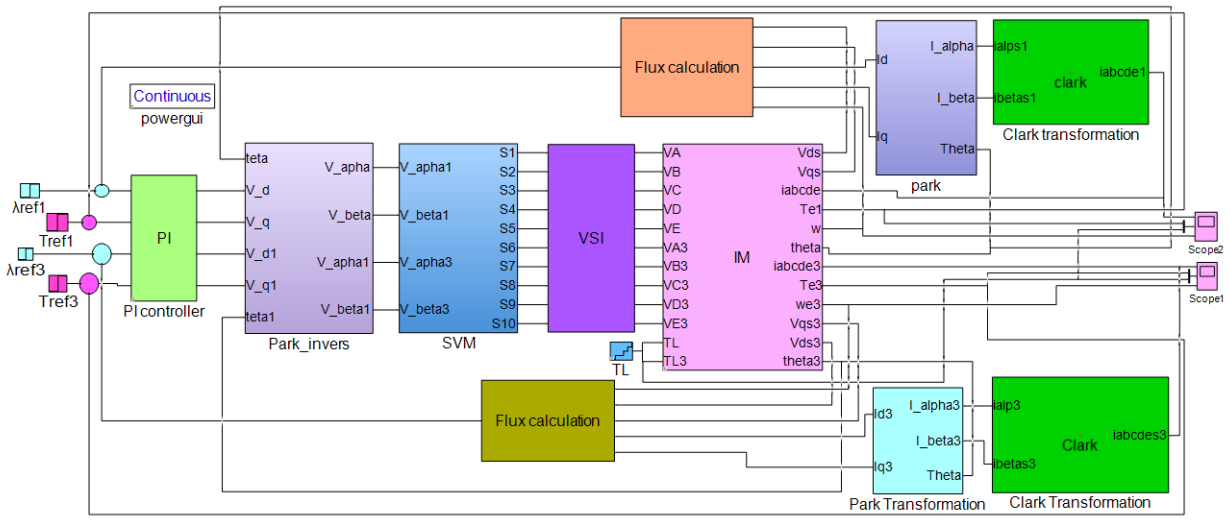

Figure 4.1-1 DTC of five phase IM system simulation block diagram

The PI controller blocks are used to minimize the flux and torque errors. The PI torque output is q-axis voltage and the PI flux output is d-axis voltage in synchronous reference frame. The outputs of PI controller are fed to park-inverse transformation sub blocks. And these voltages will generate the desired α-axis and β-axis voltage references that fed to the SVPWM sub block.

SVM Simulink block

The SVPWM simulation block, shown in figure 4.1-2, is used to determine the switching sequence and duration of the power transistors of five-phase voltage source inverters. SVPWM algorithm calculates the duty time of the five upper power transistors based on the α-axis voltage and β-axis voltage fed to it from the park inverse block. Then these outputs are compared with the output of a triangular wave repeating sequence, which is operating at frequency of PWM, to generate pulse width modulated signals accordingly. Finally the five output signals are passed through inverter logic operator to produce the inverse of them. These ten pulse width modulated signals are used to drive a five phase voltage source inverter. The source codes of sector selection, active time calculation, space vector selection and triangular wave repeating sequence generation are written in the appendix.

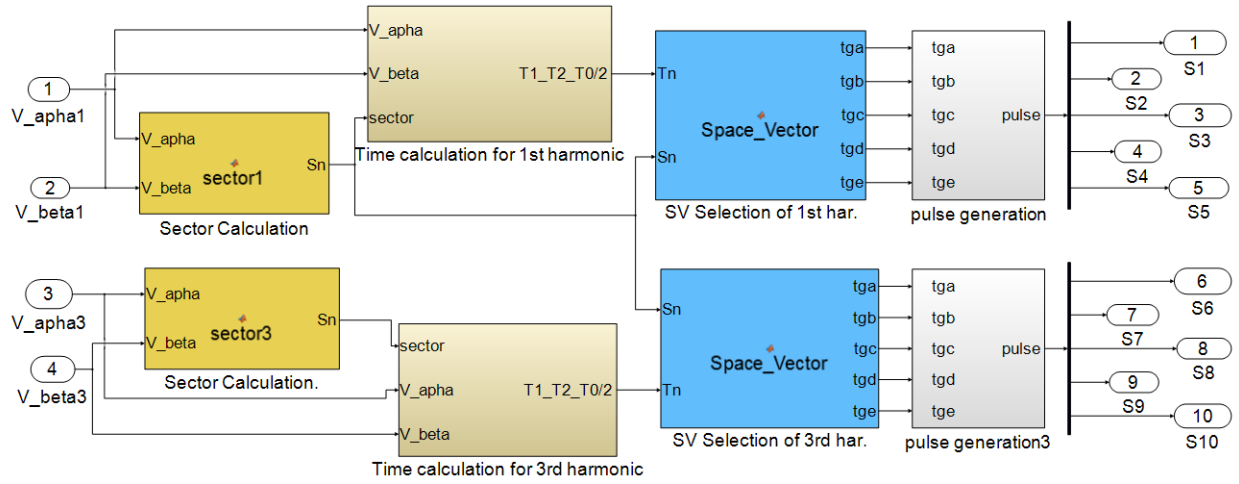

Figure 4.1-2 SVPWM generation simulation block diagram

Voltage Source Inverter block

The VSI block is used to generate five phase voltages from the DC voltage by triggering the switching states that are generated in SVM techniques. The phase voltage output of VSI feds to induction motor and also that used to estimate the actual flux and actual torque.

Coordinate Transformation blocks

The different coordinate transformations such as: Clark transformation, park transformation, Clark-inverse transformation and park-inverse transformation are written in MATLAB source code and embedded in simulation blocks. The source codes are shown in the appendix.

IM simulation model

The simulation model of five-phase IM is not available in the simulink library. However, it is designed using the stator resistance, rotor resistance, stator inductance, rotor inductance, mutual inductance and moment of inertia as shown in figure 4.1-3. The five phase VSI output voltages are transforming into α-axis voltage and β-axis voltage using the Clark transformation. These voltages also transform in to d-q axis voltages. From these voltages will be determine the actual stator flux and the rotor flux. Then, the d and q axis currents are calculated from d and q axis voltage and flux variables. After that, the electromagnetic torque is developed from the interaction of stator flux's and stator currents that is taken as actual torque. From the mechanical torque equation and torque load, the rotor speed and rotor position is calculated.

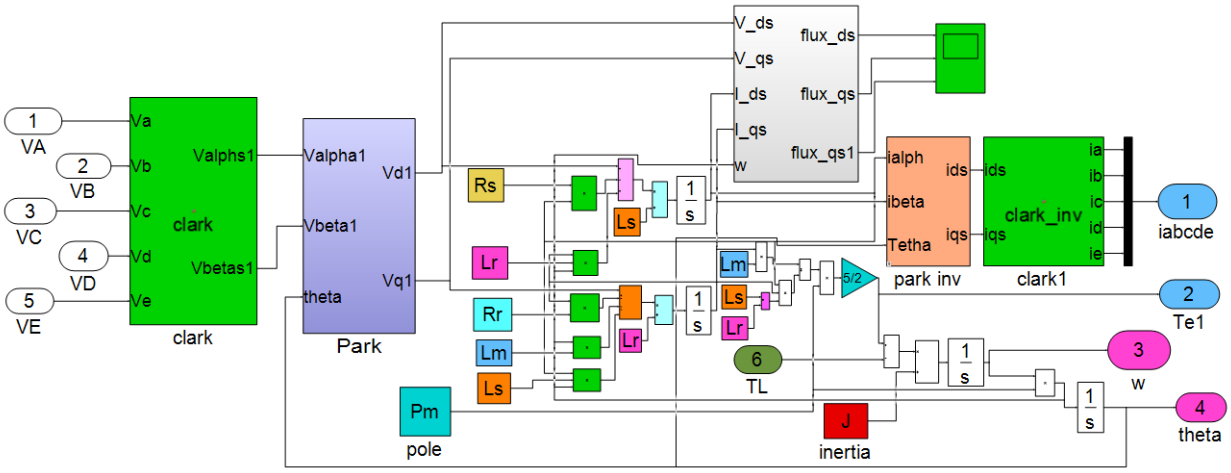

Figure 4.1-3 Induction Motor model block diagram

4.2 Simulation Results of Five-Phase IM

This section deals with the simulation results of five phase IM drive system. The parameters of the motor that are used in the simulation are shown in table 4.1-1. They are found from MATLAB documentation.

Table 4.2-1 Induction motor and VSI parameters

Dc link voltage	Vdc = 400V
Stator resistance	Rs= 2.875ohm
Rotor resistance	Rr= 2.875ohm
Stator inductance	Lls= 8.5mH
Rotor inductance	Llr= 8.5mH
Mutual inductance	Lm= 0.175H
Moment of inertia	J= 0.0008Kg.m2
Number of poles	P= 4

The simulation results are carried out for different reference torques and flux's under different loading conditions. The load torque is varied in steps (at t=0, motor is no loaded and the load is varied in steps as 25%, 50%, 75%, and full load at 0.1, 0.25, 0.45, 0.7 second respectively) and the corresponding variations in stator current, torque, and speed are observed and shown in figure 4.2-1 (a) and (b), (c), and (d) respectively. It is seen that the stator current increases and speed decreases with increasing load and the motor torque follows the load torque. The transient oscillations of the torque for a load change from no load to load torque condition is observed and shown in Figure 4.2-2. The system can follow the load torque T_L=5 Nm with a rise time of less than 0.004 second and settling time of 0.03 second. It also gives a good overshoot value of 7.62 Nm at peak time t=0.007 sec with steady state error of 1.2%. It is able to track change in the set point in a satisfactory way with error value less than 2%.

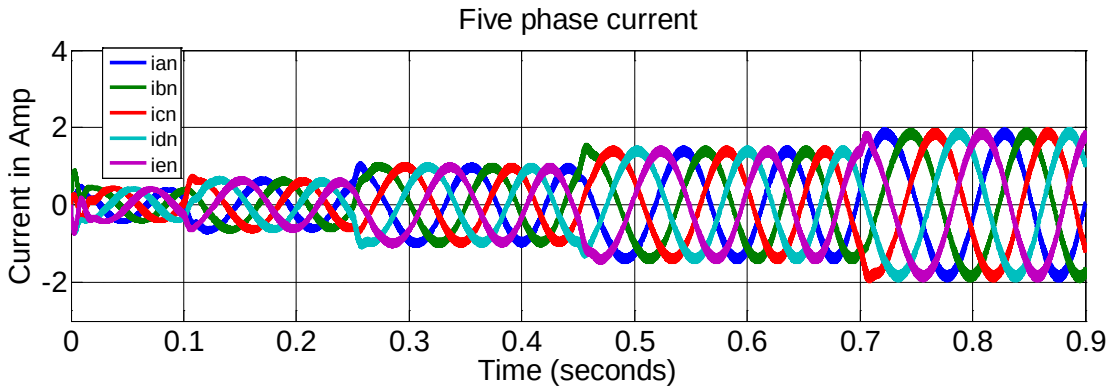

(a) Un filtered five –phase current

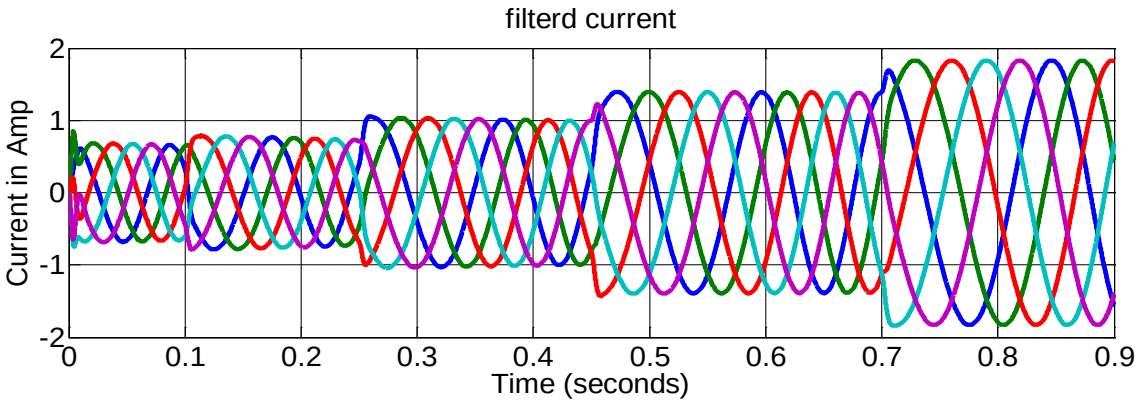

(b) After filtered

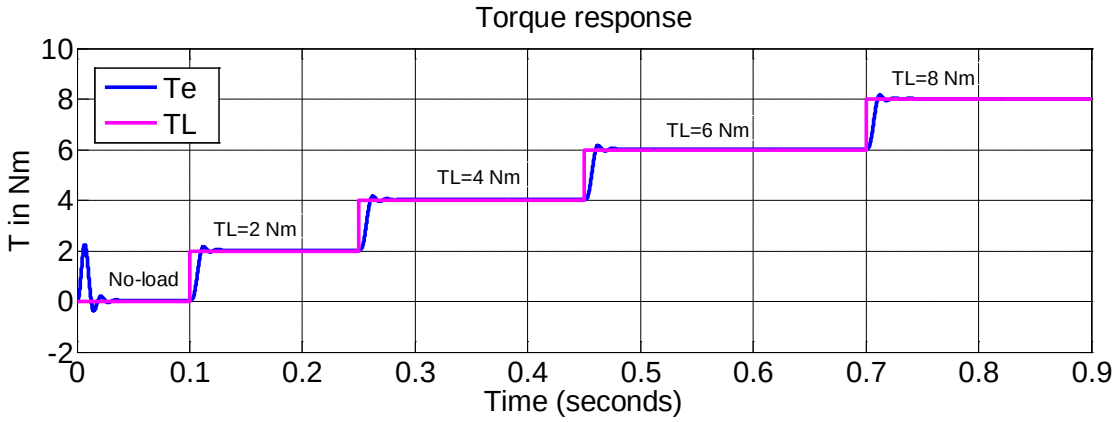

(c) Electromagnetic torque and load torque

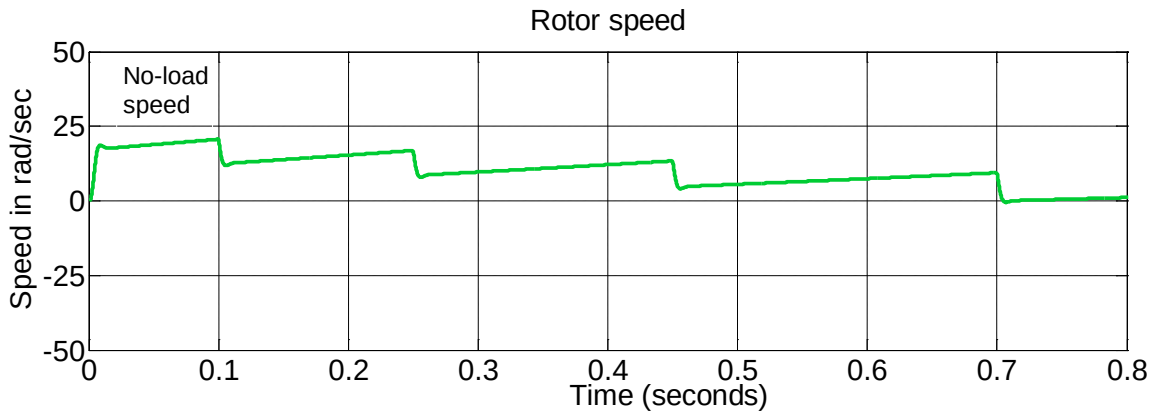

(d) Speed response of IM

Figure 4.2-1 simulation result of five phase IM with different loading conditions

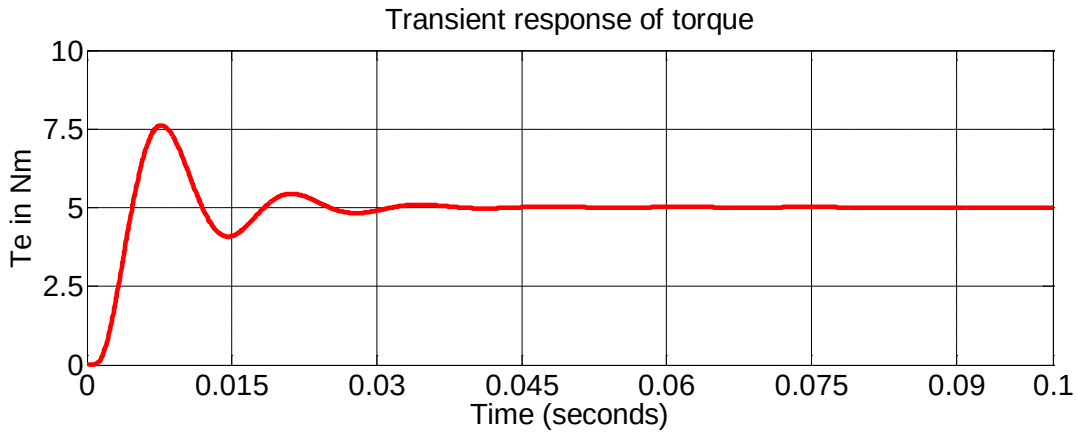

Figure 4.2-2 Transient response torque at t=0.03sec

In general, the electromagnet torque, rotor speed and Stator phase currents of the system at different load condition have good transient and steady state response. The above figures show these properties.

The simulation results of the fundamental harmonic component and third harmonic component values are deeply presented and discussed at following reference values:

- Torque reference T_{ref} = 12 N/m,
- Flux reference λ_{ref} = 2 wb and
- Load torque T_L= 6 N/m.

4.2.1 Simulation Results of First Harmonic Components

The developed stator phase voltages which are generated from the voltage source inverter output are shown in figure 4.2-3. As can be discussed in chapter three Phase voltages are of non-zero value throughout the period and their value alternates between positive and negative $2/5\,V_{dc}$ and $3/5\,V_{dc}$. This implies that the simulation result is similar to the analytical analysis. The proposed control system is able to inject sinusoidal 72^0 to the stator of the induction motor from the DC power supply available.

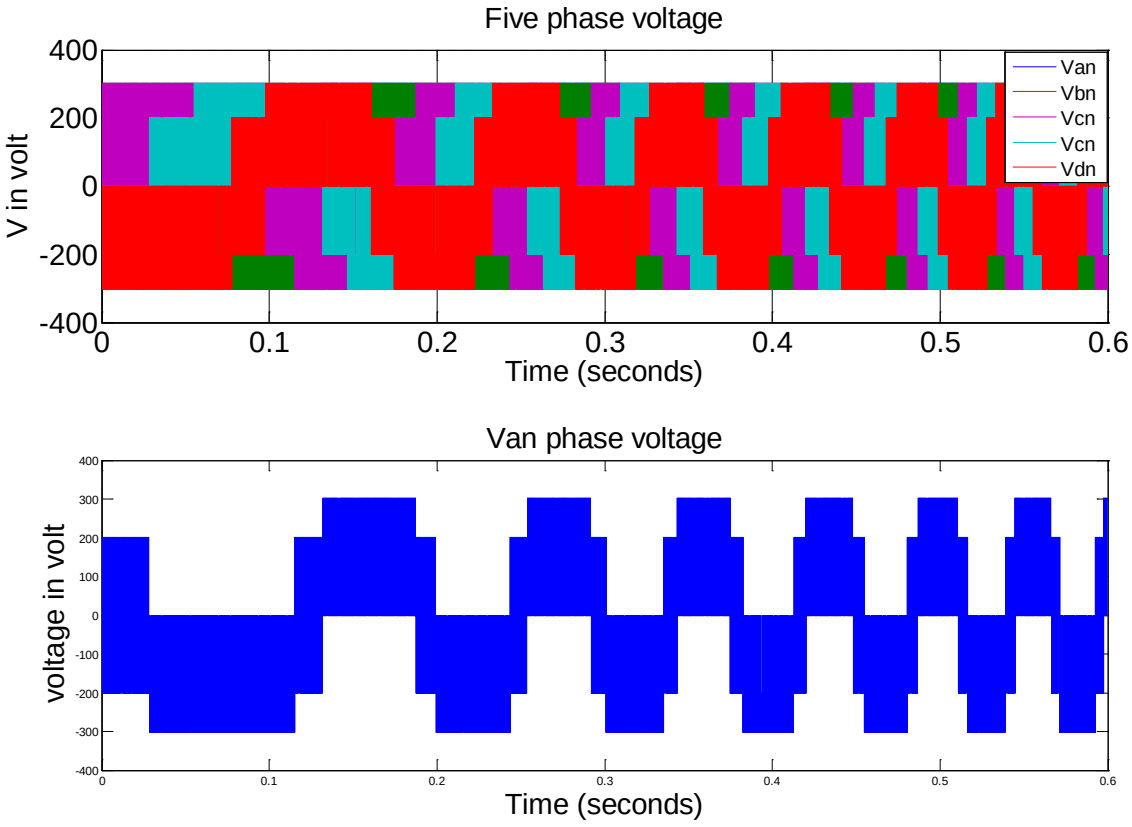

Figure 4.2-3 First harmonic components of five phase voltages

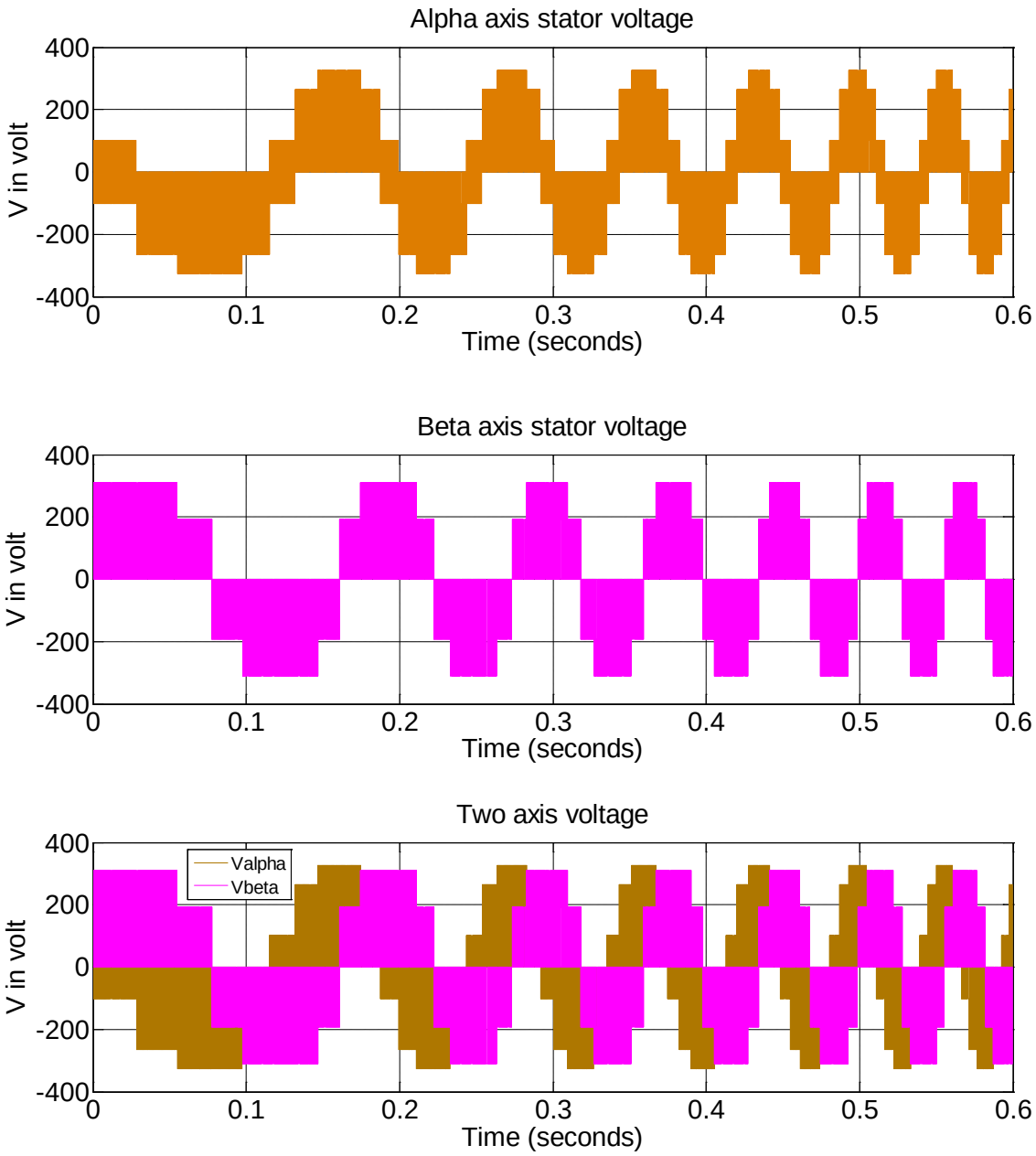

Figure 4.2-4 First harmonic component of alpha and beta axis stator voltage

Figure 4.2-4 shows the first harmonic component of two phase alpha-axis and beta-axis stator voltages. They are obtained from figure 4.2-3 by Clark transformations in the orthogonal fixed reference frame. It can be observed that these quantities are sinusoidal and have phase difference of 90^0.

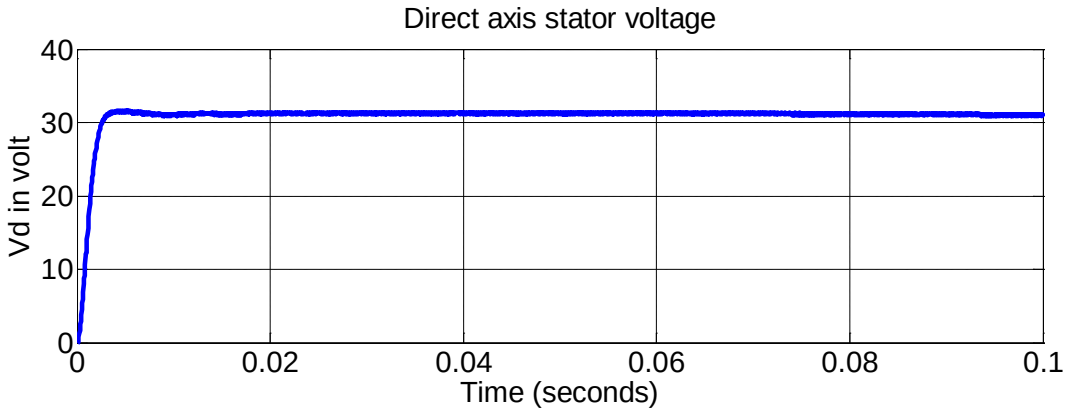

Figure 4.2-5 First harmonic component of direct axis stator voltage

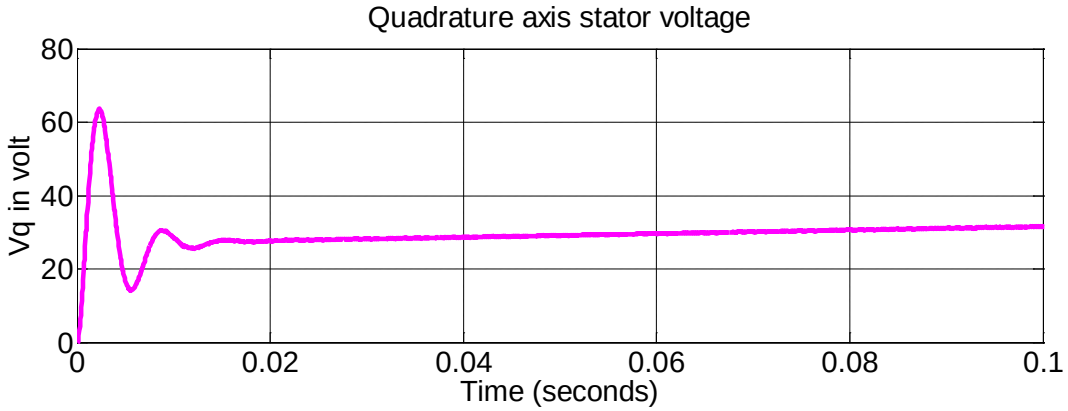

Figure 4.2-6 First harmonic component of quadrature axis stator voltage

The direct and quadrature component of voltage is given in figure 4.2-5 and 4.2-6. These voltages are obtained from park transformation and as they expected these quantities are DC values. Instated of five phase voltages, the d-q voltages are fed to the five phase IM parameters. Because, five phase induction motor is not available in the Matlab/Simulink R2013a/R2015a environment and the researcher is try to model the motor using the dynamic model stated in chapter two. Figure 4.2-7 shows the direct and quadratuare axis currents which are generated from the stator motor parameter and d-q stator voltage components.

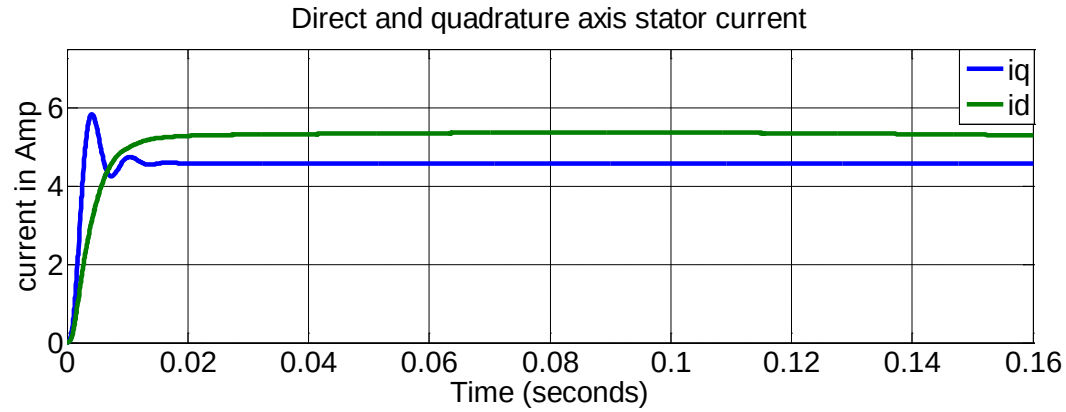

Figure 4.2-7 First harmonic component of direct and quadratuare axis stator currents

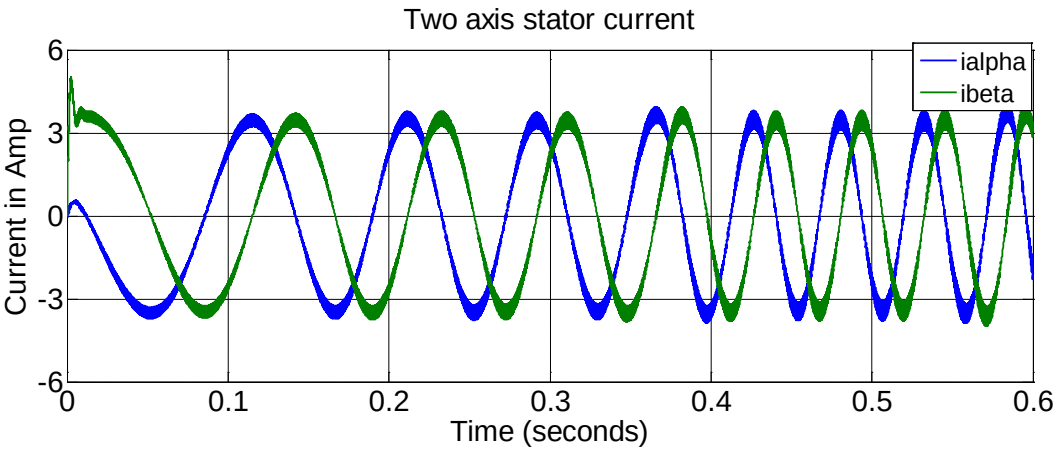

Figure 4.2-8 First harmonic component alpha and beta axis stator current

Figure 4.2-8 show the fundamental harmonics of alpha and beta currents which obtained by park inverse transformation. Both currents are orthogonal each other. The five phase induction motor shown in figure 4.2-9 is obtained from these quantities by Clark inverse transformation. In this figure after the transient response, the steady state value is constant amplitude. It is clearly that the five phase current is sinusoidal 72 electrical degrees apart each adjacent phase.

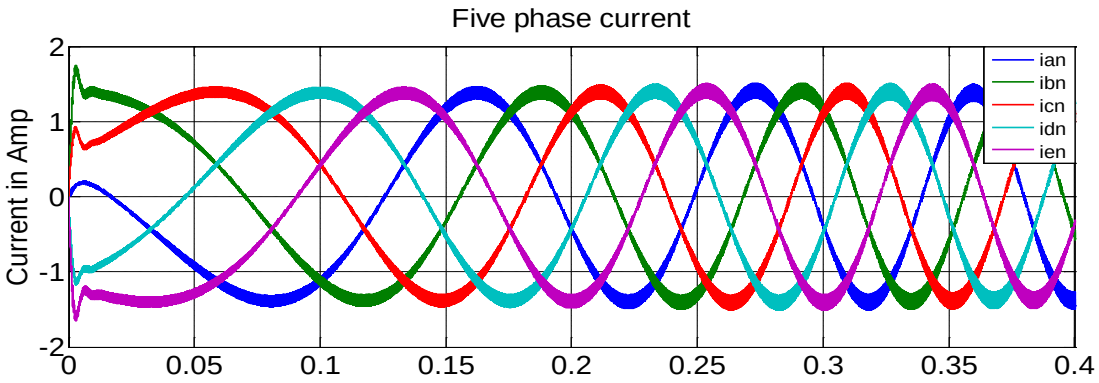

Figure 4.2-9 First harmonic component of five phase current

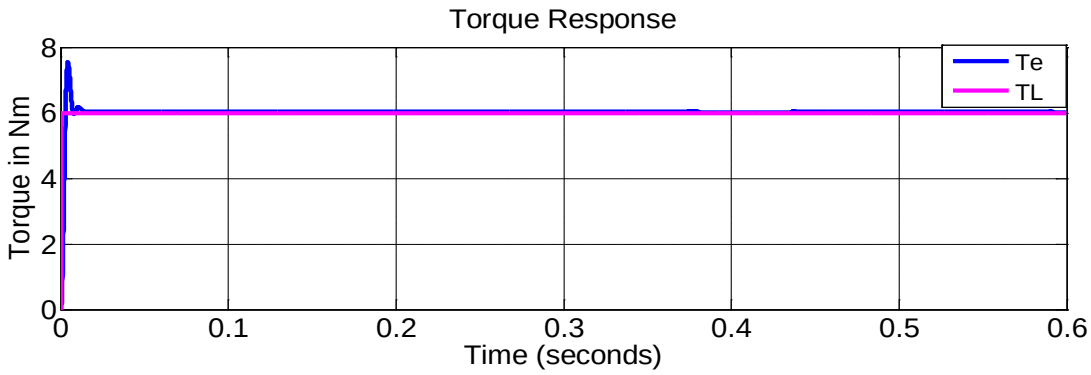

Figure 4.2-10 First harmonic component of electromagnetic torque and load torque

Figure 4.2-10 shows the developed electromagnetic torque of the motor. The starting torque is high at the transient response that oscillates for 0.03 seconds and the steady state value of torque is tracking the load torque with less than 2% error.

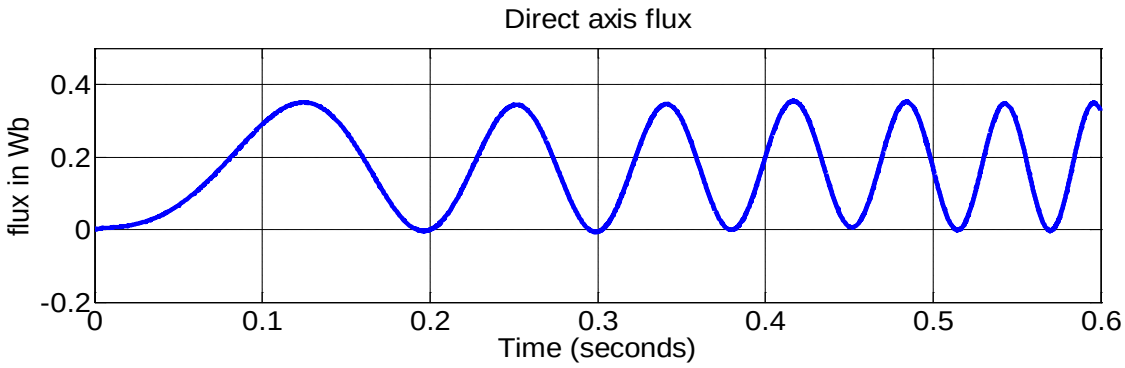

Figure 4.2-11 First harmonic component of direct axis stator flux

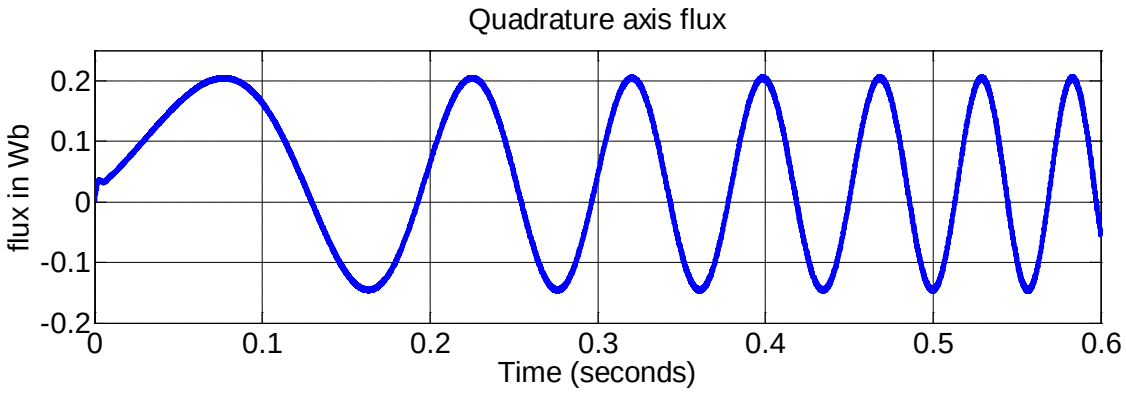

Figure 4.2-12 First harmonic component of quadratuare axis stator flux

Figure 4.2-11 and 4.2-12 are shows the direct and quadrature component of stator flux. Figure 4.2-13 shows the actual rotor position, as can be observe from the figure if the angle is reach at 2π rad or 360^0 it turns back to 0 until the simulation time is end.

Figure 4.2-14 shows sector number identification of the decagon shown in Figure 3.4-2. As stated in chapter three, in 2π rad or 360^0 there are ten sectors. As observe from the figures, in one period rotor angle (2π rad) there are corresponding ten sectors. This is one of the performance tests that indicate the simulation is quite alright.

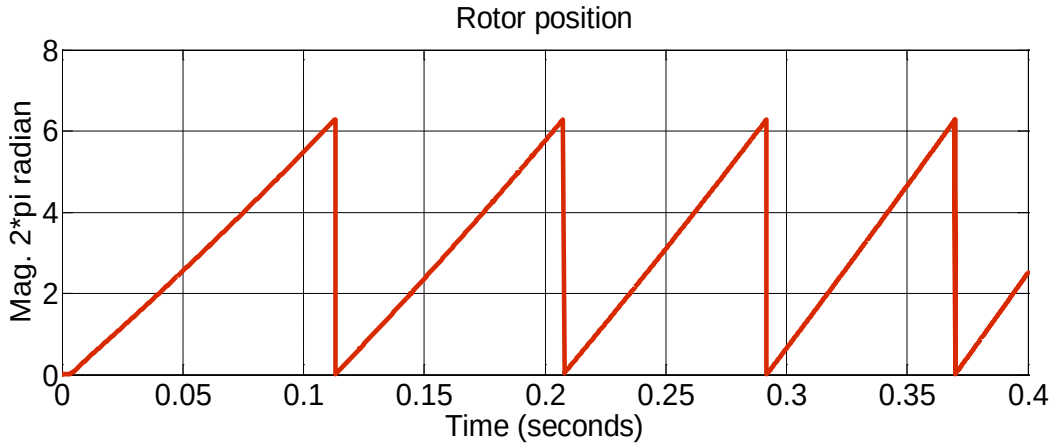

Figure 4.2-13 Rotor position

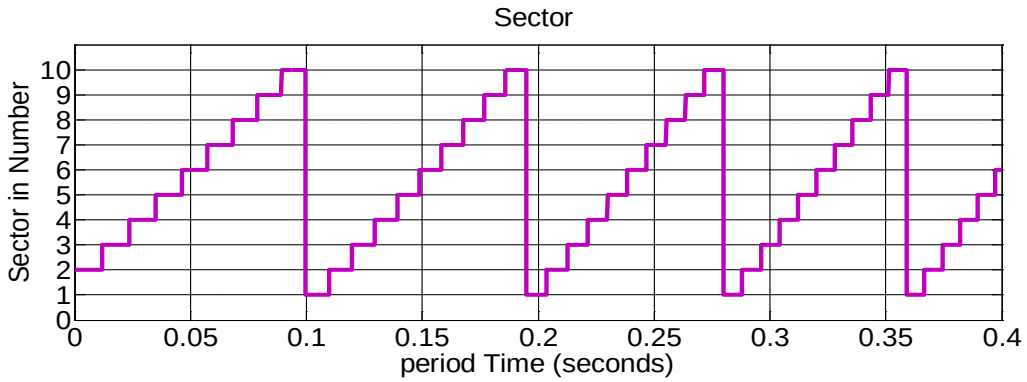

Figure 4.2-14 sector number

In chapter two was explained that direct torque control helps to independently control the flux and torque using the direct and quadrature axis variable components respectively. The electromagnetic torque is directly proportional to quadrature axis stator voltage (current) and the flux is directly proportional to direct axis stator voltage (current).

As shown in figure 4.2-15 the quadrature and direct axis stator current have approximate value of 0A and 1.757A in steady state condition at no-load. The quadrature current is increased into 1.5 A when the load torque is shifts from no-load to 2.5 Nm but the direct axis current is almost constant values. In contrast; it can be control the direct axis stator current independently at different reference value of reference flux without affecting the quadrature stator current as shown in figure 4.2-16, 4.2-17 and 4.2-18. Thus, these relationship will be indicated clearly shown that the torque and flux can be controlled independently by changing the set points.

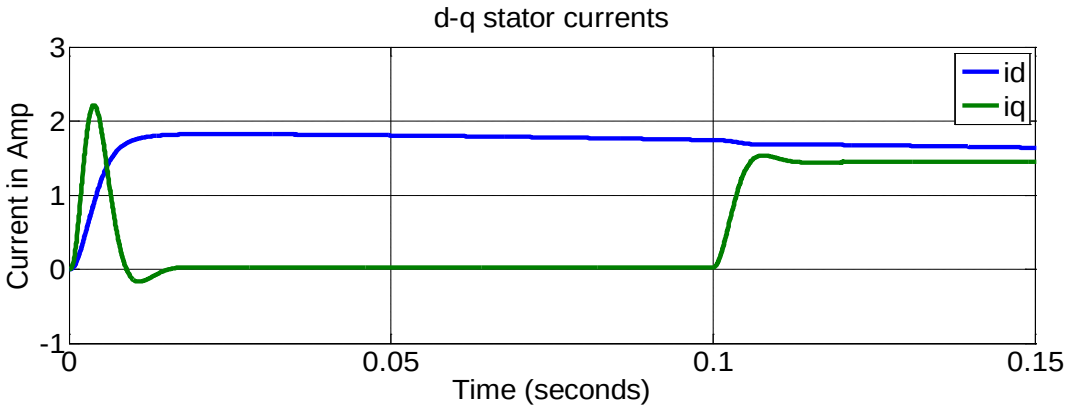

Figure 4.2-15 First harmonic component of d-q axis stator current at T_L=No load (t=0 sec), T_L=2.5.Nm (t=0.1 sec) and λ_{ref} =2 Wb

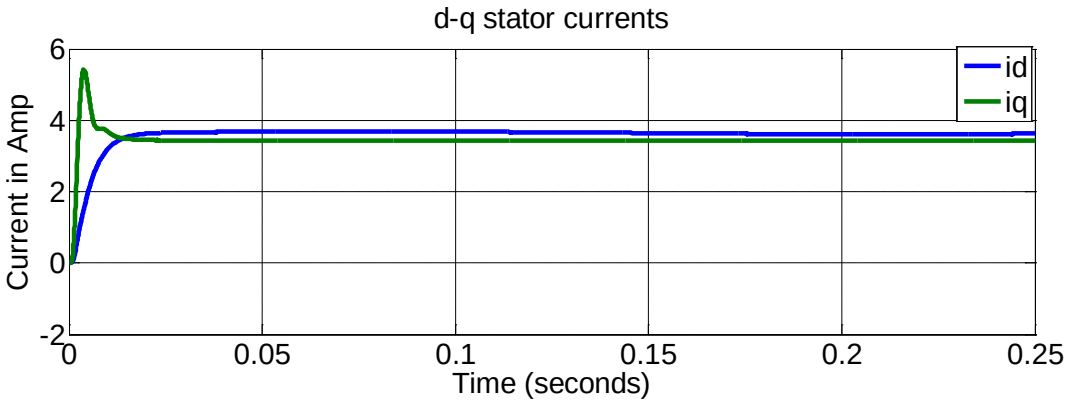

Figure 4.2-16 First harmonic component of d-q axis current at T_L=5 Nm and λ_{ref}=3.5Wb

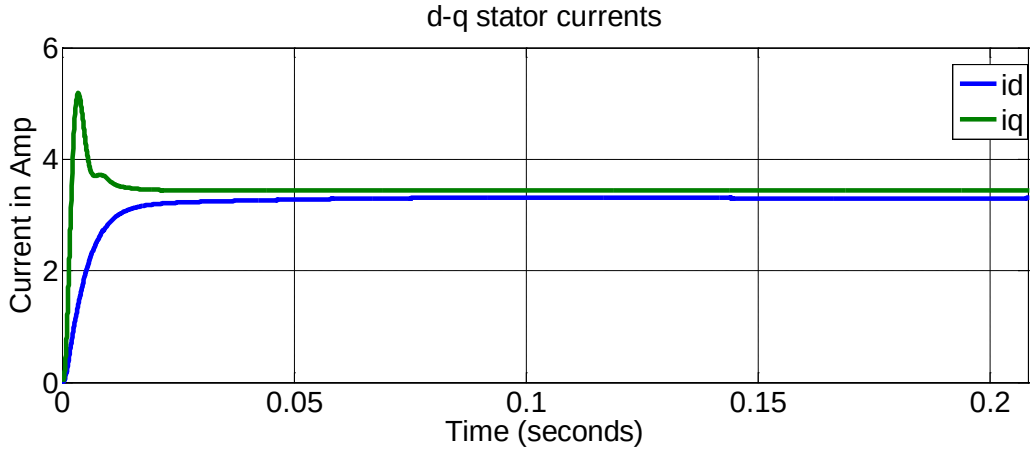

Figure 4.2-17 First harmonic component of d-q axis current at T_L=5 Nm and λ_{ref}=3Wb

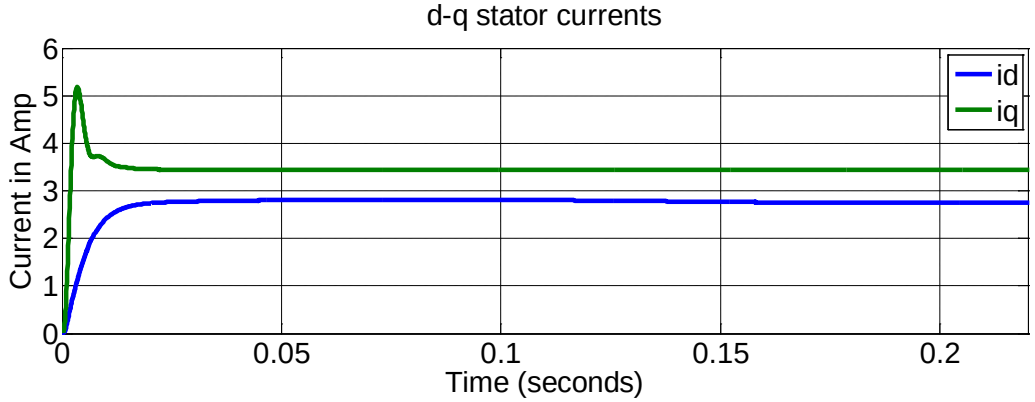

Figure 4.2-18 First harmonic component of d-q axis current at T_L=5 Nm and λ_{ref}=2.5Wb

4.2.2 Simulation Results of Third Harmonic components

Figure 4.2-19 shows the developed third harmonic stator phase voltage and figure 4.2-20 shows the Clark transformation of phase voltages.

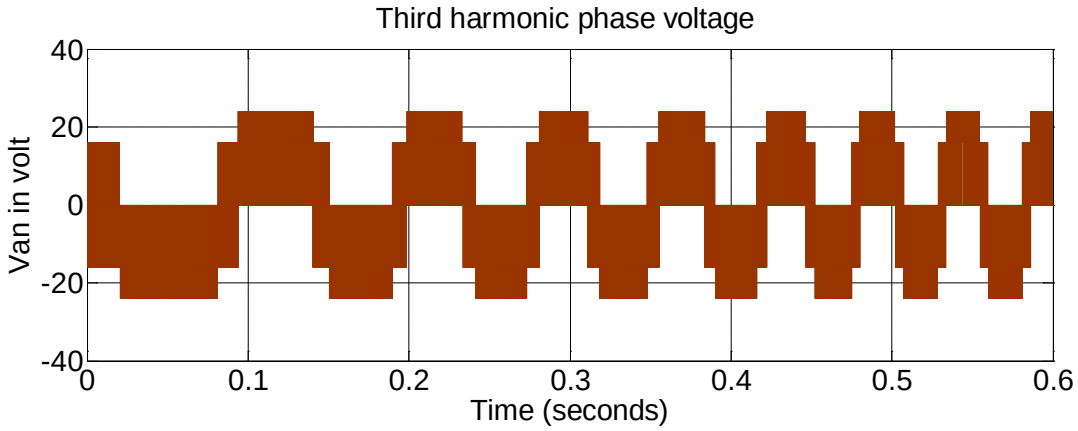

Figure 4.2-19 Third harmonic component of stator phase voltage

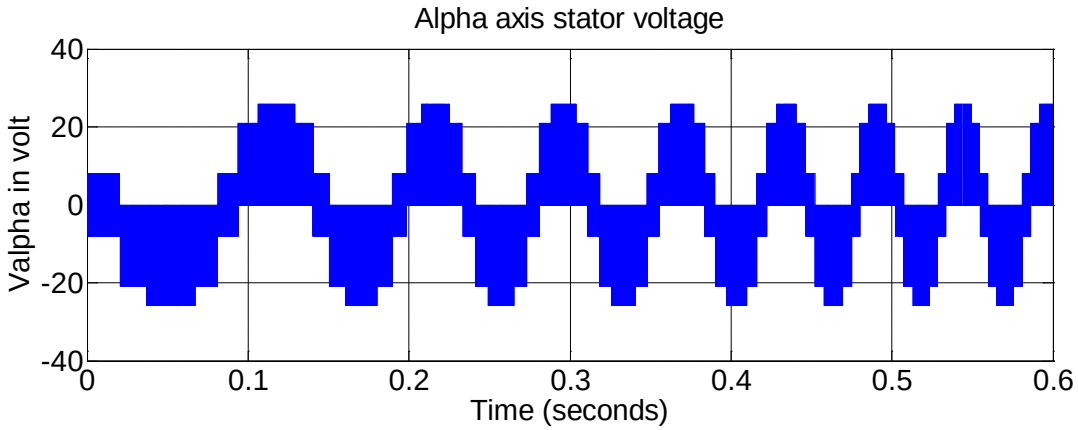

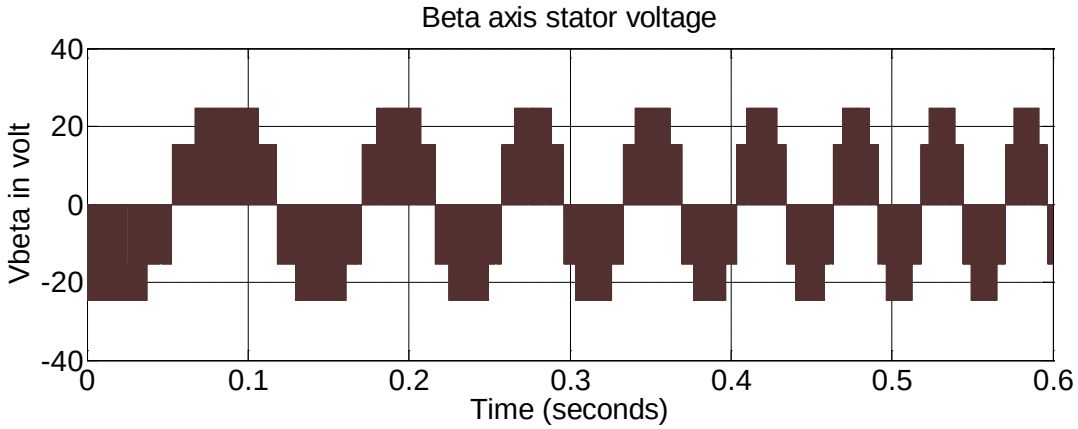

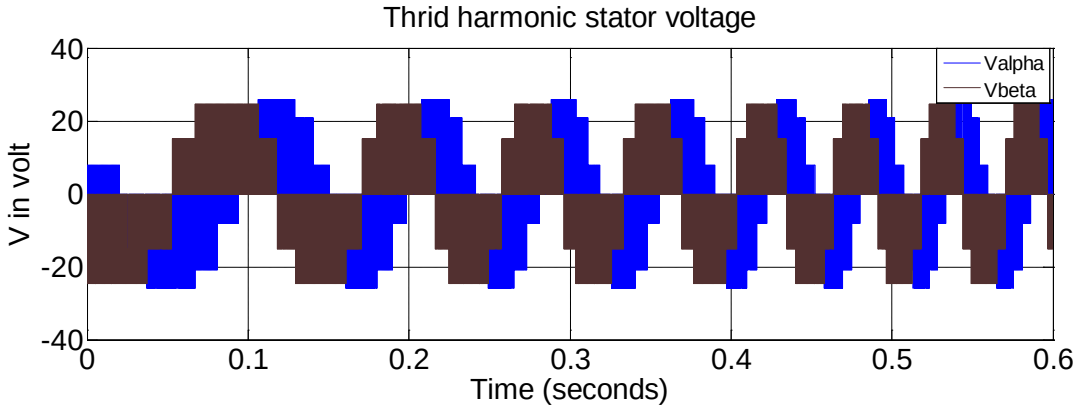

Figure 4.2-20 Third harmonic components of alpha and beta axis stator voltages

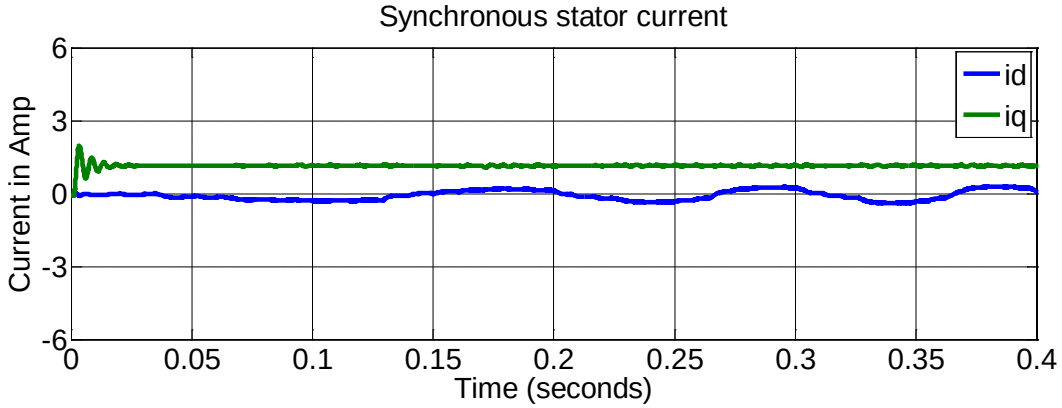

Figure 4.2-21 Third harmonic component of direct and quadrature axis stator currents

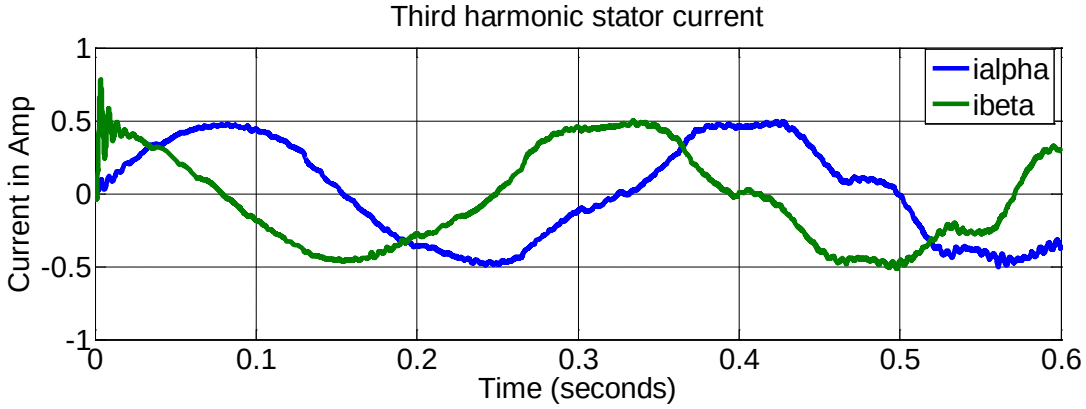

Figure 4.2-22 Third harmonic components of alpha and beta axis stator currents

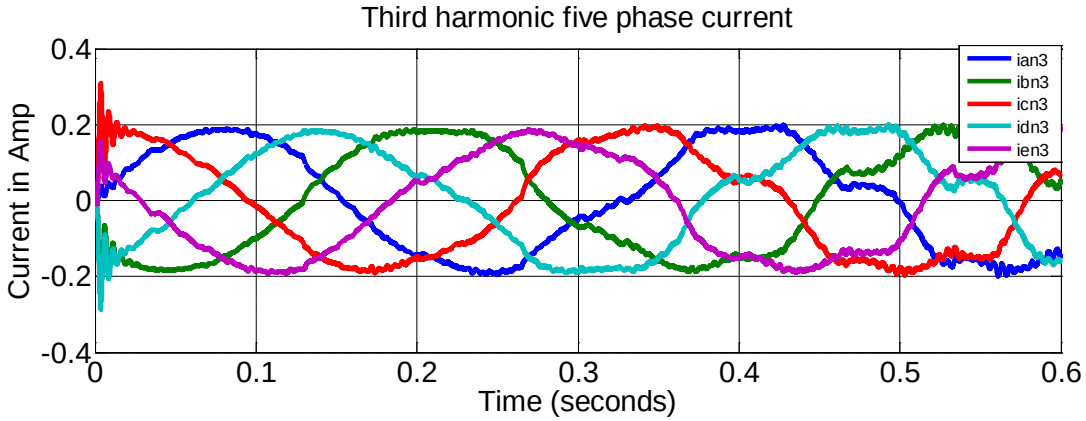

Figure 4.2-23 Third harmonic components of five phase stator currents

The third harmonic five phase induction motor current shown in figure 4.2-23 is 12.3% of the fundamental harmonic components. The spatial angle between the adjacent phases is nearly sinusoidal 72 electrical degrees.

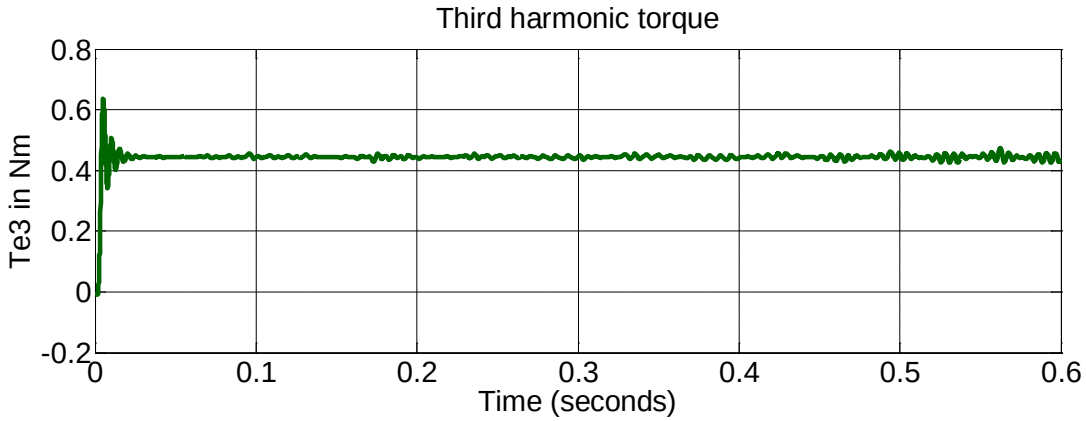

Figure 4.2-24 Third harmonic component of electromechanical torque at load of 6 Nm

4.2.3 Simulation Results of Total Electromagnetic Torque Response

Figures 4.2-25 and 4.2-26 show the total electromagnetic torque at no-load and load, respectively. This is obtained by adding the two values of electromagnetic torques, i.e. the fundamental component value and the third harmonic component value. As can observed from figure 4.2-24 the third harmonic component of electromagnetic torque is about 7.5% of the fundamental harmonic component of electromagnetic torque. Thus, DTC of five phase IM using SVM technique is used to inject a third harmonic voltage component that determine the ability of

a five phase induction motor to contribute a third harmonic torque component to the total torque component.

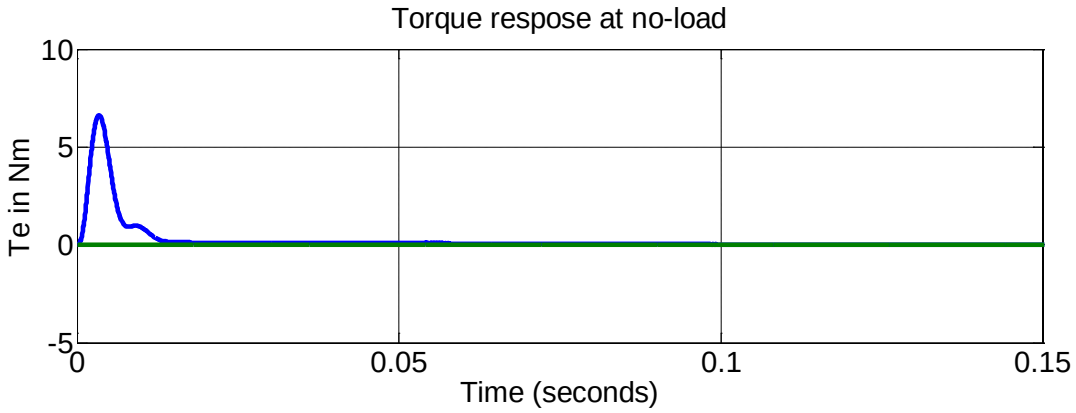

Figure 4.2-25 Total electromagnetic torque at No load torque

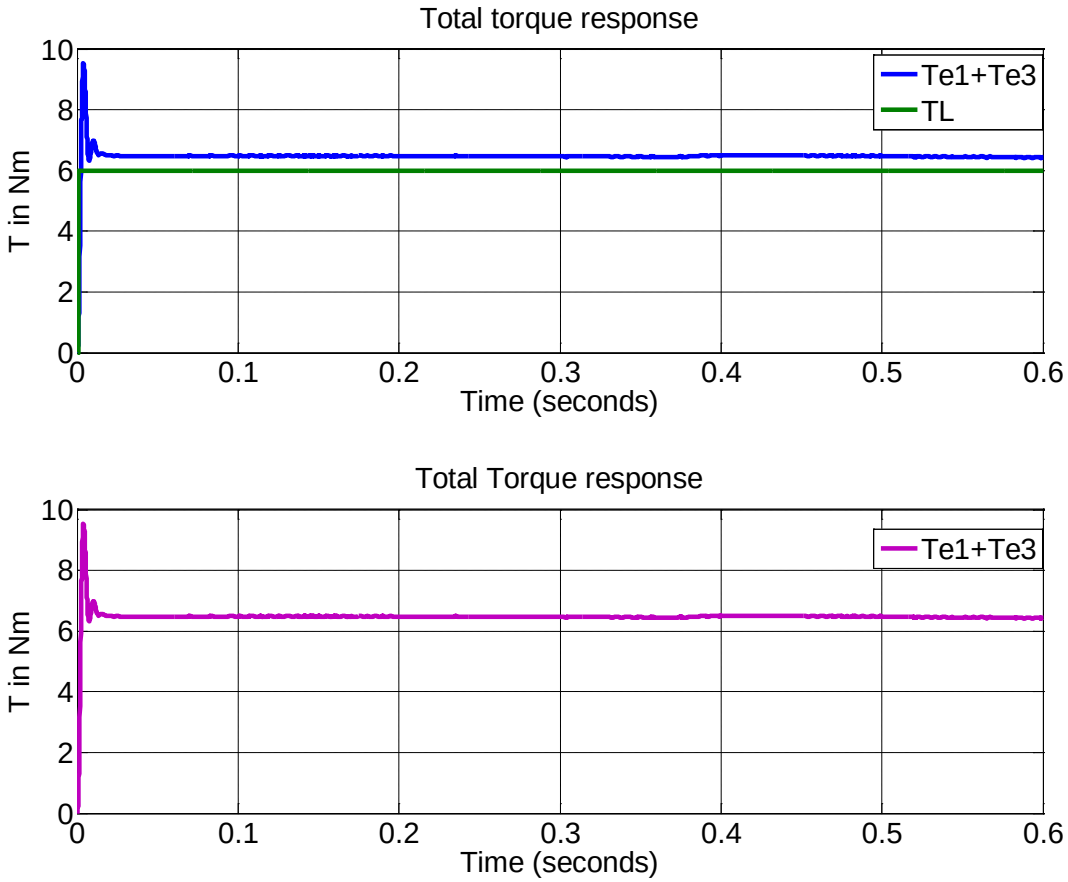

Figure 4.2-26 Total electromagnetic torque (T_{e1}+T_{e3}) at a load torque of 6 Nm

4.2.4 Fault Tolerance Simulation Results

Fault tolerant feature of the 5-phase induction motor is observed from 5th, and 2nd and 5th stator windings opened condition is shown in figure 4.2-27 and 4.2-28. It is seen that the number of lost phase increases, the starting current of the rest of the phases increases and rated torque decreases gradually.

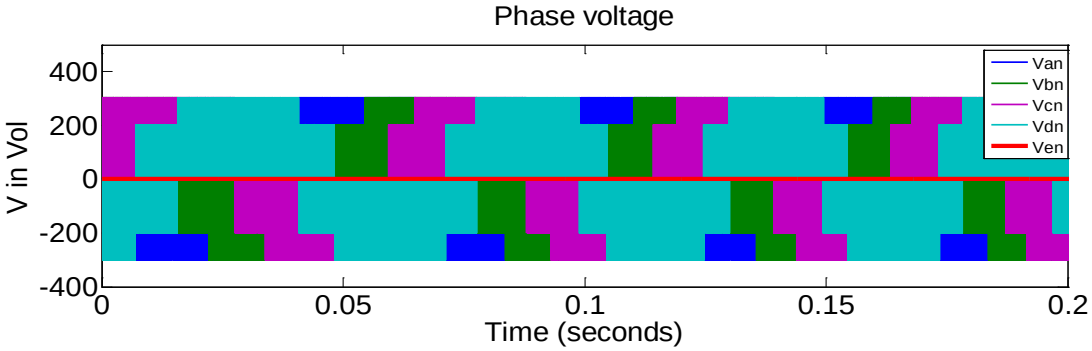

a) Five-phase voltage with One phase opened

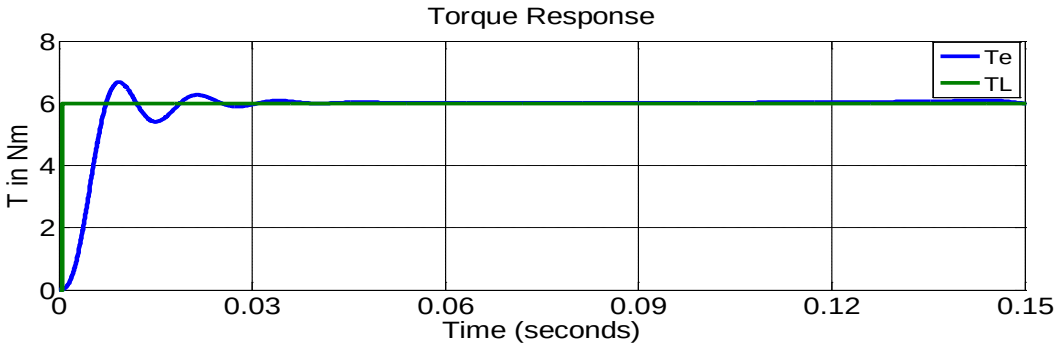

b) Electromagnetic Torque

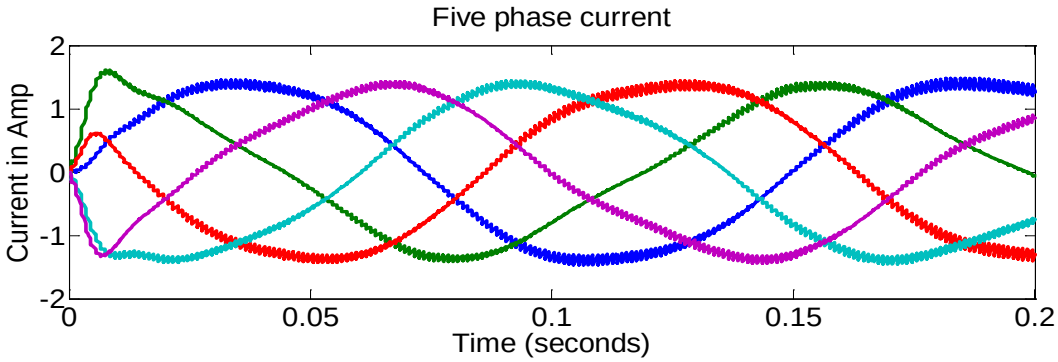

c) Stator current

Figure 4.2-27 Fault tolerant results of 5-phase IM with one (5th) of the phase is opened

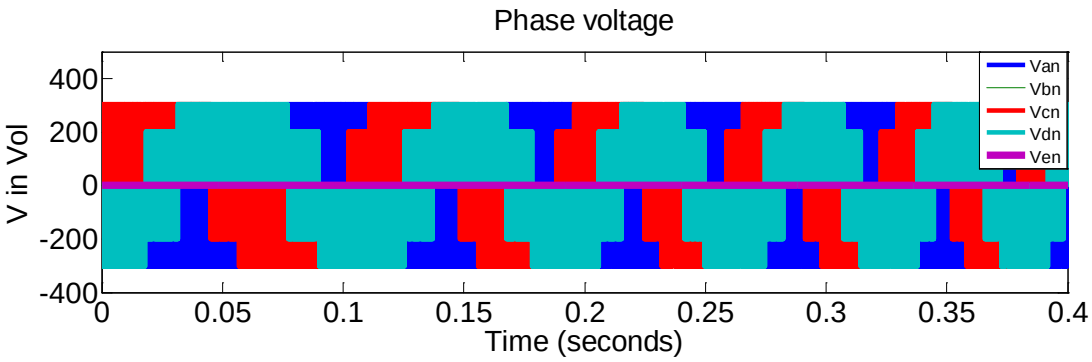

a) Five-phase voltage with two phases opened

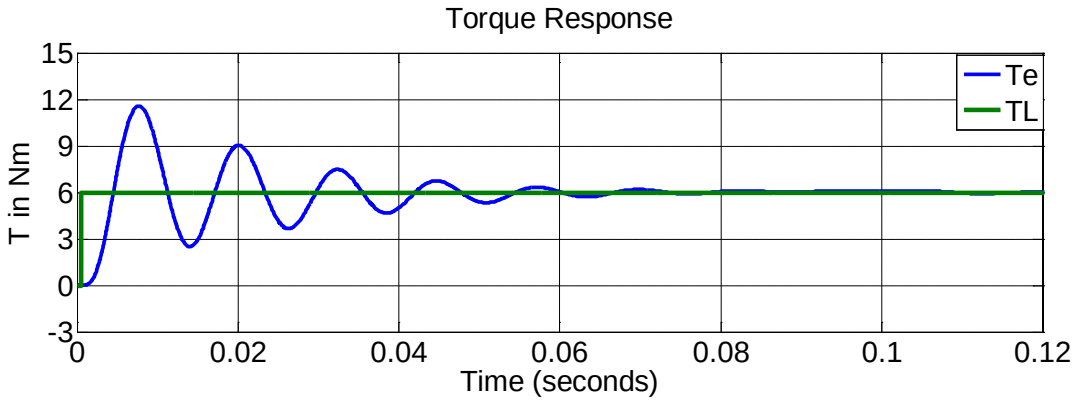

b) Electromagnetic Torque

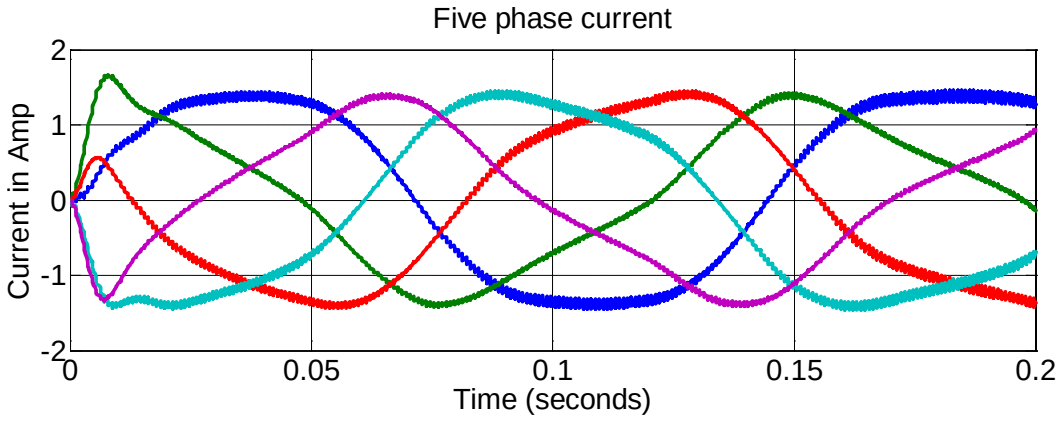

c) Stator current

Figure 4.2-28 Fault tolerant simulation of 5-phase IM with 2nd and 5th of the phases are opened

4.2.5 Comparison of Three-Phase and Five-Phase Simulation Results

It is realized that the five-phase induction motor drive systems offered some distinct advantages over three-phase drive system counterparts. The torque ripple of five-phase IM shown in figure 4.2-30 (b) is lower than the torque ripple of three-phase shown in figure 4.2-29 (b). It stays for 0.002 sec in five phase induction motor and 0.05 sec for its three phase. The current per phases in five-phase IM are reduced when compare with the three phase current as shown in figure 4.2-30 (a) and figure 4.2-29 (a) respectively. The accelerating transient response of the five-phase torque for a load change from no load to load torque condition is higher than the three-phase transient response as shown in figure 4.2-30 (c) and figure 4.2-29 (c) respectively. The simulation is incorporated with the same specification of three phase and five phase induction motor counterparts.

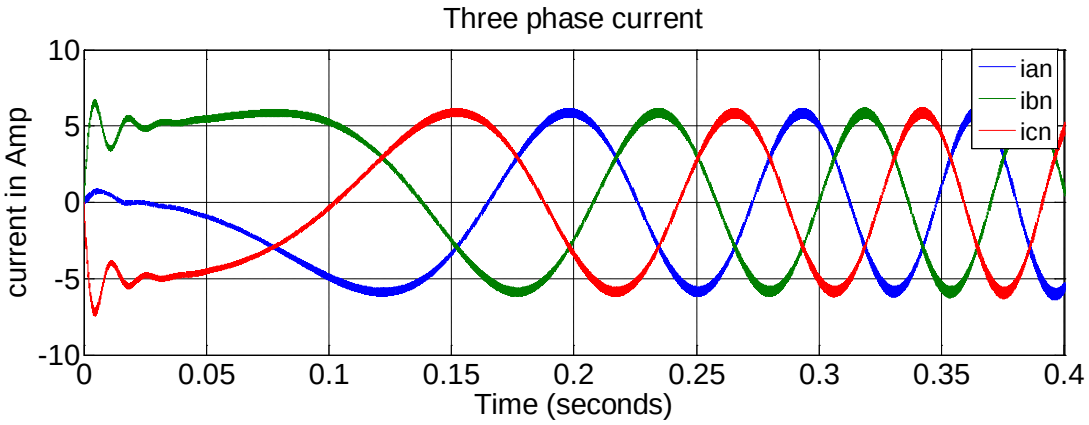

a) Three phase current

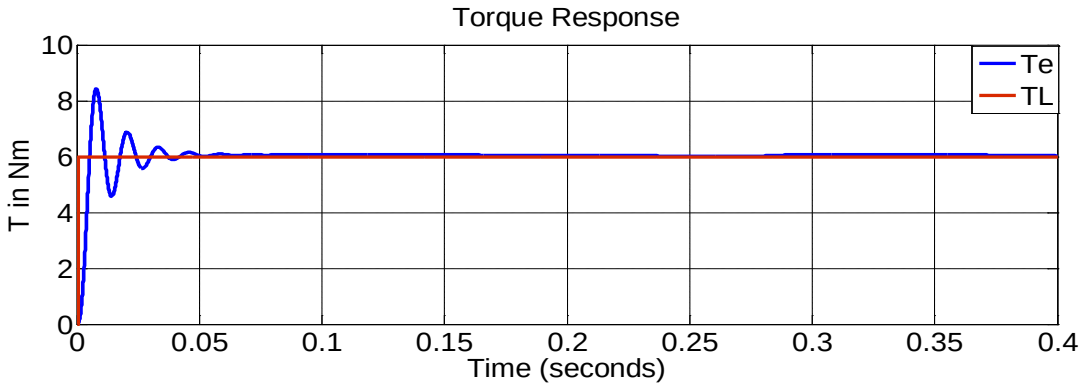

b) Electromagnetic torque at load of 6 Nm

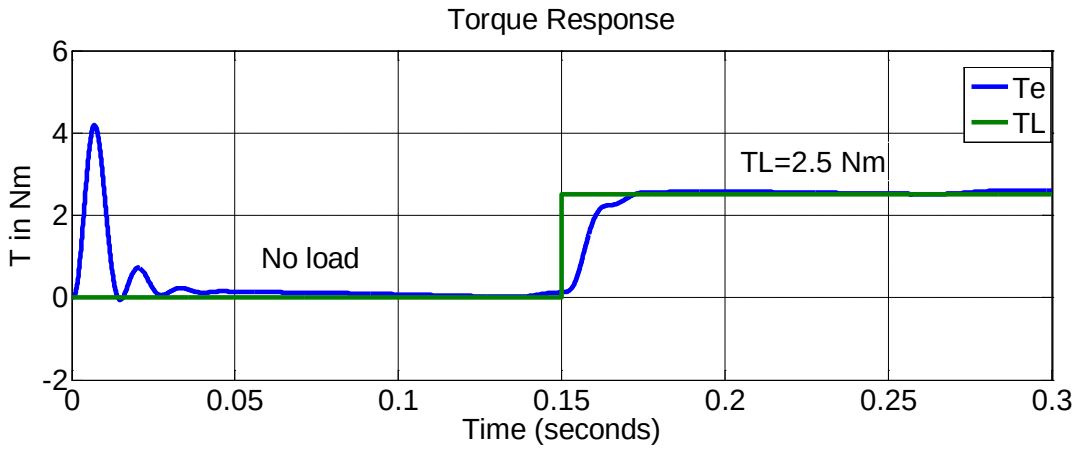

c) Electromagnetic torque at No-load and at load torque of 6 Nm

Figure 4.2-29 Simulation results for three-phase IM at different load conditions

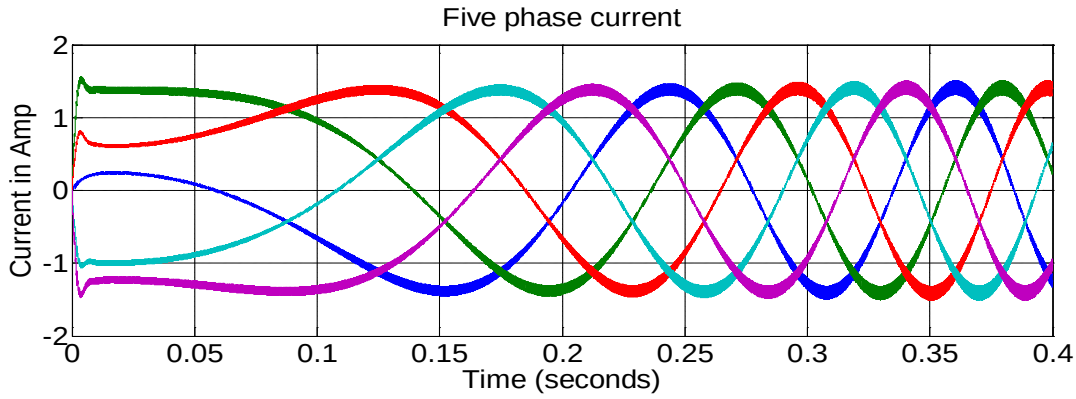

a) Five phase current

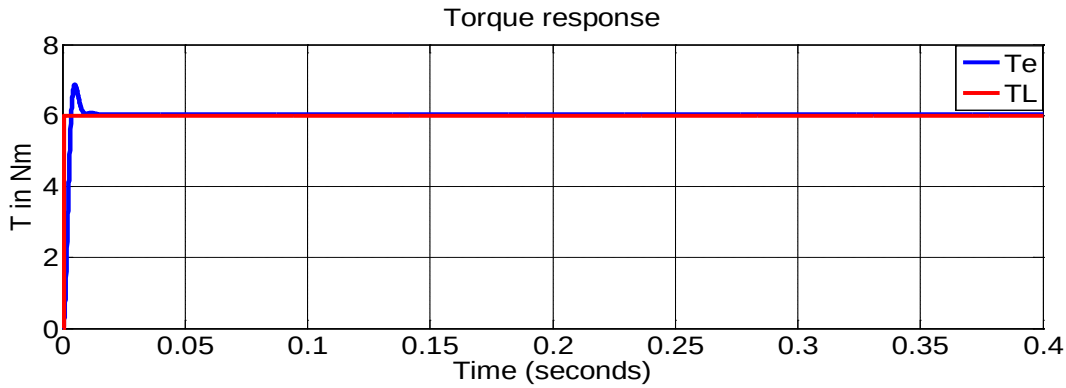

b) Electromagnetic torque at load of 6 Nm

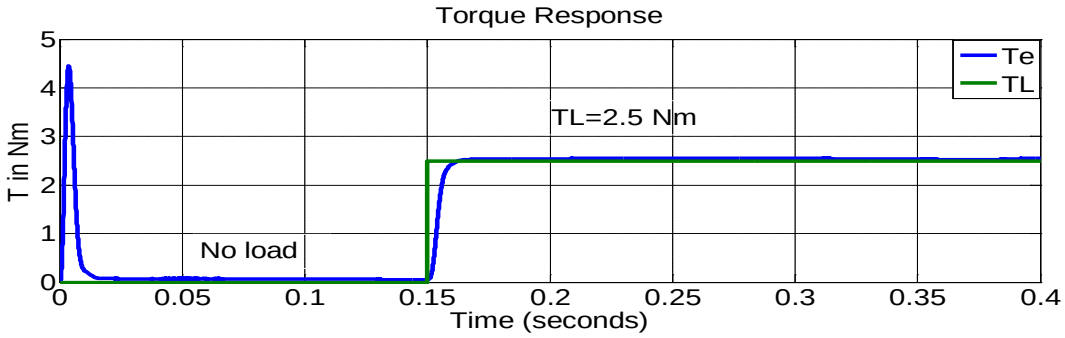

c) Electromagnetic torque at No-load and at load torque of 6 Nm

Figure 4.2-30 Simulation results for five-phase IM at different load conditions

4.2.6 Simulation Results with Varying Parameters

The model simulation also works with the following motor parameters. The parameters of the motor that are used in the simulation below are shown in table 4.2-2 and they are taken from [21].

Table 4.2-2 Induction motor and VSI parameters

Dc link voltage	Vdc = 400V
Stator resistance	Rs= 10 ohm
Rotor resistance	Rr= 6.3 ohm
Stator inductance	Lls= 0.04mH
Rotor inductance	Llr= 0.04mH
Mutual inductance	Lm= 0.42mH
Moment of inertia	J= 0.03Kg.m2
Number of poles	P= 4

The simulation results are carried out for different reference inputs under different loading conditions with the above parameters without changing the other specifications as simulated previously. The load torque is varied in steps (at t=0, motor is no loaded and the load is varied in steps as 25%, 50%, 75%, and full load at 0.1, 0.25, 0.45, 0.7 second respectively) and the corresponding variations in torque, stator current and speed are observed and shown in figure 4.2-31 (a), (b) and (c) respectively. It is seen that the stator current increases and speed decreases

with increasing load and the motor torque follows the load torque. As can be observed from the simulation result; the simulation model is generated the same output with various parameter of the induction motor.

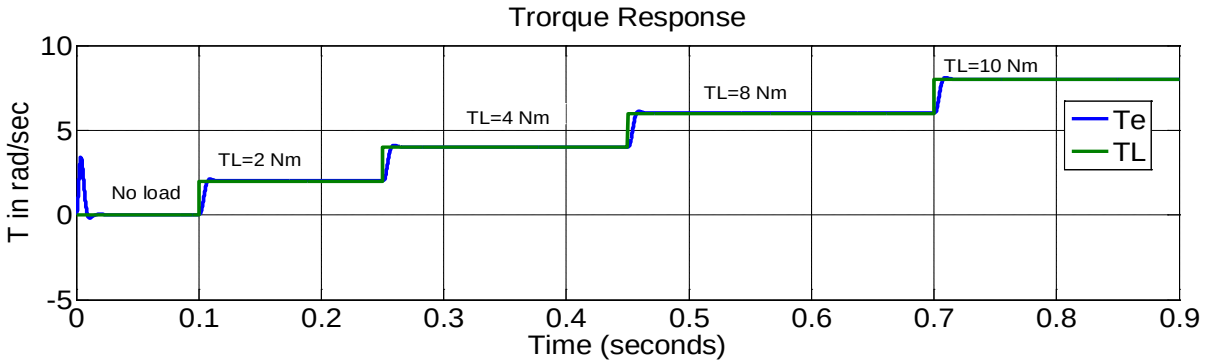

a) Electromagnetic torque and load torque

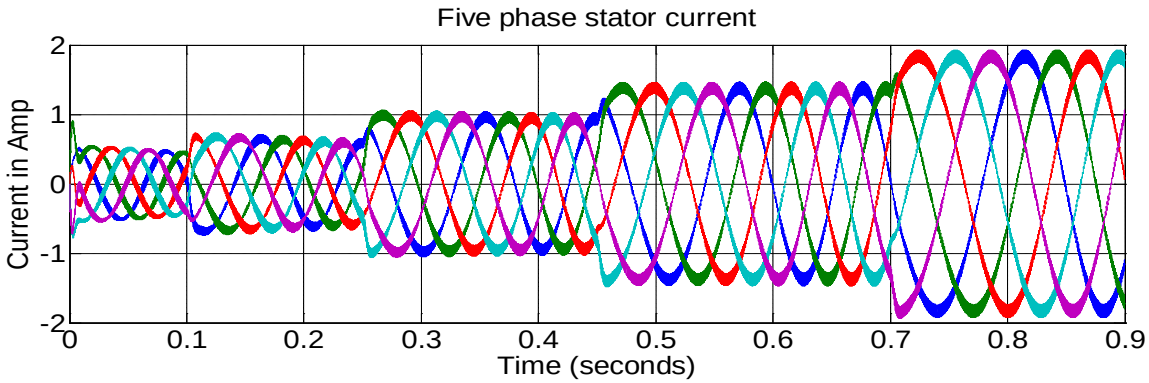

b) Five-phase stator current

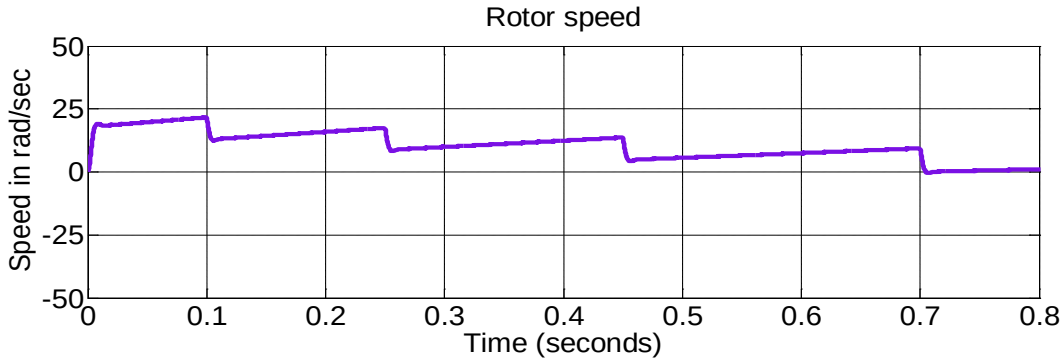

c) Speed response

Figure 4.2-31 simulation results of five phase IM with different loading conditions

Chapter Five

Conclusion and recommendation

5.1 Conclusion

In this thesis, DTC of five phase induction motor using space vector modulation (SVM) has been investigated. The dynamic model of the drive system and its d-q dynamic model in synchronous reference frame with the combined fundamental and third harmonic components have been developed. Based on estimates of the instantaneous errors in torque and stator flux magnitude, and PI controller outputs, a voltage vectors are selected. The developed SVM algorithm is used to generate the triggering signal of the voltage source inverter. Due to the additional degrees of freedom, the five-phase induction motor drive presents unique characteristics for enhancing the torque producing capability of the motor. The principle of Direct Torque Control and flux estimation method of induction motor are also elaborated and the overall model results have been analyzed with the help of MATLAB/SIMULINK. The difference between three-phase induction motor and five-phase induction motor is highlighted. Also the fault tolerance simulation results are analyzed. From the analysis of the simulation results the performance of the drive have been presented and analyzed. The main results observed from the Simulation are as shown below.

- The fast transient accelerating torque response of the drive, steady state is attained in a very short time approximately 0.03 seconds.
- The torque and flux can be control independently under different reference inputs and different load torques.
- In the first harmonic, electromagnetic starting torque is high at the transient response that oscillates for 0.03 second with rising time of 0.004second and the steady state value of torque is tracking the load torque with less than 2% error.
- The third harmonic torque can be contributed 7.5% of the fundamental harmonic torque component to the system with 4.9 % of torque ripple
- The five-phase induction motor drive systems offered better performance over three-phase drive system counterparts.

- The overall system gives good performance at no-load torque (0 Nm) and loaded torque condition (6 Nm).
- The performance of DTC-SVM can be improved further by appropriate tuning of the PI controller gains

Hence by using this proposed technique the total electromagnetic torque density can be enhanced by injecting the third harmonic components to the fundamental torque producing components. The overall simulation results show a good performance of the DTC five phase induction motor using SVM. The proposed technique may be employed in building construction for lift applications and agricultural irrigation systems for water pumping in rural areas.

5.2 Recommendation

If combined application of medium and large space vectors (five vectors per switching period) are used the torque ripped can be reduced. If intelligent controllers such as slide mode controller or fuzzy logic controller are used instead of the ordinary PI controller, system performance could be improved more. Also VSI with multilevel converters are preferable than two level converters.

References

[1] G. V. RamaKrishna, “Torque Ripple Reduction in Direct Torque Controlled Induction Motor Drive by using Fuzzy Controller”, *2007*.

[2] M. KUMAR ARYA, “Development of Direct Torque Control Model with using SVI for Three Phase Induction Motor”, International Journal of Engineering Science and Technology (IJEST), Vol. 3 No. 8 August 2011.

[3] N. Patra, “Study of Induction Motor Drive with Direct Torque Control Scheme and Indirect Field Oriented Control Scheme Using Space Vector Modulation”, masters thesis, June 2013.

[4] G. Renukadevi, and K. Rajambal “Modeling and Analysis of Multi-Phase Inverter Fed Induction Motor Drive with Different Phase Numbers”, *Issue 3, Volume 8, July 2013*.

[5] Ayman S. Abdel-Khalik, Shady M. Gadoue “Improved flux pattern by third harmonic injection for multiphase induction machines using neural network”, Alexandria Engineering Journal, August 2011.

[6] Min-Huei Kim, Nam-Hun Kim, and Won-Sik Baik, “A Five-Phase Induction Motor Speed Control System Excluding Effects of 3rd Current Harmonics Component”, *Journal of Power Electronics, Vol. 11, No. 3, pp. 294–303 May 2011*.

[7] *J. N. Bharothu, V.Gopilatha,* “Optimal Vector Sequence with Space Vector Modulation in Direct Torque Control of Induction Motor”, American Journal of Sustainable Cities and Society, Issue 2, Vol. 1 January 2013.

[8] A. Manuel, and J. Francis, “Simulation of Direct Torque Controlled Induction Motor Drive by using Space Vector Pulse Width Modulation for Torque Ripple Reduction”, Vol. 2, Issue 9, September 2013.

[9] Hamid A. Toliyat, Huangsheng Xu, “A Novel Direct Torque Control (DTC) Method for Five-Phase Induction Machines”, IEEE, 2000

[10] Huangsheng Xu, Hamid A. Toliya and Lynn J. Petersen, “Rotor Field Oriented Control of Five-Phase Induction Motor with the Combined Fundamental and Third Harmonic Currents”, IEEE, 2001.

[11] Shuai Lu, and Keith Corzine, “Direct Torque Control of Five-Phase Induction Motor Using Space Vector Modulation with Harmonics Elimination and Optimal Switching Sequence”, *Student Member*, IEEE, pp. 195–200, 2006.

[12] D.Kousalya, N. Manoj Kumar, “Torque Ripple Reduction in SVM Based Direct Torque Control of Induction Motor”, International Journal of Advanced Research in Electrical, Electronics and Instrumentation Engineering (IJAREEIE), Vol. 3, Special Issue 2, April 2014.

[13] S. Allirani and V. Jagannathan “High Performance Direct Torque Control of Induction Motor Drives Using Space Vector Modulation”, IJCSI International Journal of Computer Science Issues, Vol. 7, Issue 6, November 2010.

[14] H. Xu, H. A. Toliyat, and L. J. Petersen, “Five-phase induction motor drives with DSP-based control system,” IEEE Transactions on Power Electronics, vol. 17, No. 4, pp. 524-533, July 2002.

[15] E. Levi, R. Bojoi, F. Profumo, et al, “Multiphase induction motor drives – a technology status review”, IET Electr. Power Appl, 2007.

[16] A.Iqbal and E.Levi, “Space Vector PWM Techniques for Sinusoidal Output Voltage Generation with a Five-Phase Voltage Source Inverter”, Liverpool John Moores University, School of Engineering , Liverpool, United Kingdom Published online: 23 Feb 2007.

[17] D.Dujic, G.Grandi, M.Jones, and E. Levi, “*A Space Vector PWM Scheme for Multifrequency Output Voltage Generation With Multiphase Voltage-Source Inverters*” IEEE transactions on industrial electronics, vol. 55, NO. 5, May 2008

[18] Huangsheng Xu and Hamid A. Toliyat, “Implementing Rotor Field Orientated Control and Direct Torque Control of Five Phase Induction Motor Using TMS320C32 DSP”, Texas A&M University.

[19] *Abraham Belay, “DSP Based Vector Control Of Induction Motor” master thesis,* September 2007.

[20] Namhun Kim and Minhuei Kim, “Modified Direct Torque Control System of Five Phase Induction Motor”, *Journal of Electrical Engineering & Technology Vol. 4, No. 2, pp. 266-271, 2009.*

[21] G. Renukadevi, and K. Rajambal, “Generalized d-q Model of n-Phase Induction Motor Drive”, International Journal of Electrical Science and Engineering Vol:6 No:9, 2012.

[22] R. J. LEE, P. PILLAY and R. G. HARLEY, “D, Q Reference Frames for the Simulation of Induction Motors”, Electric Power Systems Research, 8 (1984/85) , pp 15 -26 ,Received April 9, 1984

[23] R.Toufouti, S.Meziane,and H.Benalla, “Direct Torque Control Strategy of Induction Motors”, Acta Electrotechnica et Informatica No. 1, Vol. 7, 2007.

[24] A.Verma, “Direct Torco Controlled Induction Motor Drive”, masters thesis, December 2010.

[25] Dereje Shibeshi, “DSP based Field Weakening Control of PMSM” masters thesis, October 2007.

[26] KarlJ. Astrom and Tore Hagglun, “PID Controllers: Theory, Design, and Tuning”, Printed in the United States of America , 2nd Edition, 1995

[27] Seborg, D.E., T.F. Edgar, and D.A. Mellichamp, “Process Dynamics and Control”. 3rd edition, 2004.

[28] A.Almula and G.M.Gebreel, “Simulation and Implementation of Two level and Three-Level Inverters by Matlab and Rt-Lab”, masters thesis, 2011.

[29] Sosthenes Francis Karugaba, “Dynamics and Control of a Five Phase Induction Machine”, masters thesis, December 2008.

[30] Mario J. Duran, Francisco Salas and Manuel R. Arahal, “Bifurcation Analysis of Five-Phase Induction Motor Drives with Third Harmonic Injection”, IEEE Transactions on industrial electronics, vol. 55, no. 5, May 2008.

[31] S.M. Vali and A.M. PRASAD, “Direct Torque Control of Induction Motor using Space Vector Modulation”, National Conference on Electrical Sciences (NCES-12), 2012.

[32] Atif Iqbal, “Modelling and Control of Series Connected Five-Phase and Six-Phase Two-Motor Drives”, PhD dissertation, August 2005.

Declaration

I declare that this thesis was composed by myself, that the work contained herein is my own except where explicitly stated otherwise in the text, and that this work has not been submitted for any other degree or professional qualification.

Gebrihans Yehdego _____

Name signature

Addis Ababa, Ethiopia _____

Place Date of Submission

This thesis has been submitted for examination with my approval as a university advisor.

Dr. Mengesha Mamo _____

Advisor's Name Signature